ENERGY EXCHANGE WITHIN A CORN CANOPY

ENERGY EXCHANGE WITHIN A CORN CANOPY

By

JOHN HARRY McCAUGHEY, B.Sc., M.A.

A Thesis

Submitted to the Faculty of Graduate Studies

in Partial Fulfilment of the Requirements

for the Degree

Doctor of Philosophy

McMaster University

October 1972

DOCTOR OF PHILOSOPHY (1972)
(Geography)

McMASTER UNIVERSITY
Hamilton, Ontario.

TITLE: Energy Exchange Within a Corn Canopy

AUTHOR: John Harry McCaughey, B.Sc. (Queen's University, Belfast)
M.A. (McMaster University)

SUPERVISOR: Professor J.A. Davies

NUMBER OF PAGES: x, 138

SCOPE AND CONTENTS:

The results of an investigation of the microclimate of a sweet corn canopy is reported at two stages in its development. The purpose of the experiment was to study the height dependence and diurnal variations of the net radiation, sensible and latent heat fluxes, and the turbulent transfer mechanism. Only daytime data were used.

The depletion of net radiation in the canopy was studied within the framework of the exponential model. A new model for estimating net radiation in the canopy is developed. The pattern of the sources and sinks and the apparent turbulent transfer coefficient for sensible and latent heat in the canopy space are reported.

ACKNOWLEDGEMENTS

This study was supported by a grant from the National Research Council of Canada. Their support is appreciated.

I wish to thank my supervisor, Dr. J.A. Davies, for his guidance and assistance during the course of the work. Also, I acknowledge the advice of Dr. W.R. Rouse, McMaster University, and Dr. K.M. King, University of Guelph.

I am grateful to Dr. G. Collin of the Simcoe Horticultural Experiment Station, for providing the experimental site and to my fellow students who assisted in the collection and analysis of the data.

In particular, my thanks are due to Dr. R.G. Wilson, McGill University, and to Mr. M. Nunez, University of British Columbia.

Finally, I am grateful to my wife for typing this thesis.

TABLE OF CONTENTS

Table of Contents - continued

Table of Contents - continued

LIST OF DIAGRAMS

List of Diagrams - continued

LIST OF TABLES

LIST OF APPENDICES

CHAPTER 1

INTRODUCTION

Process-oriented investigations in microclimatology have depended upon theory describing the energy exchanges between the atmosphere and an underlying surface. In such studies, the data have been collected within the surface boundary layer where the fluxes[1] of latent and sensible heat can be considered to be constant with height (Elliott 1964).

The concept of a single, well-defined surface (the active surface) at which the exchanges occur, has been implicit in most of this work. However, in tall vegetation, this surface cannot be defined. A vegetation canopy has instead, an active depth where there is a complex interaction of processes. Within a canopy, vertical fluxes are not constant with height, and this characteristic distinguishes the canopy space from the atmosphere. From measurements in the boundary layer, total fluxes from a vegetation stand can be obtained. However, these only indicate the total behaviour of the canopy (Philip 1964), and, to understand how different portions of the canopy are involved in the energy exchanges, the vertical distribution of fluxes must be known. Experiments to define the vertical variation of energy exchange

[1] In this thesis, the term flux is defined as the rate of transport of a specified quantity across unit area of a surface.

give insight into crop-climatic environment interaction.

The microclimatic approach to the study of plant activity in terms of energy fluxes provides a means of estimating plant response in the field on a short term basis, usually hourly, with minimal disturbance of the natural environment. This approach has been employed successfully by Uchijima (1962), Denmead (1964), Begg et al. (1964), Lemon (1965), Brown and Covey (1966), Allen (1969) and Gillespie and King (1971). These studies have been restricted either to analysis of energy exchanges during a single diurnal cycle or to peculiarities within the crop atmosphere. To the writer's knowledge, there have been no attempts to study canopy behaviour over the lifespan of a crop, although this step has been recommended (Monteith 1968). This is essential to successful simulation of canopy climates (Waggoner and Reifsnyder 1968). In general, there is a dearth of canopy data and, therefore, further work is required.

The purpose of this study is to examine the behaviour of energy fluxes in a dense corn canopy. Brown and Covey (1966), Lemon (1965) and Gillespie and King (1971) have presented results for field corn. Sweet corn (variety, Seneca Chief), which provides a much denser canopy, was used in this study.

The specific aims of the study are to establish the vertical distribution of available radiant energy in the canopy; to evaluate sensible and latent heat fluxes within and above the canopy; to evaluate the turbulent exchange mechanism and to determine the involvement of the canopy in the energy exchange by evaluating the vertical variation of various energy terms in the canopy space.

CHAPTER 2

THEORETICAL FRAMEWORK

A FLUXES OF LATENT AND SENSIBLE HEAT FROM THE ENERGY BALANCE

From the principle of the conservation of energy, the energy balance for any level, z, within a vegetation canopy is

$$Rn_z + \int_0^z Cp\nabla_H(\rho uT)\ \delta z + \int_0^z \frac{L\varepsilon}{R'}\nabla_H\left(\frac{ue}{T}\right)\ \delta z = H_z + LE_z + G_0 + P_z$$

$$+ \int_0^z Cc\rho c\frac{\partial T}{\partial t}\ \delta z + \int_0^z Cp\rho\frac{\partial T}{\partial t}\ \delta z + \int_0^z \frac{L\varepsilon}{R'T}\ \frac{\partial e}{\partial t}\ \delta z \quad , \qquad (1)$$

where

Rn = the net radiation flux,

H = the sensible heat flux to the air,

LE = the latent heat flux to the air,

P = the photochemical energy equivalent of the carbon dioxide flux.

The remaining symbols are defined in Appendix I.

The second and third terms on the left hand side of equation 1 are the horizontal divergence of sensible and latent heat respectively. The first four terms on the right hand side are the vertical energy fluxes, and the other three terms are the heat storage in the biomass and the sensible and latent heat storage in the air. The relationship summarized in equation 1 is shown schematically in Figure 1. The complexity of this three-dimensional energy balance has been stressed by Suomi and Tanner (1958), and King (1961). However, it can be reduced considerably by neglecting the storage and photosynthetic terms. Brown and Covey (1966) showed that the heat storage in the biomass of a mature corn crop was <1% of the net radiation. Wilson (1971) estimated that, for the corn in this experiment and a temperature and vapour pressure change of 10C hr^{-1} and 1 mbar hr^{-1}, the heat storage in the air was equivalent to an energy flux of only 0.006 cal cm^{-2} min^{-1}. This is<1% of net radiation, except for short periods at sunrise and sunset. The energy used in photosynthesis is normally <5% of net radiation in mature corn, (Yocum, Allen and Lemon 1964). Rates of photosynthesis equivalent to 10% of net radiation have been recorded for short periods in the early morning and late afternoon (Lemon 1960). Therefore, ignoring this term could cause significant error during the day for short periods.

The horizontal divergence(or advection) of sensible and latent heat will be negligible only if horizontal gradients of temperature, humidity and wind speed are negligible. Above a homogeneous surface, these gradients are insignificant within the surface boundary layer. The depth of this layer is some function of the distance (fetch) from the leading edge (the point where surface characteristics change).

FIGURE I. ENERGY BUDGET OF A CROP-AIR VOLUME (after Suomi and Tanner, 1958)

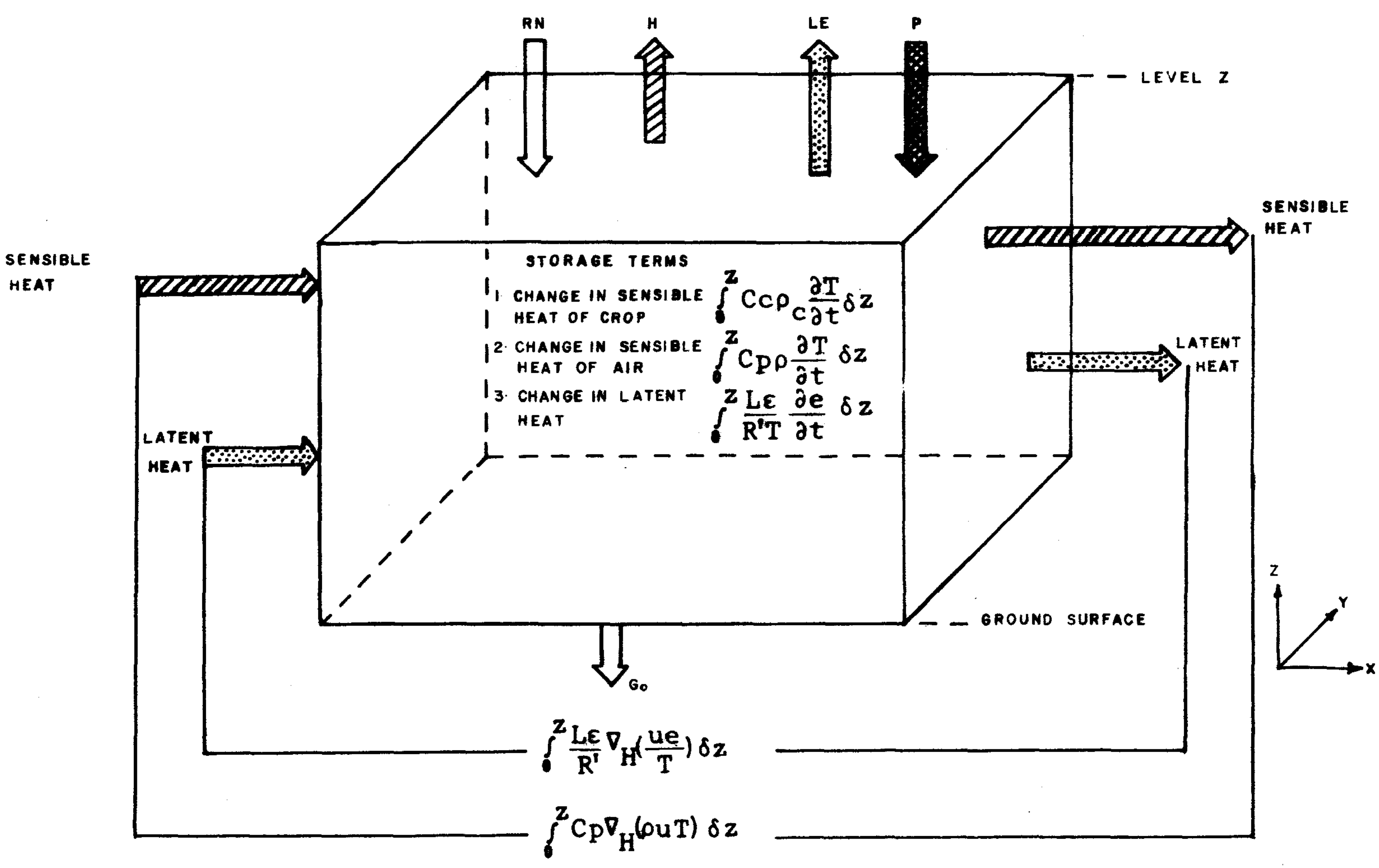

If the depth of the boundary layer is defined as a height: fetch ratio, there is general agreement that the ratio is at least 1:100 (Dyer 1968).

When the site is covered by a tall row crop, the problem is more complex. The wind blows through the roughness elements and is decelerated with distance inward, causing horizontal and vertical divergence of heat (Tanner 1957, and King 1961). The penetration and the intensity of the divergence into a canopy is a function of wind direction. They are greatest when the wind blows parallel to the rows.

It is not known if the same rule applies within a canopy for the minimization of horizontal divergence of sensible and latent heat as above homogeneous surfaces. Most studies of the transfer processes within vegetation have relied on the simplified energy balance equation where only vertical fluxes are assumed to exist.

In this study, it was assumed that horizontal homogeneity existed and that the consumption of energy in photosynthesis was negligible. Therefore, the energy balance for any level z in the canopy above is

$$Rn_z = H_z + LE_z + G_0 \quad , \tag{2}$$

where the values of the parameters are averaged over an hour to satisfy the requirement of steady state conditions. Net radiation and soil heat flux are considered positive when directed downwards, and the sensible and latent heat flux are considered positive when directed upwards.

The total net radiation and surface soil heat flux can be accurately measured (±5%) for any agricultural surface. The partitioning of the remaining energy between sensible and latent heat flux is normally done indirectly because the direct measurement of either requires sophisticated instrumentation employing the eddy correlation equations (Dyer, Hicks and King 1967) or a lysimeter (Angus 1963). The Bowen ratio method (Bowen 1926) is the best available means of accurately determining the total sensible and latent heat fluxes. The Bowen ratio, $\beta = H/LE$, is solved using one-dimensional mass transfer equations for sensible and latent heat:

$$H = -\rho C p K_H \overline{\frac{\partial \theta}{\partial z}} , \tag{3}$$

and

$$LE = -\rho L \frac{\varepsilon}{p} K_W \overline{\frac{\partial e}{\partial z}} . \tag{4}$$

In practice, the temperature and vapour pressure gradients are often replaced with finite difference ratios. If the temperature and vapour pressure differences are measured over the same height interval above the surface,

$$\beta = \gamma \frac{K_H}{K_W} \frac{\overline{\Delta \theta}}{\overline{\Delta e}} , \tag{5}$$

where γ is the psychrometric constant $(\frac{Cp\ p}{L\varepsilon})$. It is further simplified by assuming that $K_H = K_W$. This assumption has been shown to be valid over a wide range of atmospheric stability conditions (Swinbank and Dyer 1967 , Dyer 1967, Webb 1970). The latent and sensible heat fluxes are obtained from equations 2 and 5:

$$LE = \frac{Rn-G}{1 + \beta} , \tag{6}$$

and

$$H = \frac{\beta(Rn-G)}{1 + \beta} . \tag{7}$$

Calculations of LE from equation 6 have shown consistently good agreement with absolute measurements from lysimeters (Tanner 1960, Denmead and McIlroy 1970).

The Bowen ratio method is successful

(i) if energy fluxes are constant between the levels of measurement;

(ii) if the same exchange mechanism transports sensible heat and latent heat;

(iii) if the sources (or sinks) of sensible heat and latent heat are at the same level (Munn 1966).

Within a vegetation canopy, the sources (or sinks) of sensible heat and latent heat are not always at the same levels, and, therefore, the transfer coefficients are not necessarily equal. However, as a working approximation, it is assumed that $K_H = K_W$ within the canopy atmosphere.

There are two approaches to the calculation of LE and H in the canopy atmosphere. First, by assuming that the one-dimensional equations for LE and H adequately describe the energy transfer, equations 3 and 4 can be combined with 2 and solved for K, the apparent transfer coefficient for both LE and H:

$$K_z = \frac{Rn_z - G_0}{-\rho\left(Cp\overline{\frac{\partial\theta}{\partial z}} + L\frac{\varepsilon}{p}\overline{\frac{\partial e}{\partial z}}\right)} \quad . \tag{8}$$

Flux values at any height in a canopy can then be evaluated from equations 3 and 4. Secondly, if it is assumed that the finite difference ratios closely approximate the gradients of temperature and vapour pressure, and if the differences are measured over the same height interval, the latent and sensible heat fluxes can be calculated from equations 6 and 7. The computed values refer to the mid-point of the layer. It is not necessary to first compute a transfer coefficient for the flux determination. From equation 4, the value of the apparent transfer coefficient is given by

$$K_z = \frac{LE_z \,\Delta z}{-\rho L\frac{\varepsilon}{p}\overline{\Delta e}} \quad . \tag{9}$$

Both methods require net radiation, air temperature and humidity at different levels in the canopy and the soil heat flux. In the first method, smoothed temperature and humidity profiles are drawn and the gradients computed graphically for any level. These steps in the analysis are performed subjectively. Brown and Covey (1966) used this method and found that

> "Difficulty arises particularly in determining the location of the zero slopes and the inflection points on the temperature profiles."

This method is capable of success only when the profiles are smooth and when a large number of data points are available. If the profiles are not smooth, then the final shape of the profiles will be unduly influenced by the subjectivity of the researcher.

The second method is much less subjective in this respect. However, compared with the first method, it reveals less detail in the flux profile. Groom (1968) described the use of the first method using smooth profiles drawn through nine data points of temperature and humidity and gradients computed from hand-drawn tangent lines at thirty-three points. If the second method had been employed, only eight points of determination would have been possible. This writer prefers the second method since less subjectivity is introduced into the analysis.

The apparent transfer coefficient evaluated from equation 8 or 9 is a weighted mean value of K_H and K_W. It is not known if or by how much these transfer coefficients diverge from equality at any time, and the method fails to specify any differences which might exist.

B SOURCES AND SINKS

The source or sink strength for net radiation, latent and sensible heat is a measure of the intensity of the flux divergence and, from the principle of the conservation of energy,

$$\frac{\partial H_z}{\partial z} = \frac{\partial Rn_z}{\partial z} - \frac{\partial LE_z}{\partial z} \quad , \tag{10a}$$

where

$$\frac{\partial LE_z}{\partial z} = -\frac{\partial}{\partial z}\left(\rho L \frac{\varepsilon}{p} K_z \overline{\frac{\partial e}{\partial z}}\right) \quad , \tag{10b}$$

and

$$\frac{\partial H_z}{\partial z} = -\frac{\partial}{\partial z}\left(\rho Cp K_z \overline{\frac{\partial \theta}{\partial z}}\right) \quad . \tag{10c}$$

When equations 10b or 10c are positive, they are treated as source strengths. Conversely, when the flux divergence of net radiation is positive, it is treated as a sink strength.

The vertical variation of the sources and sinks of energy in the canopy is a measure of the involvement of the different portions of the vegetation in the energy exchange. It is reasonable to postulate that the normal daytime situation will be characterized by sinks of net radiation throughout the depth of the canopy and the converse for latent heat, because it is extremely unlikely that condensation will occur within the vegetation except early in the morning or late in the evening.

In this study, the relationships summarized in equation 10 were used with finite difference approximations replacing the differential forms.

C NET RADIATION IN THE CANOPY

Net radiation is the most important term in the energy balance since it is usually the largest. The vertical distribution of net radiation in vegetation is poorly understood. Wide use has been made of the assumption that its decrease with depth is approximately exponential and can be described by a modification of Beer's Law. This approximate exponential decrease has been found in vegetation where the biomass is not concentrated in a single thin layer (Munn 1966).

Beer's Law describes the attenuation of monochromatic radiation by a homogeneous medium as

$$I = Io \exp(-k_* m) \quad , \tag{11}$$

where

Io = the initial monochromatic flux,

m = the optical air mass or path length,

I = the monochromatic flux after traversing the path length,

k_* = the extinction coefficient,

$k_* m$ = the optical density.

For use in vegetation, equation 11 has been modified to approximate solar or net radiation attenuation by replacing m with a canopy parameter. Allen et al. (1962) found that the vertical variation of net radiation in corn was adequately described by

$$Rn_z = Rn_h \exp\{-k(h-z)\} \quad , \tag{12}$$

where

Rn_h = net radiation at the canopy top,

Rn_z = net radiation at level z,

h = canopy height,

k = the extinction coefficient.

This model is unlikely to have general application because the predictor (h-z) does not account for important canopy features such as density. A more realistic model was suggested by Uchijima (1962). He used the same exponential framework but replaced (h-z) with the cumulative leaf area index. Thus,

$$Rn_z = Rn_h \exp(-kFc) \quad , \tag{13}$$

where

Fc = downward cumulative leaf area index.[2]

This model has the same form as the one proposed for shortwave radiation depletion in vegetation by Monsi and Saeki (1953). They assumed that crop leaves could be treated as a series of infinitely thin planes all inclined at the same angle to the horizontal. Anderson (1966) showed that the extinction coefficient for direct beam shortwave radiation depends on this angle and the angle that the beam makes with the horizontal. Since the direct shortwave radiation is the principal component in the net radiation during cloudless conditions, it is reasonable to postulate that the extinction coefficient for net radiation will also be dependent on these angles. However, the extinction coefficient

---

[2]The leaf area index is defined as the ratio of the area of leaves (one side) to unit area of ground, and it is a measure of canopy density.

for net radiation is usually assumed to be constant or to have a small diurnal variation from 0.5 to 0.6. Impens and Lemeur (1969) showed a diurnal trend in the extinction coefficient but did not attempt an explanation. On the other hand, Brown and Covey (1966) found no significant diurnal variation in the extinction coefficient. Using daily mean data, they found that the decrease with depth of the relative intensity of net radiation (Rn_z/Rn_h) departed from an exponential decay and showed an overestimation of Rn towards the top of the canopy and an underestimation towards the base. A similar finding was reported by Allen, Yocum and Lemon (1964). Impens and Lemeur (1969) modified the exponent in equation 13 to account for this departure:

$$Rn_z = Rn_h \exp(-k_1Fc + k_2Fc^2). \tag{14}$$

In energy balance studies where hourly average values of net radiation are required, it cannot be assumed that an exponential model employing a constant extinction coefficient will suffice. Therefore, an understanding of the variables contributing to the variation in the extinction coefficient is necessary. It is hoped that the data from this study of canopy net radiation will contribute to this understanding.

CHAPTER 3

DATA COLLECTION AND ANALYSIS

A EXPERIMENTAL SITE

The study was conducted at the Simcoe Horticultural Experiment Station, Simcoe, Ontario. The experimental site was a 2.2 hectare field (200 X 110 metres). It was flat, with no slope greater than 2°. To the east and south, it was bounded by low-growing field crops for distances of at least 500 metres. A gravel road and railway cutting defined the western and northern boundaries.

The crop was sown in N.W.-S.E. rows, 1 metre apart, with an average planting density of 4.7 plants per square metre. The crop reached maturity at the end of July, at a maximum height of 186 centimetres. A growth curve of the crop is shown in Figure 2.

B DATA COLLECTION

The following parameters were measured during the experiment:

(i) net radiation above and within the canopy;

(ii) dry-bulb and wet-bulb temperature at five

FIGURE 2. GROWTH CURVE OF CORN (SIMCOE, 1969)

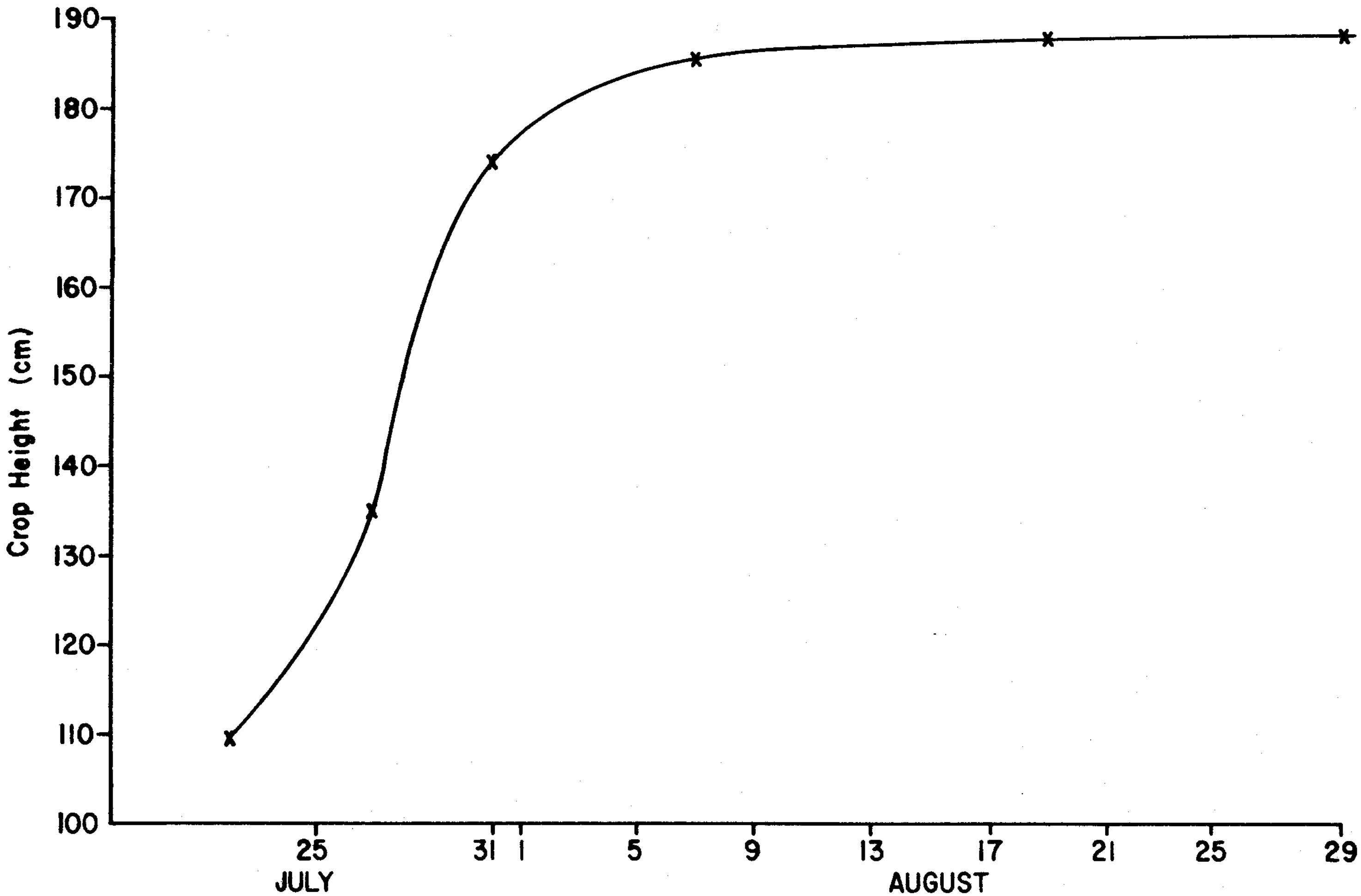

levels in the canopy and at three levels above the canopy;

(iii) soil heat flux;

(iv) wind speed and wind direction above the canopy;

(v) leaf area index.

The instrumental array for measuring parameters (i) to (iv) was positioned close to the eastern edge of the experimental site (see Figure 3). This position was chosen to maximize the fetch from the prevailing wind direction (S.W.). The variation of fetch in relation to the instrumental array is shown in Figure 4. The data were collected between July 26 and August 29 during selected runs. A summary of the measurement schedule of energy balance data is shown in Table 1. The duration and frequency of runs was determined mainly by weather conditions with wind direction the most important criterion. Most runs were made with winds from the S.S.W. and W. No data collection was started during east winds. On some occasions, the wind direction was favourable for adequate fetch for most of a run, with some periods with unfavourable wind direction. These periods will be discussed during the examination of the results.

The leaf area index of the crop was determined on July 26, August 1, 7 and 13.

FIGURE 3. EXPERIMENTAL SITE

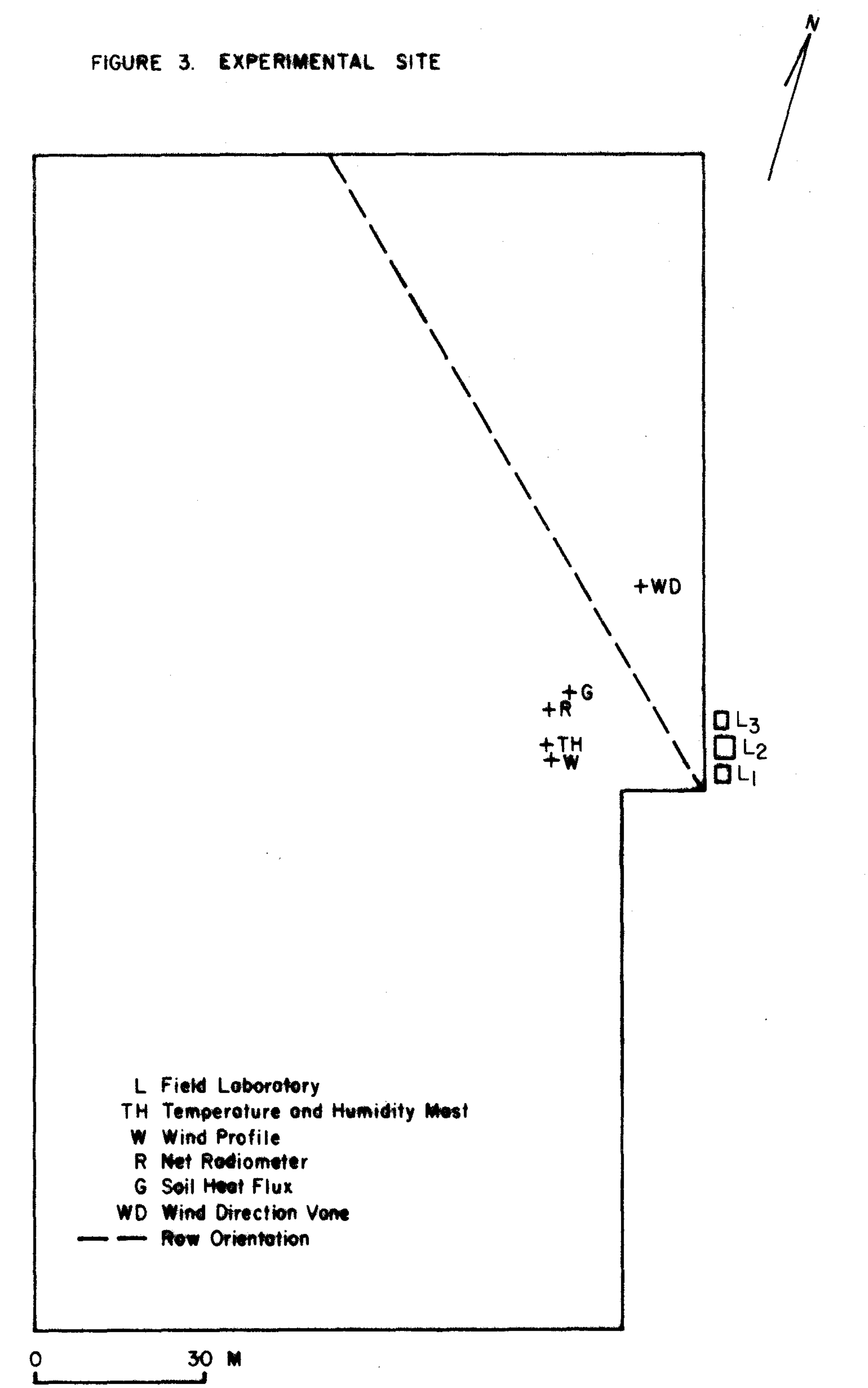

FIGURE 4. VARIATION OF FETCH ON EXPERIMENTAL SITE

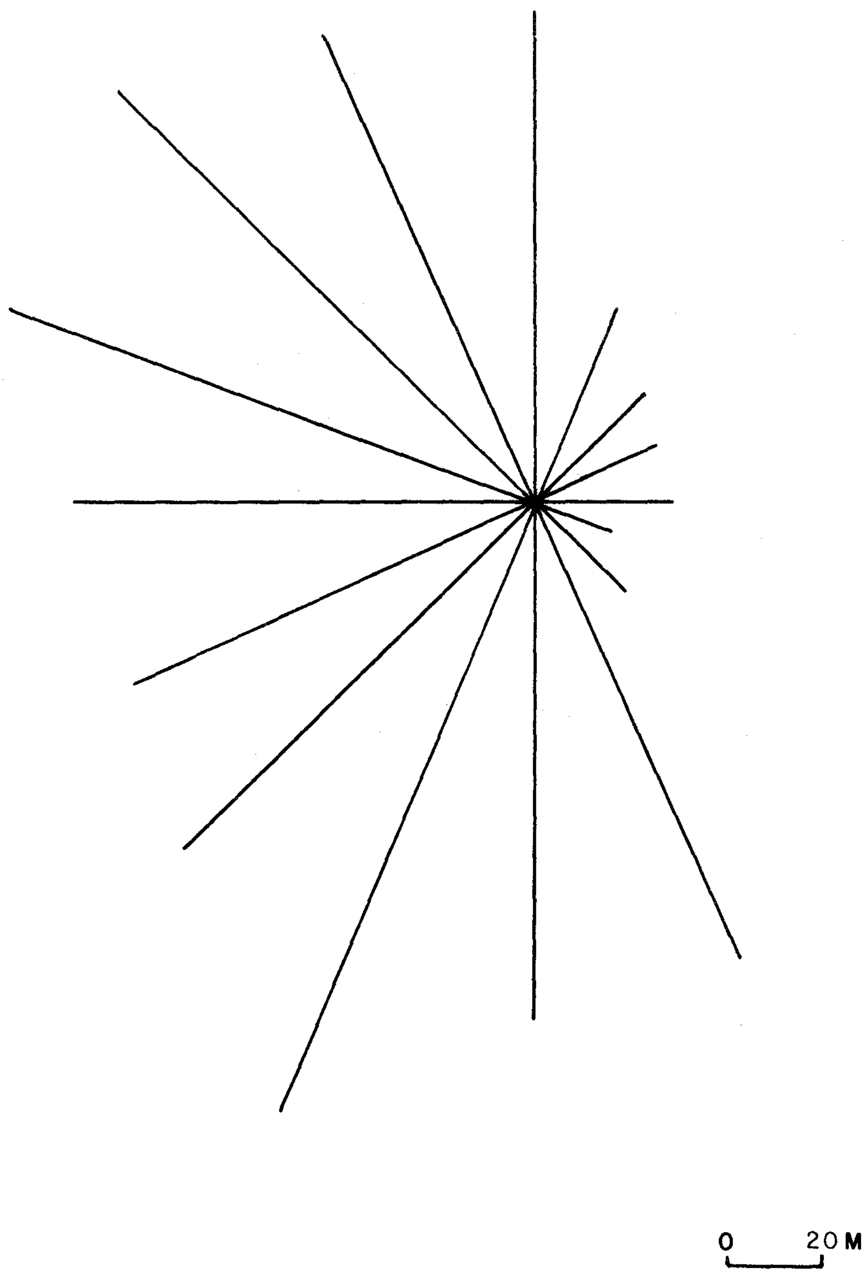

TABLE 1

DATA COLLECTION SUMMARY

Run No.	Date	Duration E.S.T.	T.	H.	W.	S.	Rn_1	Rn_2	Rn_3
1	July 26	0700-1100 1300-1700	X	X	X	X	X		
2	30	0800-1500	X	X	X	X	X		
3	31	0700-1200	X	X	X	X	X		
4	Aug. 1	0700-1700	X	X	X	X	X	X(2)[3]	
5	3	0700-1500	X	X	X	X	X	X(1)	
6	5	0700-1600	X	X	X	X	X		
7	6	0900-2100	X	X	X	X	X	X(6)	
8	7	0700-1400	X	X	X	X	X	X(3)	
9	8	0700-2000	X	X	X	X	X	X(7)	
10	10	0800-2000	X	X	X	X	X	X(5)	
11	11	0600-2000	X	X	X	X	X	X(2)	
12	12	0700-1800	X	X	X	X	X		
13	13	0700-2000	X	X	X	X	X		X
14	14	0700-1800					X		X
15	20	0800-1800					X		X
16	21	0700-1800					X		X
17	22-23	0600-0800	X	X	X	X	X		X
18	23	0800-1900					X		X
19	24	0700-1800					X		X
20	25	0800-1700					X		X
21	26	0700-1700					X		X
22	27	0700-1800	X	X	X	X	X		X
23	28-29	0800-1900	X	X	X	X	X		X

T = Temperature Profile Data

H = Humidity Profile Data

W = Wind Profile Data

S = Soil Heat Flux

Rn_1 = Rn above canopy; Rn_2 = Rn within canopy (periodic samples)

Rn_3 = Rn within canopy (continuous)

[3]Number in parentheses indicates number of samples.

C INSTRUMENTATION

1. Temperature and Humidity

Dry-bulb temperature was determined using five-junction thermopiles to measure the dry-bulb temperature difference (ΔT) between successive levels, and a single thermocouple at the lowest level to give an absolute temperature. The vapour pressure at each level was determined by the psychrometric method, with the additional measurement of wet-bulb depression (D), using a five-junction thermopile. A single thermocouple was incorporated into each D-thermopile to ensure a record of dry-bulb temperature if any of the ΔT-thermopiles failed.

(a) Thermopile and thermocouple construction. All thermopiles were made from 36 a.w.g. copper/constantan wire (Thermo Electric (Canada) Ltd.). Each thermojunction consisted of a copper and a constantan wire twisted together and soldered with low thermal e.m.f. solder. In addition, each junction was dipped in polyester resin which electrically insulated it without significantly increasing its bulk.

The thermopile wires were mounted in two stainless steel tubes, and each set of five sensing elements was encased in thin-walled (0.025 cm), aluminum tubes. The exposed wires at the ends of the steel tubes were encased in polyvinyl chloride (PVC) tubing and the joins sealed with epoxy resin. The aluminum tips were filled with polyester resin to provide rigidity.

(b) Thermopile and thermocouple calibration. A calibration bath was constructed by mounting two thermos bottles filled with oil in a styrofoam box and packing mica chips around them to provide thermal insulation. The temperature of one reference bottle was allowed to equalize with room temperature, while the temperature of the other bottle was raised in steps by inserting a heated copper rod. The absolute temperature of each bottle was monitored by a precision platinum resistance thermometer (Rosemount Eng. Co.) to an accuracy of ±0.01C.

The calibration for one thermopile was determined over a range of 7C. The thermopile was reversed several times during the calibration, and its sensitivity was symmetrical. It was found that the calibration was linear and was described by the equation,

$$\Delta T(C) = 0.009 + 4.9131 \text{ (mv output)}. \quad (15)$$

The correlation coefficient (r) is 0.99, and the standard error (Sy) is 0.007(C). All other thermopiles were compared with the standard thermopile. All were symmetrical and conformed to the established calibration.

A sample thermocouple for calibration was chosen from the batch of sensors. It was necessary to replace the oil with water in the calibration bath because the temperature range required could not be established with oil. In this experiment, the temperature in the reference thermos bottle was maintained close to 0C with an ice-water mixture. The calibration, performed over a range of 34C, was non-linear and was fitted by the equation,

$$\Delta T(C) = \frac{\text{mv output}}{0.03730 + 0.00162\ (\text{mv output})},$$

$$r = 0.95;\ Sy = 0.05(C). \tag{16}$$

The calibration data for both the thermopiles and thermocouples are shown in Figure 5.

At the end of the field season, the calibration of one thermopile was checked with the same equipment, and there had been no change in the interim.

(c) Thermopile time constant. The time constant of any sensor is the time required for the sensor to respond to 63.2% of a discrete change in the parameter being measured. For a temperature sensor, it depends on instrument size and aspiration rate. Munn (1966) recommended a time constant of at least one minute for meaningful average temperature profiles. Although the time constant of the

FIGURE 5. THERMOCOUPLE & THERMOPILE CALIBRATIONS

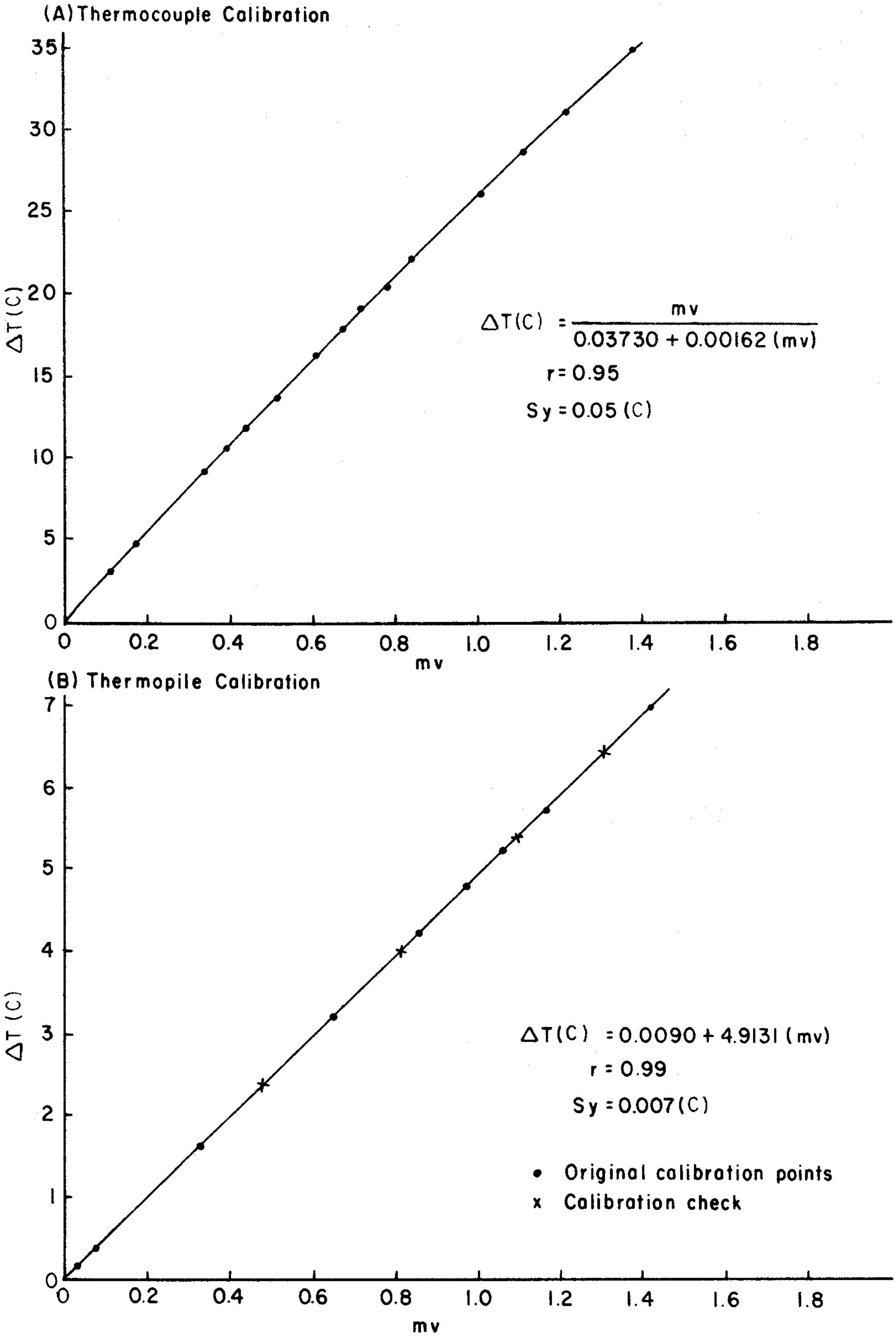

thermopiles used in this study was not measured, it was found, in a previous experiment, that the average time constant of a Rosemount resistance thermometer was one minute when ventilated at 3m sec^{-1}. Since the sizes of a thermopile and a resistance sensor are approximately equal, the time constants should be approximately equal under the same ventilation velocity. Therefore, a time constant of one minute was assigned to the thermopiles. Confirmation that this figure is of the proper magnitude was provided when tests on similar thermopiles were performed later (Munro, personal communication).

(d) Radiation shielding and aspiration. When large sensors are used for measuring air temperature, it is necessary to shield them from direct solar radiation and to aspirate them to ensure representative measurements (Tanner 1963).

Radiation shields were constructed by encasing plastic tubes in 1 cm-thick cylinders of styrofoam. The cylinders were made by pouring liquid styrofoam into cardboard moulds fitted around each tube. Each shield was wrapped with silver-backed polyester film tape which has a high reflectivity for shortwave radiation and a high emissivity (Fuchs and Tanner 1965). Since styrofoam is a poor heat conductor, radiant heating of the sensor is minimized.

Each radiation shield was fitted into a PVC pipe tee and the sensor inserted, through a rubber stopper, into the tube from the other end of the tee. The rubber stopper provided a rigid holder for the sensor.

The ΔT- and D- thermopiles were mounted in separate housings (see Figure 6). All housings were aspirated at the recommended rate of 3m sec^{-1} (Middleton and Spilhaus 1956, Wylie 1962). Aspiration of both sets of housings was achieved with identical systems. Each consisted of a vacuum motor mounted at the end of a plastic box (0.06 m^3 capacity) with plastic garden hose running from each housing to an intake on the end of the box opposite the vacuum motor. The box acted as a volume controlling device and ensured equal aspiration of all housings.

The two complete aspiration systems were tested in the laboratory before field installation, and the flow-rate on each line was measured. All aspiration rates were within 2% of an average value of 3.2 m sec^{-1}.

(e) Wet-bulb depression and water feed. The wet-bulb sensor was mounted 2½ cm behind the dry-bulb sensor in the radiation shield ensuring that the evaporation of water from the wet-bulb did not influence the dry-bulb. The wet-bulb was kept moist by a continuous supply of distilled water from a reservoir mounted at the outside of the radiation shield. The water was conducted from the reservoir to the wet-bulb, by a muslin wick, under a combination of capillary

FIGURE 6. DETAILS OF TEMPERATURE AND HUMIDITY SENSOR UNITS

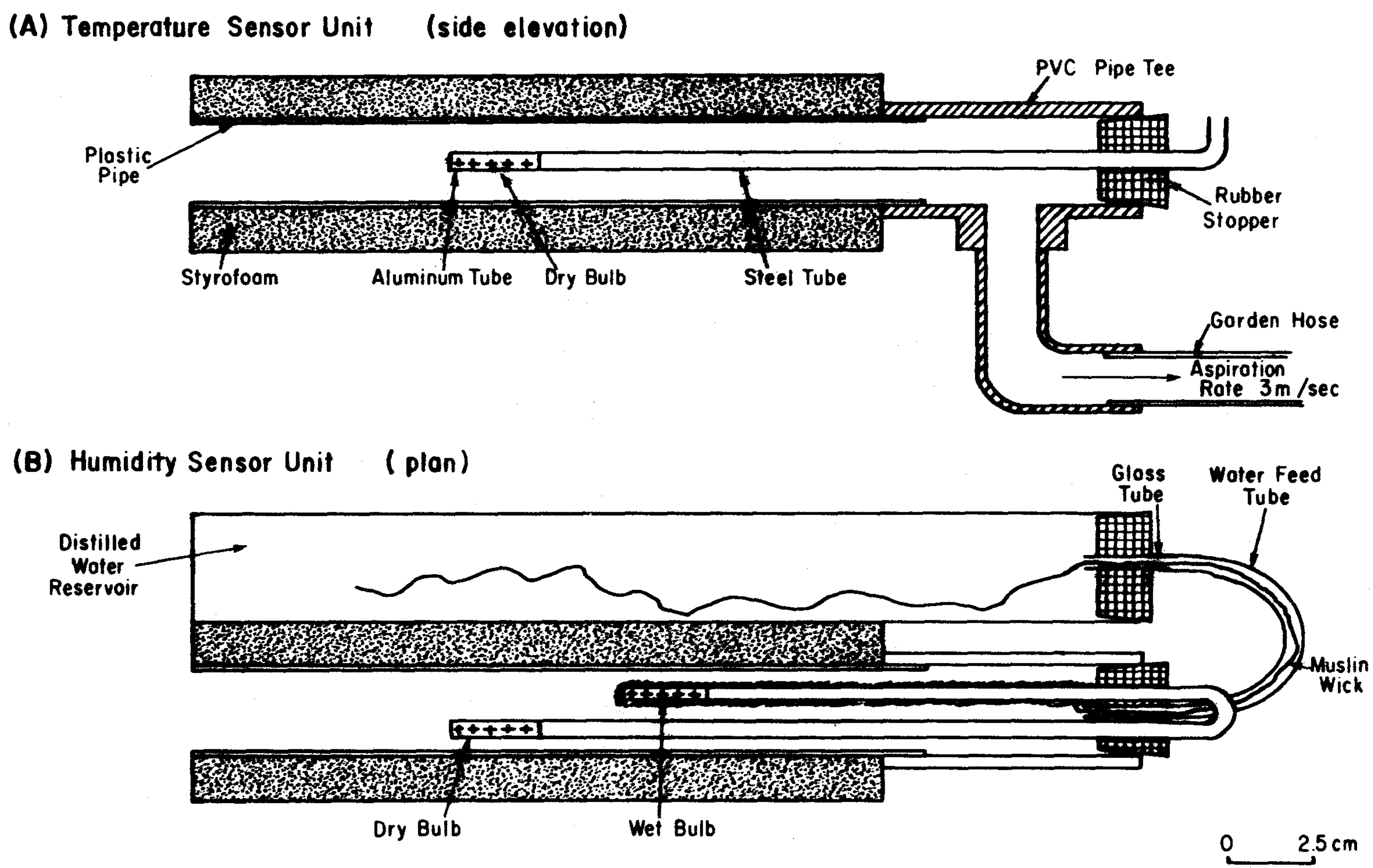

and gravity feed. The wick was threaded over the wet-bulb and ran along the steel tube for a distance of 11 cm before passing through a glass tube inserted through the rubber stopper and into a clear plastic tube to the reservoir (see Figure 6b). The wet-bulb was also wrapped with "Kleenex" tissue to further ensure an even distribution of water (Collins 1963)

The water reservoir was made from clear plastic tubing which was wrapped in silver-backed polyester film tape to minimize radiative heating of the water. However, it is probable that the water in the reservoir was above ambient air temperature, and therefore, a temperature gradient was expected along the wick inside the radiation shield. Lourence (1967), using a ceramic cup to conduct the water to the wet-bulb, found that it was necessary to expose the ceramic cup to the air stream in the housing for a distance of 10 cm behind the sensor before the temperature gradient was dissipated. In this experiment, the wick was exposed to the air stream inside the housing for a distance of 11 cm before reaching the sensor, and therefore, no unrepresentative wet-bulb temperature measurements are anticipated from this possible source of error.

(f) Evaluation of temperature sampling system. The measurement of properties of the air within a vegetation canopy requires special efforts to obtain representative spatial samples. In general, there are three ways to obtain good spatial samples:

i) by placing a large number of sensors in every horizontal plane of measurement;

ii) by drawing the air through perforated tubes placed across several rows and conducting it to an instrument for analysis;

iii) by moving a sensor in space and averaging continuously the output signal.

In order to overcome the sampling problem and the associated problem with the use of aspirated sensors, the writer attached a plastic tube, 1.5 m long, to the end of each sensor housing for use in the canopy space. Each tube was wrapped with silver-backed polyester film tape, and a series of small holes was bored on each side in the horizontal plane. The total area of the intake holes was equal to the cross-sectional area of the intake of the sensor housing. This conserved the aspiration rate of 3 m sec^{-1} past the sensors, but the flow rate of air through each small hole was only 0.15 m sec^{-1}.

The housings were tested for radiation error before installation in the canopy. A standard above-canopy housing was exposed horizontally, 1 m above a grass surface to a high radiation load on a clear, sunny day. An aspirated, dry, wet-bulb depression thermopile was installed and allowed to come to equilibrium. The absolute temperature was measured. The minimum detectable change in temperature was 0.01C.

There was a zero wet-bulb depression indicating the absence of any temperature gradient in the housing. There was no detectable change in temperature in the housing when the air intake was pointed directly at the sun. When the unit was shaded from direct solar radiation, there was no detectable change in temperature. It was concluded that the radiation shielding was satisfactory. This standard unit was then placed alongside a canopy sampling unit, and the temperatures in the housings were allowed to come to equilibrium. A systematic radiation error was present in the canopy sensor unit. The average absolute magnitude of the error was 1.5C. A hemispherical radiation shield was attached to the upper surface of the long sampling tube but did not reduce the error significantly. Thus, it was concluded that the long tubes could not be used, and they were removed. This means that the sampling of temperature and humidity in the canopy was not as satisfactory as originally envisioned. However, the writer is confident that there was no large radiation error present in any unit of the system. Also, since the canopy was very dense during the experiment, it is probable that the sampling problem was less severe than in more open stands of vegetation.

(g) Field installation. Two four-metre masts were erected side by side in a corn row. The temperature and humidity housings were attached to the masts in pairs so that five were within the canopy space and three in the atmosphere above. The air intakes to the two housings at each level were positioned only 5 cm apart to ensure that the temperature and humidity of the same air sample was measured.

The aspiration hoses from each level extended to a third mast which had been placed three corn rows distant and, from there, to the intake ports on the aspiration boxes. Each hose was attached to the third mast by tee-junction fittings, thus preventing undue sagging which could have resulted in a reduced aspiration rate past the sensors.

All reference junctions for the thermocouples in the array were encapsulated in a single plug which was placed in a covered styrofoam box containing an ice-water mixture. The latter was placed into a larger covered styrofoam box filled with mica chips for insulation. The complete reference temperature unit was buried flush with the surface of the ground, two metres from the base of the instrument masts. The temperature of the ice-water mixture was monitored continuously using a platinum resistance bulb. The field placement of the dry-bulb temperature profile system is shown schematically in Figure 7.

FIGURE 7. SCHEMATIC TEMPERATURE PROFILE SAMPLING ARRAY

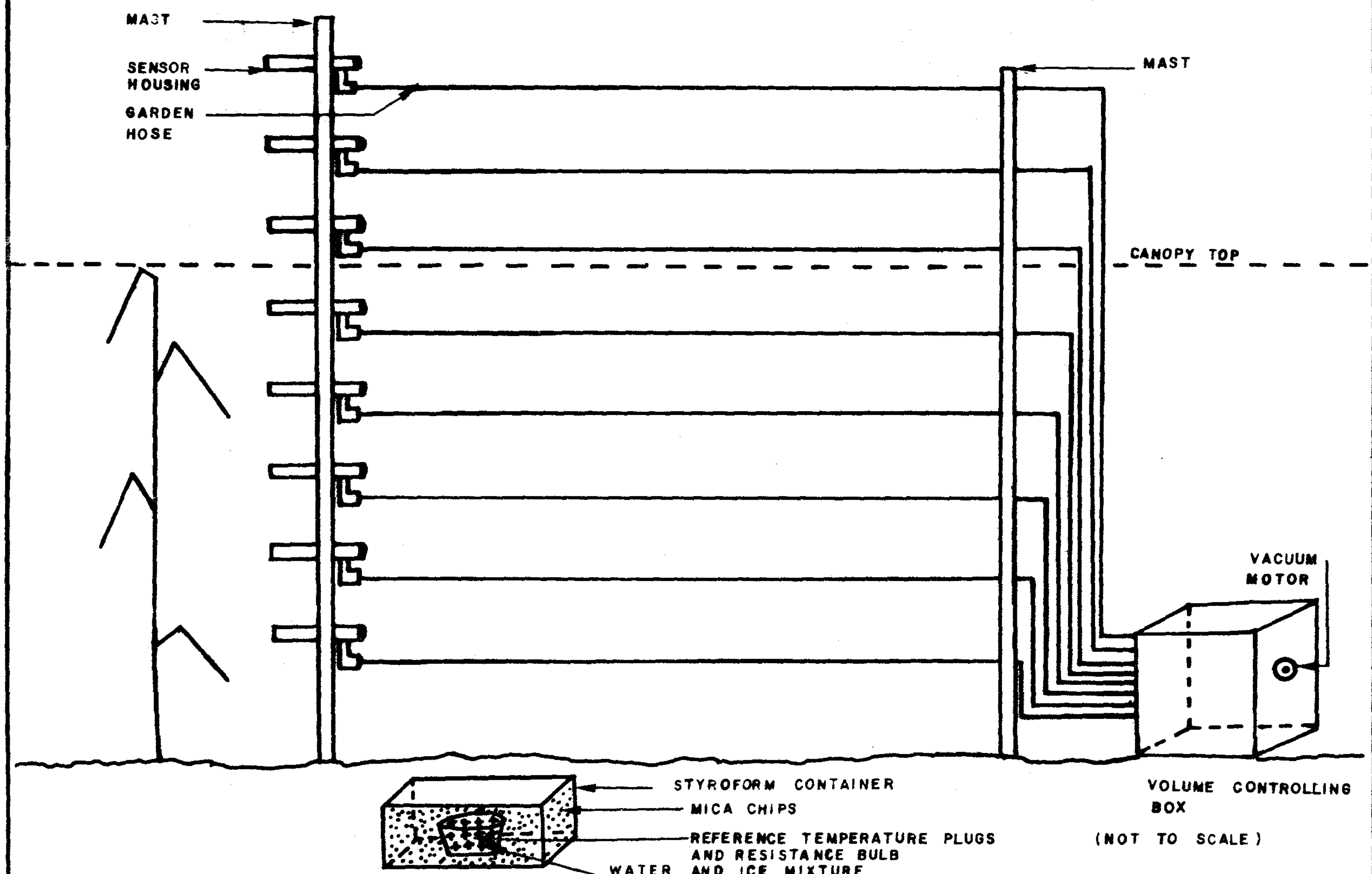

2. Net Radiation

(a) Net radiation above the canopy. Net radiation was measured with a Swissteco (model SS1) net radiometer (Funk 1959) mounted at 1 m above the canopy. Its protective polyethylene domes were inflated and purged continuously by nitrogen during the early part of the study. Later, nitrogen was replaced by dry air obtained by passing air from an aquarium pump through a container of silica gel. The latter method is preferred for routine field use since it is much more compact and easy to maintain.

The radiometer calibration was provided by the National Radiation Laboratory of the Atmospheric Environment Service.

The longwave and shortwave calibration constants were equal, and the symmetry (top/bottom) was 0.981.

Moisture accumulation on the domes, due to rain or dew, was removed before each run. Domes were changed at least once a week.

(b) Net radiation within the canopy. The measurement of net radiation within the canopy is a difficult problem since radiation intensity varies horizontally because of the horizontal heterogeneity in the vegetation. Tanner et al. (1960), Denmead, Fritschen and Shaw (1962), and Impens and Lemeur (1969) used arrays of net radiometers arranged spatially at the levels of measurement to attempt to define a representative average value. The number of stationary sensors required to give a meaningful average value varies with the position in the canopy and from crop to crop. In general, the radiation intensity shows maximum variability in the uppermost position of a canopy. Impens, Lemeur and Moermans (1970) concluded that, for some crops, at least 100 sensors would be necessary at the uppermost measurement level (2/3 canopy height) to determine 12-hour totals of net radiation within 10% at the 95% confidence level.

Linear net radiometers seem to be more suitable because they have been designed specifically for use in vegetation (Monteith, Szeicz and Dos Santos 1964, Denmead 1967).

In this study, three 53 cm-long linear net radiometers (Swissteco Mfg. Co.) were used. These were mounted in a vertical profile within a representative stand of corn close to the above-canopy net radiometer. Anderson (1969) has emphasized that, when using linear radiometers in row crops, one must sample row and inter-row spaces. Since the rows were 1 metre apart, it was not possible to sample a complete row and inter-row space. Instead, each sensor was positioned so that one end was almost touching a row of corn and projected into the centre of the inter-row space without actually passing through a corn row. It was felt that this was the best position considering the generally erect nature of the corn leaves.

All the linear sensors were purged with dry air using aquarium pumps and silica gel. The high humidity in the canopy made it difficult to keep the sensors dry, and the silica gel dessicant had to be changed daily.

The sensors arrived uncalibrated after the experiment had begun, and there was insufficient time to perform a satisfactory calibration in the field. The sensors were mounted at 20, 80 and 120 cm in the canopy. Continuous measurements began on the afternoon of August 13.

Prior to the arrival of the linear sensors, an attempt was made to define the form of the net radiation profile using a standard radiometer as a moving probe. A small mast was erected in a corn row, and clamps attached to it acted as supports for the hand-held instrument. The radiometer was moved across the row, and a minimum of five samples were taken at each level. The output was read on a portable potentiometer. A complete profile was sampled in ten minutes. The main problems with this method were

(i) that it was difficult to keep the instrument level;

(ii) that the measurements at all levels were not simultaneous;

(iii) that at least two people were required.

(c) Calibration of linear net radiometers. In June, 1970, the linear sensors were calibrated against a standard net radiometer (Swissteco, Type SS1) of known calibration. All the instruments were exposed at a height of one metre on a flat roof. Each linear sensor was oriented with the long axis facing east-west. During the period of calibration, the sky was cloudless and the radiation intensity very steady. The output of all sensors was sampled every minute by a Solartron data logging system, and 30-minute average values were computed. The variation in the relative sensitivity of the linear sensors is shown in Figure 8. The data were weighted by the radiation intensity. This procedure biases the calibration towards the value around solar noon. The variation in the sensor calibrations was small. Linear No. 3 showed the maximum variation, ±3.5%.

Anderson (1969) stated that the sensitivity of linear radiometers is azimuth dependent. Also, the sensitivity is likely to decrease with high zenith angles[5] because of reflection of direct beam radiation from the tubes. No systematic trend was apparent in the sensitivity of the linear sensors as a function of azimuth or zenith angle. The maximum value of zenith angle during the experiment was 50°, and the azimuth angle varied through 140°. Therefore, if the instruments are sensitive to either azimuth or zenith angle, the dependence is slight and will only be apparent when the zenith angle approaches 90°, and the azimuth angle exceeds 70°. Both of these conditions occur near sunrise and sunset when the radiation intensity is very low, and, therefore,

[5] Zenith angle is defined as the angle between the zenith line and a ray striking the surface.

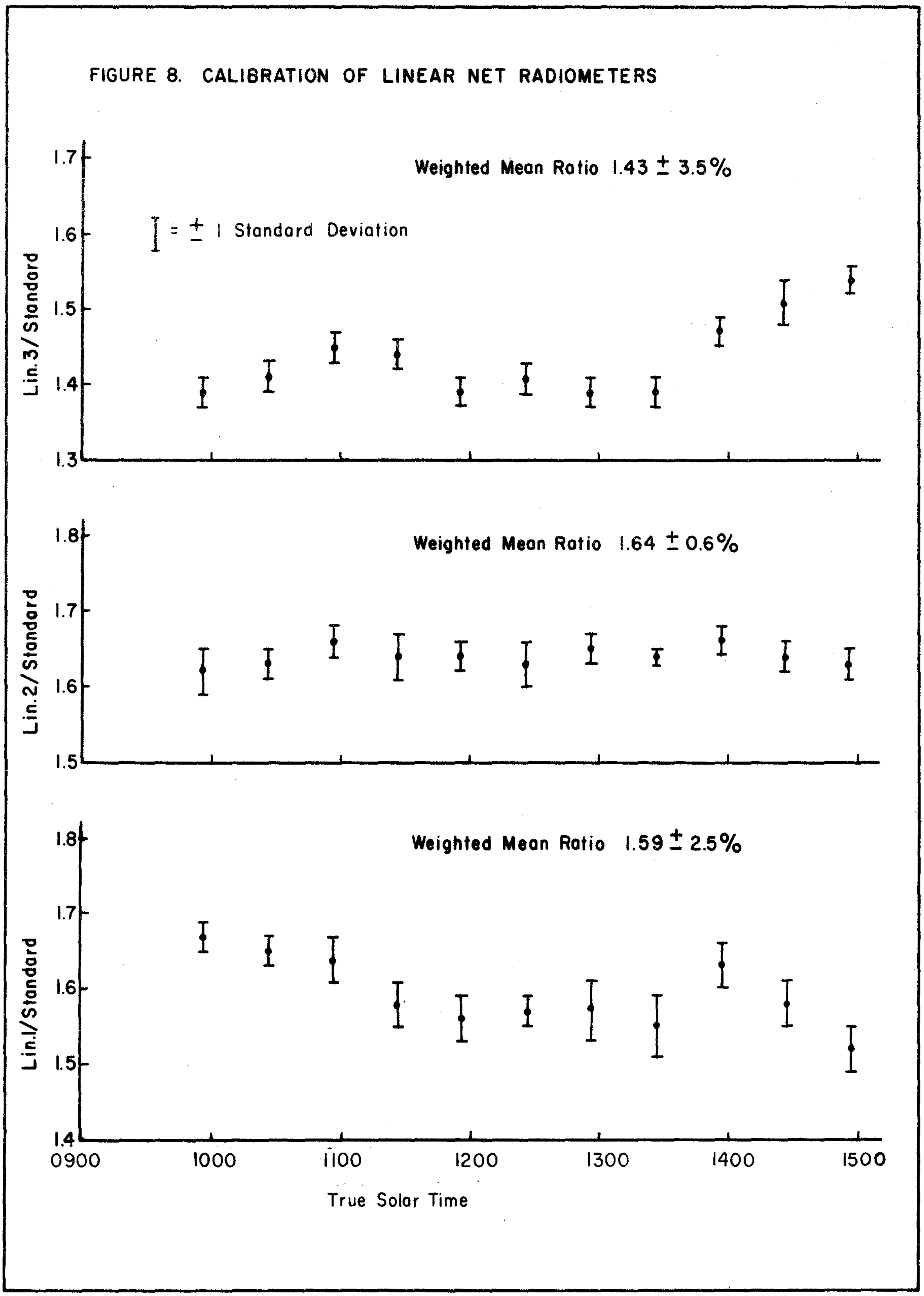
FIGURE 8. CALIBRATION OF LINEAR NET RADIOMETERS
Weighted Mean Ratio 1.43 ± 3.5%
= ± 1 Standard Deviation
Lin. 3/ Standard
1.7
1.6
1.5
1.4
1.3
Weighted Mean Ratio 1.64 ± 0.6%
Lin. 2/ Standard
1.8
1.7
1.6
1.5
Weighted Mean Ratio 1.59 ± 2.5%
Lin. 1/ Standard
1.8
1.7
1.6
1.5
1.4
0900
1000
1100
1200
1300
1400
1500
True Solar Time

the other terms of the energy balance are small.

3. Soil Heat Flux

The soil heat flux at the surface is given by

$$G_0 = -\lambda \left(\frac{\partial Ts}{\partial z}\right)_0 \quad , \tag{17}$$

where

λ = the thermal conductivity of the soil,

Ts = the soil temperature.

This relationship is difficult to use because the temperature gradient at the surface cannot be easily measured, and the thermal conductivity of soil is highly variable. The problem is circumvented by measuring the flux with several heat flux plates placed as near the surface as possible. They cannot be placed right at the surface because they can impede moisture movement in the soil, thereby creating an unrepresentative local condition. They should be buried at a depth of several centimetres where the flux is small, and a large fractional error in measurement can be tolerated. However, this can cause serious error in the surface flux if there is significant flux divergence between the plates and the surface (Van Wijk 1965, Fuchs and Tanner 1968). The most reliable estimate of the surface flux is found by measuring the flux at a depth (z) of at least 5 cm and the flux divergence. Thus,

$$G_0 = G_z + Cs\frac{\Delta\overline{Ts}}{\Delta t}z \quad , \tag{18}$$

where $\Delta\overline{Ts}/\Delta t$ is the change per unit time of the average temperature of the layer from the soil surface to depth z, and Cs is the heat capacity of the soil. This was the method adopted in this experiment.

The heat capacity is

$$Cs = CmXm + CoXo + CwXw + CaXa \quad , \tag{19}$$

in which Cm, Co, Cw and Ca are the heat capacities of the mineral and organic matter, water and air respectively, and Xm, Xo, Xw and Xa are the corresponding volume fractions. The heat capacity of air is negligible compared to the others, and it was assumed to be zero. Average values of 0.46 and 0.60 for Cm and Co (De Vries 1963) were adopted. The volume fractions of mineral and organic matter of the soil (Caledon fine sandy loam) were assumed constant for the experimental period, and the average value of each was found from laboratory analysis on five soil samples. The values found were Xm = 0.459 and Xo = 0.024.

The soil heat flux at a depth of 5 cm was measured with three heat flux plates (Middleton Pty.) connected in series. Each plate was mounted on a rigid wire frame to ensure that it remained parallel to the soil surface. Two of the plates were placed under adjacent corn rows with the third in the centre of the inter-row space.

The average temperature of the soil layer above the plates was measured by a five-junction thermopile referenced to a plug at a depth of two metres. The plug consisted of a 10 cm-long aluminum tube (0.06 cm wall), filled with polyester resin to seal the junctions from moisture and to provide rigidity. The temperature of the plug was measured by a single thermocouple referenced to an ice-water bath. The thermo-junctions, mounted on wooden dowels (1.9 cm diameter) were at depths of 0.5, 1.5, 2.5, 3.5 and 5.0 cm. 15 cm of thermocouple wire were wrapped around each rod at the measurement depth to prevent heat conduction down the wire to the sensor. The rods were arranged around the heat flux plates to provide a spatial sample. The thermo-junctions at 0.5 cm and 1.5 cm were placed under a row, those at 2.5 cm and 3.5 cm under the adjacent row, and the one at 5.0 cm was positioned in the centre of the inter-row space.

The average soil moisture content of the top 5 cm layer of soil was determined once a day by gravimetric analysis of ten samples.

4. Leaf Area Index

The leaf area index (L.A.I.) is a measure of the density of the canopy. It is calculated from the mean area of leaves per plant and the plant density. In this experiment, the L.A.I. was determined on a stratified basis, the depth of each stratum being determined by the position of the temperature sensors in the canopy. The leaf area density distribution was computed from the leaf area index data by dividing each stratum L.A.I. value by the depth of the stratum. The leaf area density is defined as the total area of leaves per unit volume of space. The plant density was determined at the net radiation and the temperature sites from a plant count in two, eight square metre plots. It was found to be 4.9 plants m^{-2} at the net radiation site and 4.5 plants m^{-2} at the temperature and humidity site.

Two methods were used to calculate the leaf area:

(i) by a relationship between leaf weight and leaf area;

(ii) by planimetering leaf tracings.

The first method was used for the initial determination. Each of five plants was sampled at random from a remote location in the field and taken immediately to the laboratory where it was sectioned into the required strata. Every leaf was weighed, ten punch samples of known area were taken and their weights recorded. The leaf area (A) was calculated using the equation,

$$A = \frac{W \ X \ DA}{DW} \quad , \tag{20}$$

where

W = leaf weight,

DA = disc area,

DW = disc weight.

On one plant, the area was also computed by the second method, and the results agreed to within 5%.

The first method was found to be too laborious, and thus, the second method was employed for the remainder of the experiment. The latter method was relatively quick; it was possible to analyze one plant per hour. For the determinations on July 31 and August 7, six plants were sampled.

The L.A.I. of the crop reached a maximum value of 5.6. This was very high for corn and was due to the presence of a large number of tillers. There was an average of three tillers per plant in the sample plots. In some cases, the tillers were two-thirds the height of the main plant.

5. Recording and Data Reduction

The signals were recorded on a variety of strip-chart recorders housed in an air-conditioned field laboratory. All sensors were connected to recorders by shielded cable, and all signal cables were grounded to a copper rod near the recorders.

The net radiation above the canopy and the soil heat flux were recorded continuously on a Honeywell two-pen recorder (Model 194), while the signals from the linear sensors were recorded continuously on three TOA polyrecorders

(Model EPR-2T). Integrated hourly totals were found by planimetry.

Wind speeds were recorded with anemometers and counters (C.W. Thornthwaite Associates) which were read every half-hour.

The dry-bulb temperature differences were recorded sequentially, every two minutes, by means of a 12-channel stepping switch and a second two-pen Honeywell recorder (Model 194). All other temperatures, except the soil temperature reference for the soil heat flux array, were recorded every thirty-six seconds on an Esterline-Angus, 24-point recorder (Model E1124E). The soil reference temperature was sampled once during each run after it had been established at the beginning of the experiment that it showed no diurnal variation.

Thirty samples per hour of dry-bulb temperature differences, dry-bulb temperatures and wet-bulb depressions were read from the charts. The individual millivolt signals were converted to temperature readings and hourly average values computed. The vapour pressure (e) for each sample was calculated using the psychrometric equation,

$$e = e_s(Tw) - \gamma D \quad , \tag{21}$$

where

e_s = saturation vapour pressure,

Tw = wet-bulb temperature,

D = wet-bulb depression,

γ = psychrometric constant,

and the hourly average value was computed. The saturation vapour pressure was calculated using the equation,

$$e_s(Tw) = \alpha \exp \{\beta' Tw/(Tw + \gamma')\} \quad , \qquad (22)$$

where

$$\alpha = 6.1078$$

$$\beta' = 17.269$$

$$\gamma' = 237.3$$

This equation was developed by Tetens (1930) and transformed to its present form by Murray (1967). It gives values of saturation vapour pressure within 0.02% of values from the accepted standard equation relating e_s and Tw due to Goff and Gratch (1946). The vapour pressure was calculated in two ways: first, by using ΔT data to obtain dry-bulb temperature (T) and secondly, by using the direct measurements of T.

The ΔT data from above the canopy were extremely erratic and seldom steady over any one-hourly period. This was attributed to the difficulty in recording the extremely small signals which were often no larger than 5 microvolts. These data were not used in the analysis. In contrast, the temperature differences from measurements of absolute temperature at each level above the canopy were very steady over the sample periods as were the vapour pressure differences, and, therefore, those data were used in the computation of the energy balance components.

During the data reduction from the charts, any spurious wet-bulb depression data were discarded. The most likely cause was accidental drying out of a wet-bulb.

The temperature and humidity data for the period from August 1 to August 13 were selected for analysis. The principal reason for this choice was that, after August 20, the crop degenerated rapidly from maturity to senescence and was assailed by a fungus infection, *Ustilago zeae*.

D ERROR ANALYSIS

The absolute and relative errors in each independent temperature measurement have been assessed and combined to show errors in calculated vapour pressures. These were then combined with the errors in Rn and G to estimate the errors in LE, H and K.

1. Error in Temperature and Humidity Measurement

The two main errors in temperature measurement are the calibration and recorder errors. Other errors, due to thermal radiational heating of the sensor, and inadequate sampling in the environment could not be assessed.

(a) Temperature. The general reduction equation for dry-bulb temperature (T), temperature difference (ΔT), and wet-bulb depression (D) is

$$V = CR \quad , \tag{23}$$

where

V = T, ΔT or D,

C = calibration constant,

R = recorder output.

The absolute error, δV, is given by

$$\delta V = \frac{\partial V}{\partial C}\delta C + \frac{\partial V}{\partial R}\delta R \quad . \tag{24}$$

Since both sources of error are independent and random, the relative error is the root mean square solution to equation 24 (Cook and Rabinowich 1963). Thus,

$$\left(\frac{\delta V}{V}\right)_{r.m.s.} = \pm \left\{\left(\frac{\delta C}{C}\right)^2 + \left(\frac{\delta R}{R}\right)^2\right\}^{\frac{1}{2}} \quad . \tag{25}$$

The values for δC and δR in this experiment were ±0.25%. For the ΔT data, the recorder error represented 2.5 μv, and for the T and D-data, 5 μv. Equation 25 was evaluated for a representative range of values of the three parameters (Table 2).

The wet-bulb temperature, Tw, at any level, n, in

TABLE 2

ABSOLUTE AND RELATIVE ERRORS IN T, ΔT, AND D

Function	Value (C)	Absolute Error (C)	Relative Error (%)
T	5.0	0.125	2.50
	10.0	0.127	1.27
	20.0	0.135	0.67
	25.0	0.140	0.56
	30.0	0.147	0.49
ΔT	2.00	0.0134	0.67
	1.00	0.0127	1.27
	0.50	0.0126	2.51
	0.10	0.0125	12.50
	0.01	0.0125	125.00
D	1.0	0.025	2.51
	2.0	0.025	1.27
	3.0	0.026	0.87
	5.0	0.028	0.56
	10.0	0.035	0.35

the profile is calculated as

$$Tw_n = T_n - D_n \quad . \tag{26}$$

The values of T within the canopy were calculated from a value of dry-bulb temperature at the lowest level, T_1, and the ΔT data. Thus,

$$T_n = T_1 - \Delta T_1 \,\ldots\ldots\ldots\, - \Delta T_{n-1} \quad . \tag{27}$$

From equation 26, the error in Tw_n is

$$\delta Tw_n = \frac{\partial Tw_n}{\partial T_n}\delta T_n + \frac{\partial Tw_n}{\partial D_n}\delta D_n \quad . \tag{28}$$

In the wet-bulb temperature, the error component which depends on the error in the dry-bulb temperature consists of a systematic component, δT_1, and the sum of the random components which result from the errors in dry-bulb temperature difference measurements. Therefore, from equation 27 and 28, the error in Tw_n, within the canopy, is

$$\left(\frac{\delta Tw_n}{Tw_n}\right)_{\text{r.m.s.}} = \frac{\delta T_1}{Tw_n} \pm \left\{\left(\frac{\delta \Delta T_1}{Tw_n}\right)^2 \ldots + \left(\frac{\delta \Delta T_{n-1}}{Tw_n}\right)^2 + \left(\frac{\delta D_n}{Tw_n}\right)^2\right\}^{\frac{1}{2}} . \tag{29}$$

Since the number of ΔT values used increased from the bottom to the top of the canopy, the random error component similarly increased. However, the increase was small (see Table 3).

TABLE 3

VARIATION IN ABSOLUTE ERROR IN

Tw WITHIN THE CANOPY[4]

Level	Systematic Component (C)	Random Component (C)
1 (bottom)	0.135	0.026
2	0.135	0.030
3	0.135	0.033
4	0.135	0.036
5 (top)	0.135	0.038

[4]When T = 20.0 C and D = 3.0 C.

(b) Humidity. The vapour pressure at each level was computed using equation 21, and the vapour pressure difference, Δe, found by subtraction. The error in vapour pressure is

$$\delta e = \frac{\partial e}{\partial e_s}\delta e_s + \frac{\partial e}{\partial D}\delta D \quad . \tag{30}$$

The errors in the saturation vapour pressure at any levels, i and j, in the profile, consisted of a systematic component due to the systematic error in the measurement of the dry-bulb temperature, T_1, and the random component in the determination of wet-bulb temperature. The systematic error was of the same magnitude for all levels in any one profile, since the temperature difference between levels 1 and 5 never exceeded 2C. Therefore, the error in the vapour pressure difference consisted of the random error in e_{s_i} and e_{s_j} due to the random error in Tw_i and Tw_j and the random error in D_i and D_j. These errors have been combined to give the r.m.s. error in Δe. Thus,

$$\left(\frac{\delta\Delta e_{ij}}{\Delta e_{ij}}\right)_{\text{r.m.s.}} = \pm\left\{\left(\frac{\delta e_{s_i}}{\Delta e_{ij}}\right)^2 + \left(\frac{\delta e_{s_j}}{\Delta e_{ij}}\right)^2 + \left(\frac{\gamma\delta D_i}{\Delta e_{ij}}\right)^2 + \left(\frac{\gamma\delta D_j}{\Delta e_{ij}}\right)^2\right\}^{\frac{1}{2}} . \tag{31}$$

For a wet-bulb temperature of 20C, $\delta\Delta e$ varied from 0.06 to 0.08 mbars, for a variation in D from 1.0C to 10C. As the wet-bulb temperature increases, the error increases because of the non-linearity in the saturation vapour pressure-temperature relationship. If Tw = 25C, $\delta\Delta e$ = 0.09 mbars. However, since the wet-bulb temperature varied between 15C and 22C in this experiment, the average error in Δe was ±0.07 mbars.

2. Error in LE, H and K

From equations 6 and 7, it is apparent that the errors in LE and H are dependent on the same independent sources of error. Thus, in general, the error in the flux (F) is

$$\delta F = \frac{\partial F}{\partial Rn}\delta Rn + \frac{\partial F}{\partial G}\delta G + \frac{\partial F}{\partial \overline{\Delta\theta}}\delta\overline{\Delta\theta} + \frac{\partial F}{\partial \overline{\Delta e}}\delta\overline{\Delta e} \quad , \qquad (32)$$

and the relative error is

$$\left(\frac{\delta F}{F}\right)_{r.m.s.} = \pm \left\{\left(\frac{\partial F}{\partial Rn}\right)^2\left(\frac{\delta Rn}{F}\right)^2 + \left(\frac{\partial F}{\partial G}\right)^2\left(\frac{\delta G}{F}\right)^2 + \left(\frac{\partial F}{\partial \overline{\Delta\theta}}\right)^2\left(\frac{\delta\overline{\Delta\theta}}{F}\right)^2 + \left(\frac{\partial F}{\partial \overline{\Delta e}}\right)^2\left(\frac{\delta\overline{\Delta e}}{F}\right)^2\right\}^{\frac{1}{2}}. \qquad (33)$$

Equations 32 and 33 were solved for LE and H. The solution to the partial derivatives are given in Appendix II. An error of 5% was assigned to the soil heat flux (Fuchs and Tanner 1970), and one of 10% to net radiation. When the temperature and humidity differences were large, reasonable accuracy (±10% to ±15%) was achieved in the estimation of LE and H. However, as the temperature and humidity differences approached 0, the errors in LE and H approached infinity (Fuchs and Tanner 1970). This condition was apparent particularly during the turn-over periods.

The error in the turbulent transfer coefficient is a function of the errors in LE and the vapour pressure difference (equation 9). Thus,

$$\delta K = \frac{\partial K}{\partial LE}\delta LE + \frac{\partial K}{\partial \overline{\Delta e}}\delta \overline{\Delta e} \quad . \tag{34}$$

The derivatives are given in Appendix II. Both sources of error are random, and, therefore, the relative error in K is given by the r.m.s. solution to equation 34 which is

$$\left(\frac{\delta K}{K}\right)_{r.m.s.} = \pm \left\{ \left(\frac{\partial K}{\partial LE}\right)^2 \left(\frac{\delta LE}{K}\right)^2 + \left(\frac{\partial K}{\partial \overline{\Delta e}}\right)^2 \left(\frac{\delta \overline{\Delta e}}{K}\right)^2 \right\}^{\frac{1}{2}} \quad . \tag{35}$$

When the temperature and humidity data within the canopy were used, equation 35 gave an average error in K of ±25%. However, in the atmosphere, absolute temperature data were measured with single thermocouples, and this resulted in a significant increase in the errors in the computed values of LE, H and K.

The temperature difference between any two levels is given by

$$\Delta T = T_n - T_{n-1} \quad . \tag{36}$$

The error in ΔT is

$$\delta\Delta T = \frac{\partial\Delta T}{\partial T_n}\delta T_n + \frac{\partial\Delta T}{\partial T_{n-1}}\delta T_{n-1} \quad . \tag{37}$$

Since the errors in each temperature measurement are independent and random, the error in the temperature difference is

$$\left(\frac{\delta\Delta T}{\Delta T}\right)_{r.m.s.} = \pm \left\{ \left(\frac{\delta T_n}{\Delta T}\right)^2 + \left(\frac{\delta T_{n-1}}{\Delta T}\right)^2 \right\}^{\frac{1}{2}} \quad . \tag{38}$$

If the absolute temperature equals 20C, $\delta T = \pm 0.135$C (see section D, 1a), and, therefore, $\delta\Delta T = \pm 0.19$C. The error in the vapour pressure difference increases to ±0.30 mbars.

When these data were used, the average relative error in LE and H became at least ±30% and ±50% respectively, and the error in the transfer coefficient increased to at least ±75% and often was >±100%. Since the accuracy in this determination of the transfer coefficient was so low, these data have not been considered in further analysis.

CHAPTER 4

CANOPY NET RADIATION RESULTS

Canopy measurements of net radiation with linear sensors were made later (August 14 to 25) than the main period of temperature and humidity profile measurement (August 1 to 13). This was the result of late arrival of the sensors. To evaluate energy balance components within the canopy during the earlier period, a model for estimating net radiation was developed. It is based upon the exponential framework (equation 13).

A DATA

Hourly average radiation values from the linear net radiometers are used in the analysis. Probe data are not included since only a small number of samples were obtained, and these data exhibited a high degree of scatter, thereby illustrating the measurement problem within the canopy. The large scatter, due to the variability of net radiation at a level, is greatest at the centre of the canopy (Figure 9). The uncertainty (±1 standard deviation) reaches a maximum value of 78% at 60 cm.

The cumulative leaf area index distributions for the

FIGURE 9. NET RADIATION PROFILE IN CORN USING MANUAL PROBE. August 8, 1969 (1230 E.S.T.)

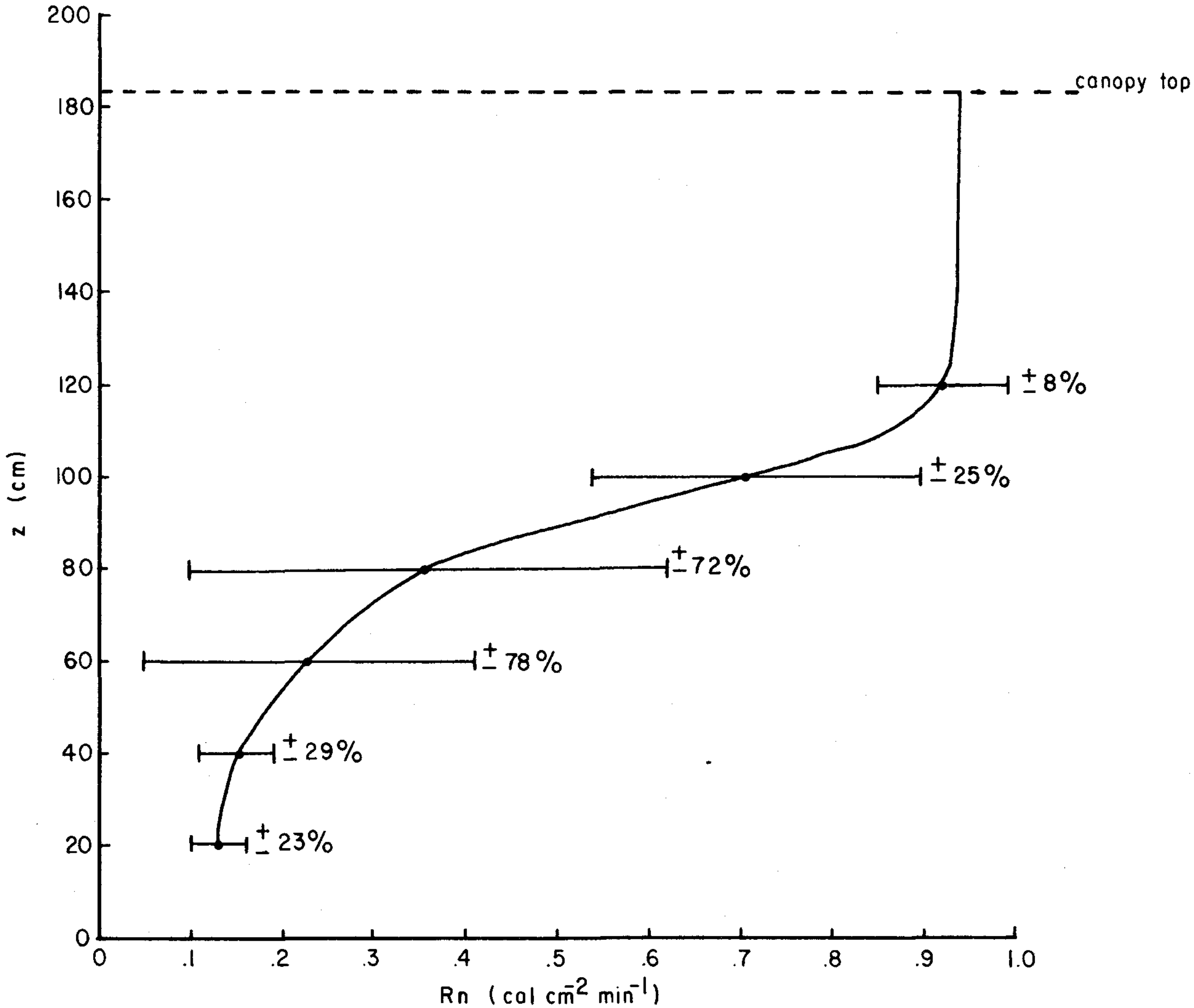

corn crop are shown in Figure 10. The L.A.I. increased rapidly from 4.3 (July 24) to 5.6 (July 31), corresponding to an increase in crop height of 50 cm. It did not increase between July 31 and August 7, even though the crop height increased by 20 cm. Over the latter period there was a marked decline in the lower half of the canopy and an increase in the upper half (Figure 11). The vertical distributions did not change between August 7 and 14 and, throughout the experiment, it was virtually Gaussian. It is assumed that the L.A.I. did not change from August 14 to 25. This assumption is valid for the upper two-thirds of the canopy but not for the lower third where the leaves had reached senescence and withered by August 25. Since the L.A.I. is cumulated from the top of the canopy downwards in the model for net radiation, its probable change at the base of the canopy is not significant in terms of net radiation estimation.

The maximum value of L.A.I. for this crop is very high. Daynard (1971) reported a maximum value of L.A.I. for corn >5, but, normally, the maximum values for corn crops on which micrometeorological studies have been done have not exceeded 4.5 (Brown and Covey 1966, Impens and Lemeur 1969).

FIGURE 10. CUMULATIVE LEAF AREA INDEX AT NET RADIATION SITE

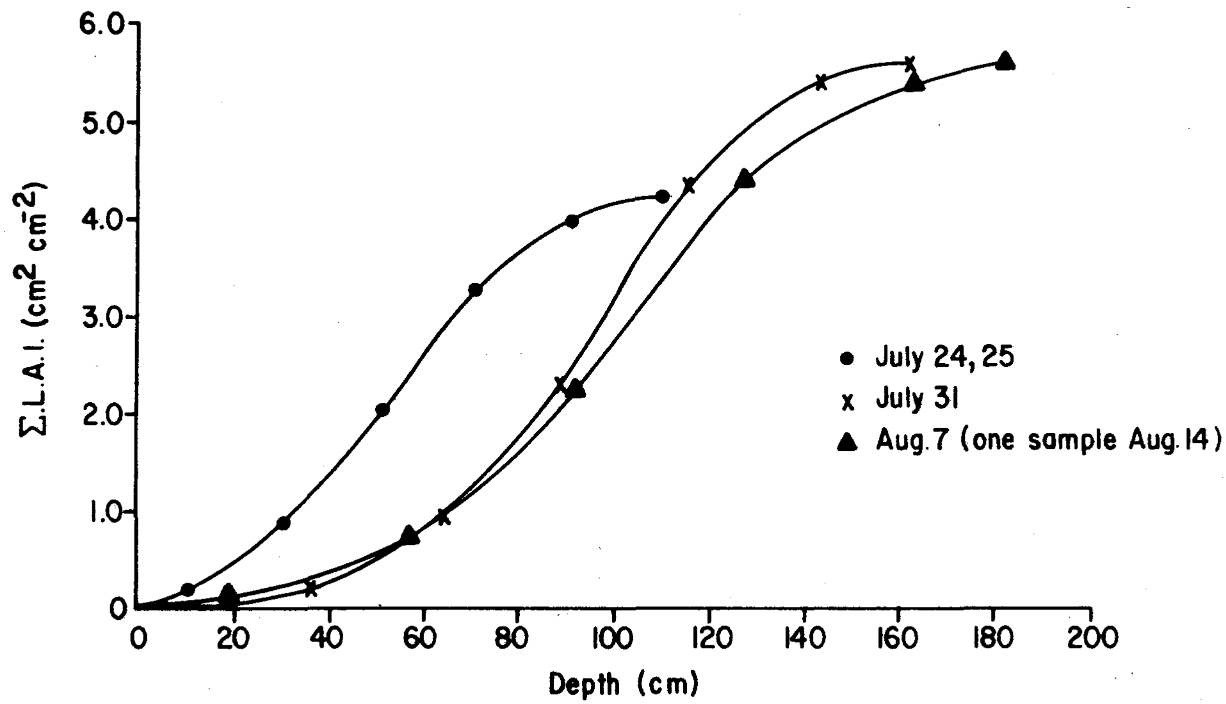

Figure II. Leaf Area Density Distribution in Corn

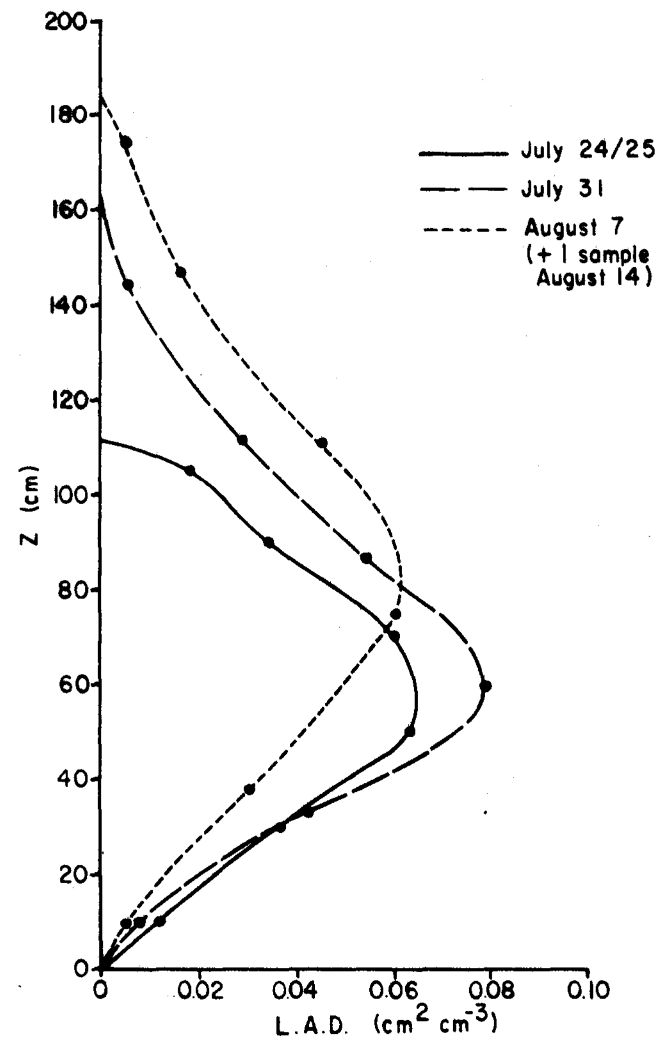

B NET RADIATION PROFILE CHARACTERISTICS

All net radiation profile data normalized with the above-canopy value are listed in Appendix III. Diurnal variation in relative intensity occurred at all levels with a maximum at 1030 (E.S.T.) on all days. At this time, the net radiation within the canopy was frequently larger than that above. This could have been due to reradiation by the upper leaves of trapped, reflected radiation from below (Kalma and Stanhill 1969).

The hourly average net radiation profiles for a sample day are shown in Figure 12. All show little depletion from the top of the canopy to 120 cm. Depletion was high between the second and third measurement levels where the leaf area density was at a maximum. The intensity of depletion varied through the day and was not symmetrical around solar noon. Characteristically, an afternoon profile shows a greater depletion than the comparable morning profile. This is evident if the 1430 profile is compared to the 1030 profile. This means that the optical density varied throughout the day, and, for this crop, the variation was not symmetrical with respect to time.

C EXPONENTIAL MODEL RESULTS

The extinction coefficient in equation 13 was computed for each profile as the slope of the least squares line

FIGURE 12. NET RADIATION PROFILES IN CORN, AUGUST 14

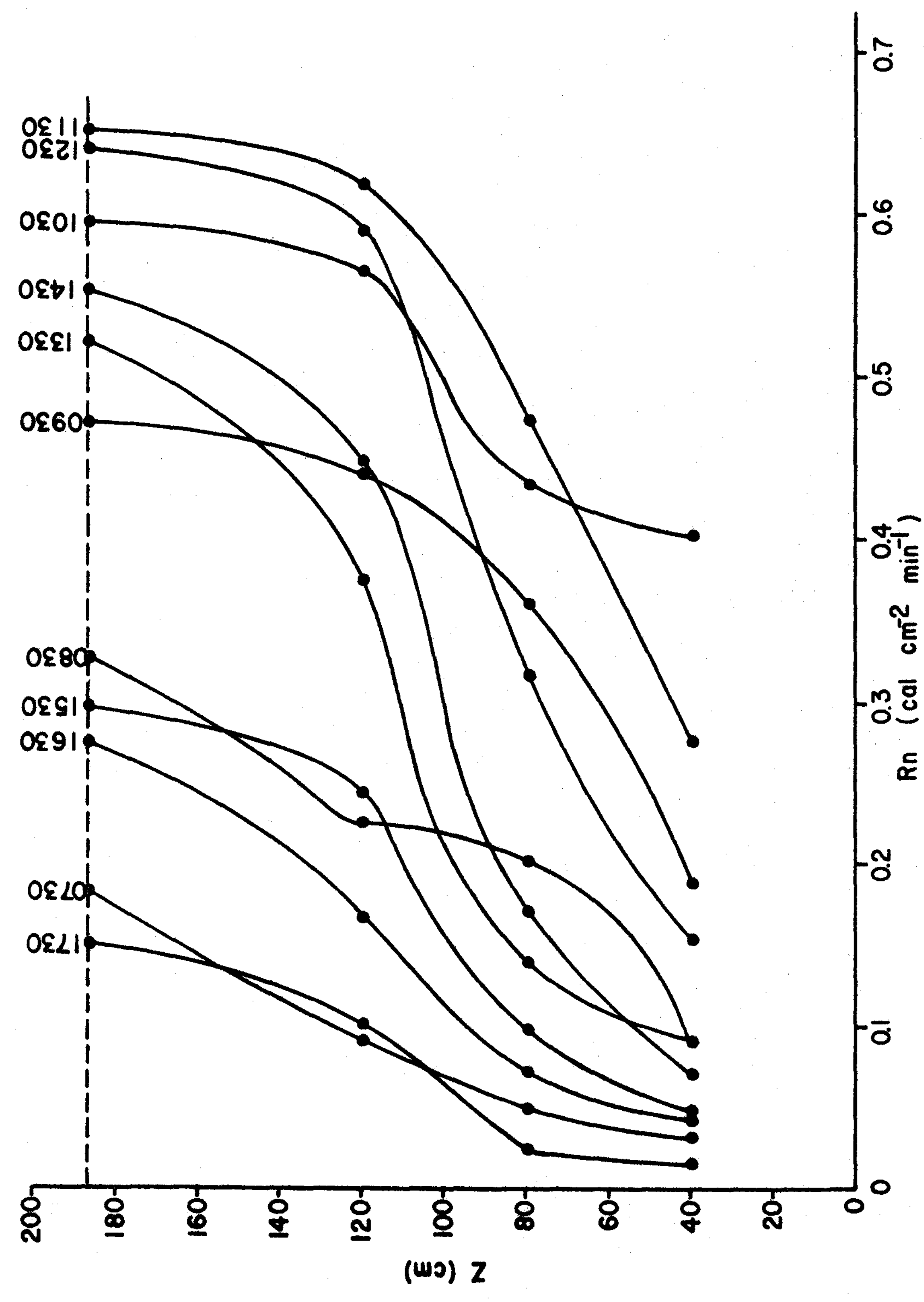

relating the logarithm of relative intensity of net radiation to the cumulative leaf area index. The intercept of the regression line was constrained at zero.

The extinction coefficient exhibited a marked diurnal variation on all days. This is shown in Figure 13 for August 14, where k varies between 0.08 and 0.46. When the mean daily extinction coefficient was used, equation 13 predicted poorly for hourly values (Figure 14). The relationship between model values (Rn') and experimental values (Rn) is

$$Rn' = 0.047 + 0.630\ Rn \quad ,$$
$$r = 0.90,\ Sy = 0.05\ (\mathrm{cal\ cm^{-2}\ min^{-1}}) \quad . \qquad (39)$$

Even though the correlation coefficient is high and the standard error of estimate is low, the model does not give satisfactory results since it underestimates the flux consistently for $Rn > 0.2$ cal cm^{-2} min^{-1}.

When the same data (August 14) are used, the Impens and Lemeur model, with $k_1 = 0.6220$ and $k_2 = 0.0553$, does not give superior results (Figure 15):

$$Rn' = 0.03 + 0.456\ Rn \quad ,$$
$$r = 0.87,\ Sy = 0.05\ (\mathrm{cal\ cm^{-2}\ min^{-1}}) \quad . \qquad (40)$$

Equations 39 and 40 illustrate that, for this canopy, an exponential model which employs a constant extinction coeff-

Figure 13. Diurnal Variation of Rn Depletion and of the Extinction Coefficient k, in Corn
August 14, 1969

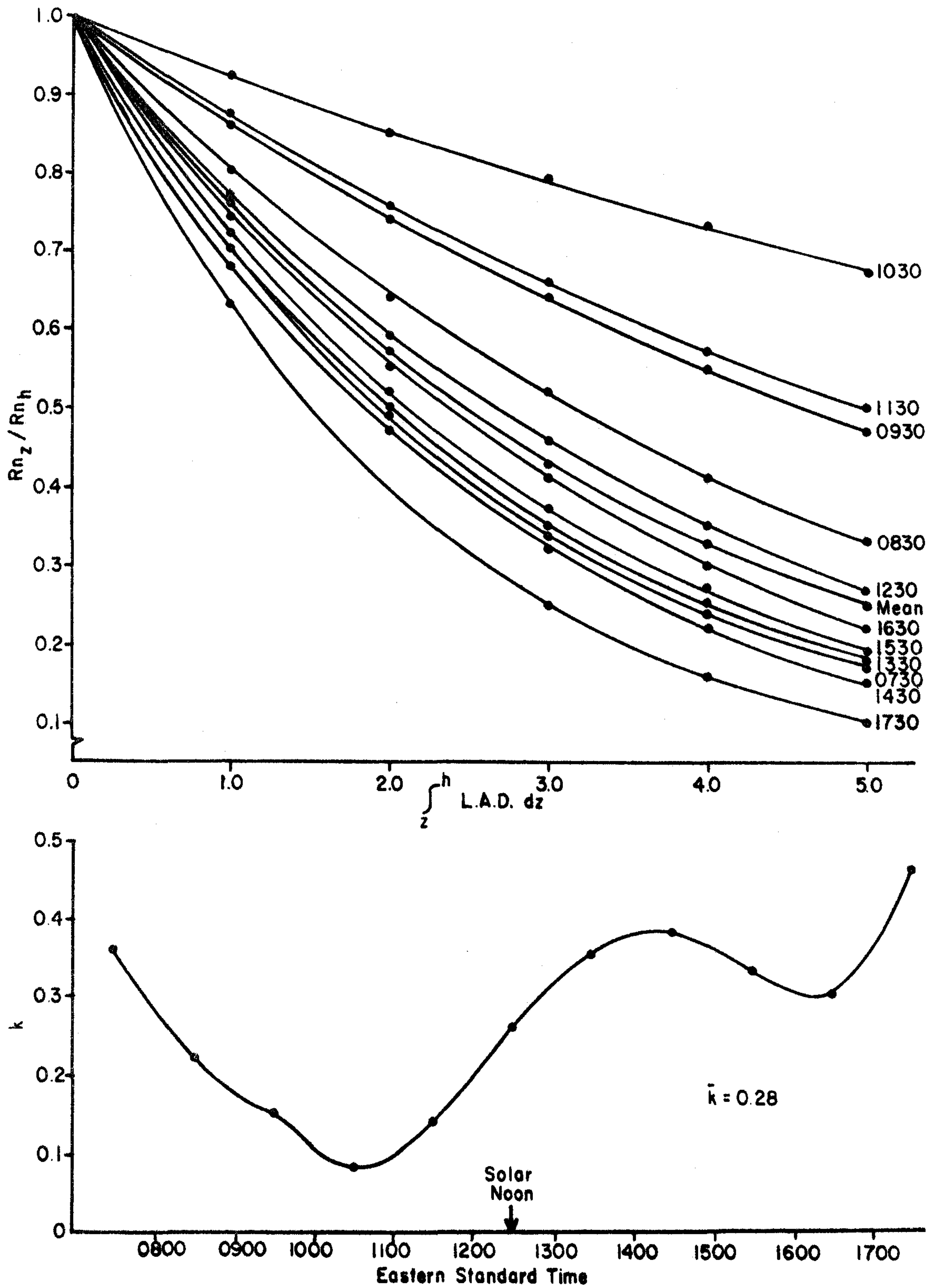

FIGURE 14. PREDICTION OF HOURLY NET RADIATION IN CORN USING THE EXPONENTIAL MODEL

$Rn_z = Rn_h \exp(-k\,Fc)$

k = 0.28 (mean daily value)

August 14

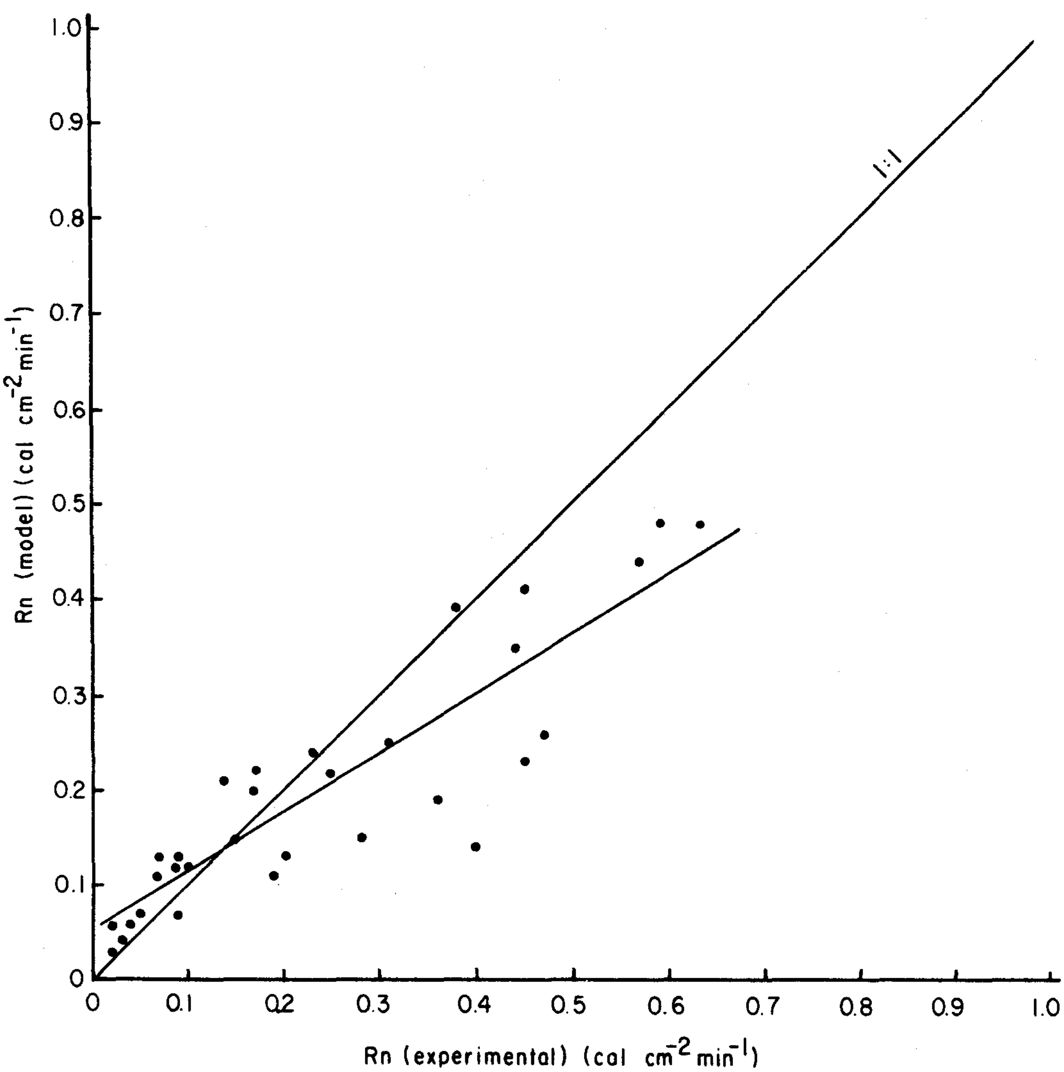

FIGURE 15. PREDICTION OF HOURLY NET RADIATION IN CORN USING THE IMPENS AND LEMEUR MODEL

$$Rn_z = Rn_h \exp(-k_1 Fc + k_2 Fc^2)$$

$k_1 = 0.6220$

$k_2 = 0.0553$

August 14

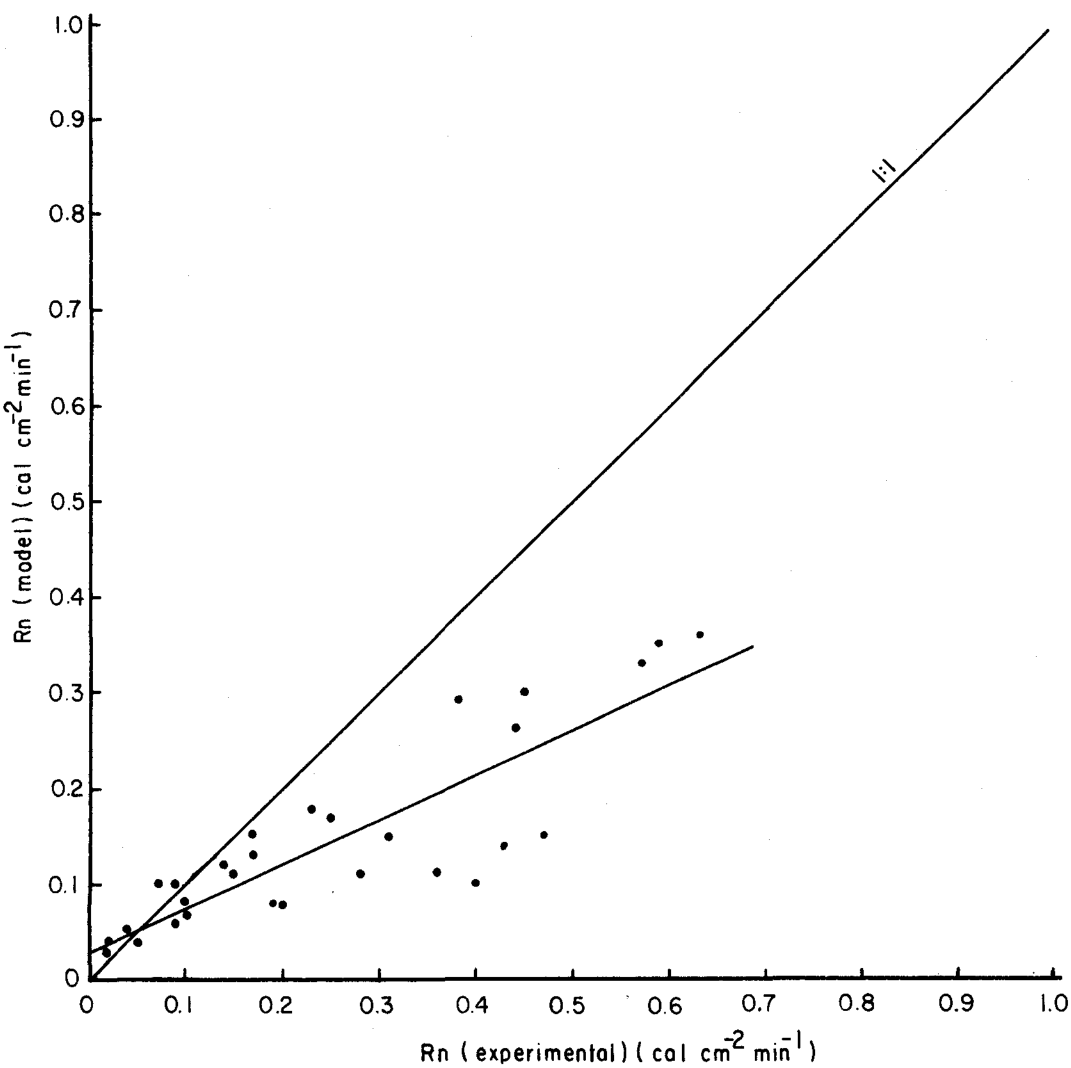

icient is insufficient.

D MODIFICATION OF THE EXPONENTIAL MODEL

The diurnal variation in k (Figure 13) indicates that the attenuation of net radiation in this crop departs significantly from Beer's Law. Beer's Law is only strictly applicable to radiation attenuation in a homogeneous medium where the variation of path length adjusts the optical density for different zenith angles. A row crop is heterogeneous, and, to achieve a satisfactory prediction of hourly values of canopy net radiation, either the diurnal variation of k must be predicted empirically, or other variables must be incorporated into the model to modify the path length (cumulative L.A.I.) and achieve a constant k. The latter is preferable because it should provide insight into the factors which control the attenuation of net radiation in the canopy. The most logical variable to use in modifying the L.A.I. is the zenith angle because the path length for the direct beam component of net radiation depends explicitly on it. This is done by defining the effective L.A.I. (Fc') as

$$Fc' = Fc \sec \zeta \quad , \tag{41}$$

where

ζ = the zenith angle.

However, the diffuse fraction of the radiation increases with penetration into the canopy (Begg et al. 1964). Assuming that the diffuse radiation is isotropic in the canopy space, the dependence on zenith angle should decrease with depth. This is accomodated by modifying equation 41:

$$Fc' = Fc\ (\sec \zeta)^{\frac{h-z}{h}} \quad , \qquad (42)$$

where

h = crop height.

Towards the base of the canopy, $\frac{h-z}{h}$ approaches 0 and Fc' approaches Fc.

However, the variation in optical density in a row crop is not completely determined by kFc' because, irrespective of the zenith angle, the optical density, and, therefore, the attenuation of net radiation is at a minimum when the sun shines directly down the row. This is shown in Figure 13 when the minimum value of k occurs at 1030, at which time the relative solar azimuth (ϕ)[6] is 0°. This feature is replicated when all data are grouped (Figure 16). The strong positive correlation between k and ϕ is shown in Figure 17. As ϕ approaches zero, k approaches zero, and as ϕ approaches 90°, k approaches its maximum value of 0.60. Thus, a function of relative solar azimuth, $\cos\ (\phi - \frac{\pi}{2})$, is

[6] Relative solar azimuth is defined as the horizontal angle between the sun and the row.

FIGURE 16. RELATIONSHIP BETWEEN THE EXTINCTION COEFFICIENT (k) FOR HOURLY NET RADIATION AND SOLAR AND RELATIVE AZIMUTH IN CORN

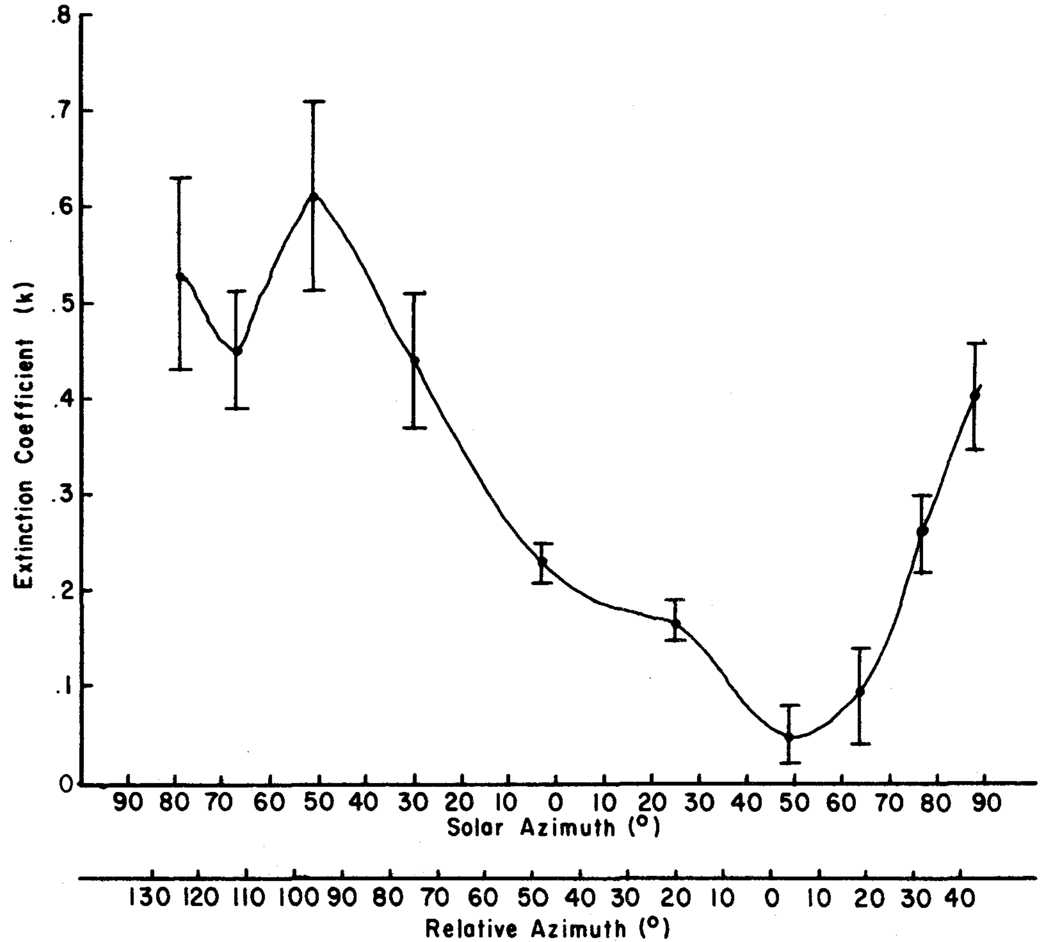

FIGURE 17 RELATIONSHIP BETWEEN THE EXTINCTION COEFFICIENT (k) FOR HOURLY NET RADIATION AND RELATIVE AZIMUTH IN CORN

The line is an eye fit to the scatter

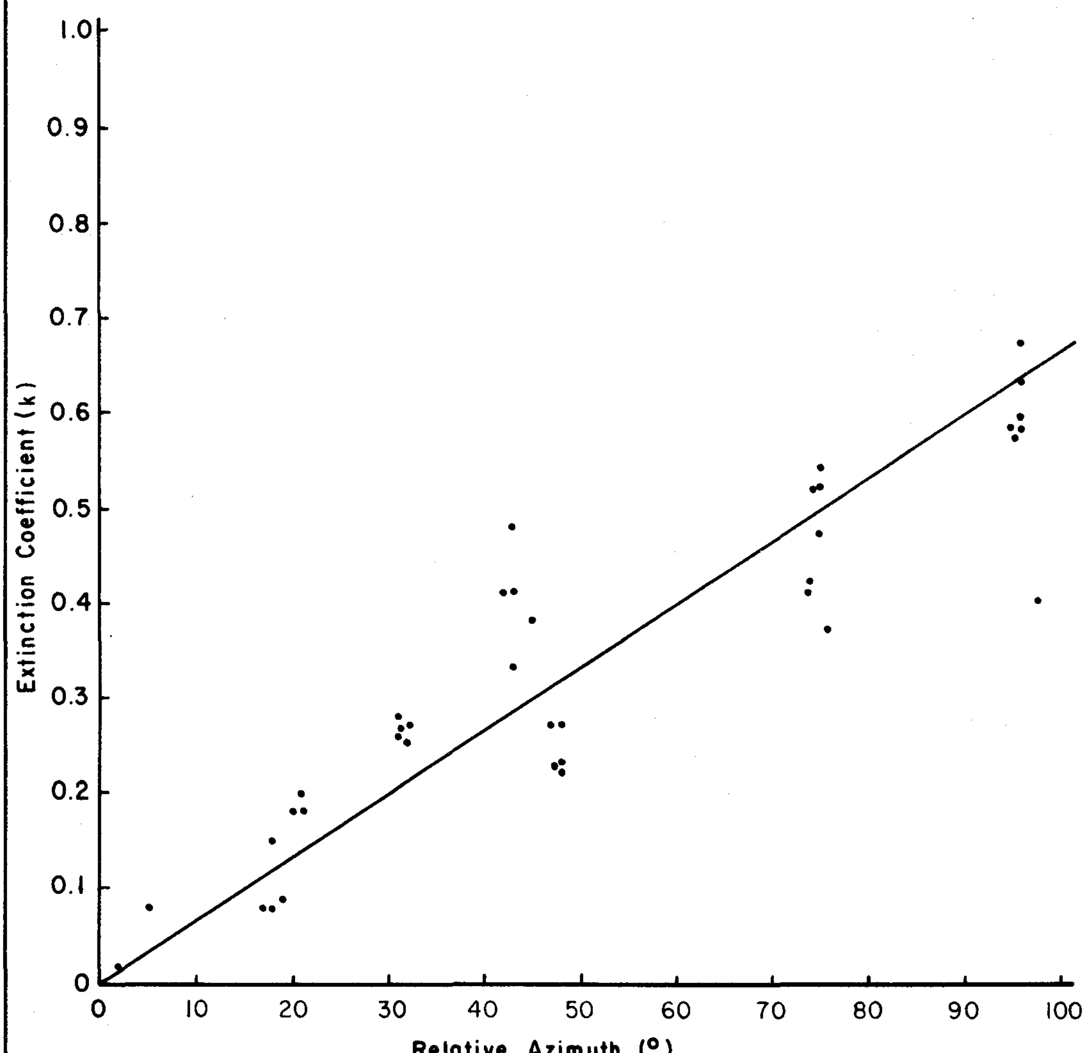

incorporated into the model. This function varies diurnally in such a manner that it adjusts the optical density to a minimum at minimum relative azimuth. Hence,

$$Fc' = Fc\ (\sec \zeta)^{\frac{h-z}{h}} \cdot \cos\ (\phi - \frac{\pi}{2}) \quad . \tag{43}$$

The modified model for canopy net radiation is obtained by combining equations 43 and 13:

$$Rn_z = Rn_h \exp\{-k\ Fc\ (\sec \zeta)^{\frac{h-z}{h}} \cdot \cos\ (\phi - \frac{\pi}{2})\} \quad . \tag{44}$$

The values of k computed from this equation for each day are shown in Table 4. There was no significant difference at the 95% confidence level (using Student's t-test) between these values. The mean extinction coefficient, 0.436, was used in the model. The performance of the model is shown in Figure 18. The scatter is fitted by

$$Rn' = 0.04 + 0.87\ Rn,$$
$$r = 0.96,\ Sy = 0.05\ (\text{cal cm}^{-2}\ \text{min}^{-1}) \quad . \tag{45}$$

The model underestimates at high radiation intensities and overestimates at low intensities, but the departure is <10%. The underestimation is partly a result of the occurrence on some days of higher values of net radiation within rather than at the top of the canopy, around solar noon. The model

TABLE 4

VARIATION IN THE EXTINCTION COEFFICIENT FOR NET RADIATION IN CORN

Date	k	95% Confidence Limits for k
Aug.		
14	0.371	0.07
20	0.470	0.12
21	0.462	0.09
22	0.495	0.14
23	0.422	0.08
24	0.422	0.09
25	0.413	0.07

FIGURE 18. PREDICTION OF HOURLY NET RADIATION IN CORN USING THE MODIFIED EXPONENTIAL MODEL

$$Rn_z = Rn_h \exp\left[-k\, Fc\, (\sec z)^{\frac{h-z}{h}} \cos(\phi - \tfrac{\pi}{2})\right]$$

$k = 0.436$

All Data

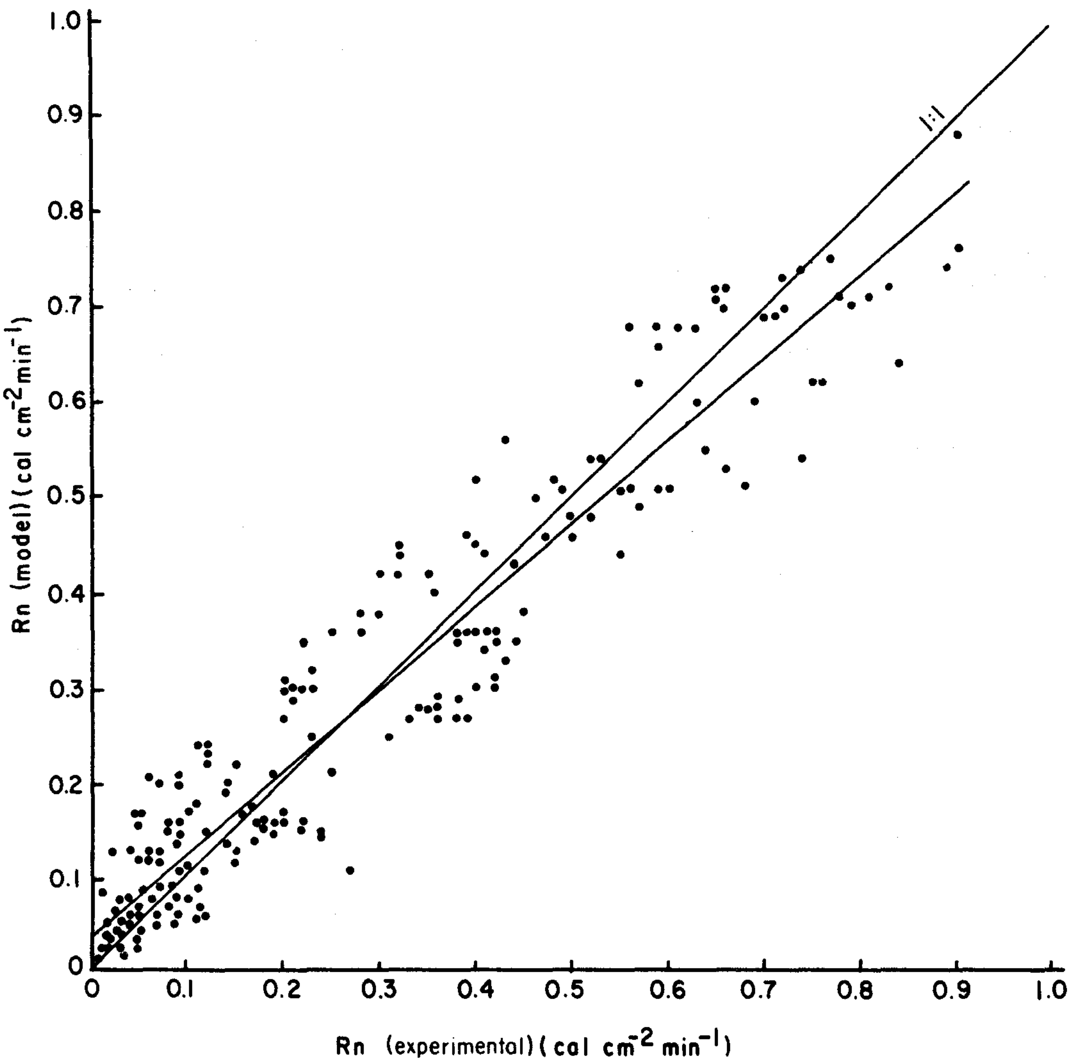

fails to predict such a condition. The data for August 14 did not exhibit this anomaly, and the model performs well (Figure 19). The line of best fit to the scatter is

$$Rn' = 0.01 + 0.91\ Rn \quad ,$$
$$r = 0.97,\ Sy = 0.04\ (\text{cal cm}^{-2}\ \text{min}^{-1}) \quad . \qquad (46)$$

In conclusion, it has been shown that for this corn canopy, the attenuation of net radiation varies significantly through the day. This variation has not been accounted for by the simple exponential model which employs a constant extinction coefficient.

It has also been shown that the extinction coefficient depends on both the zenith angle and the relative solar azimuth angle. Functions of these angles were incorporated into the model to modify the path length and to account for its variation. In particular, the effect of row orientation on the diurnal variation of net radiation in the canopy space has been demonstrated. The predictive power of the modified exponential model is significantly greater than that of the simple exponential model for hourly values of net radiation.

Since the data used to test the models were collected under primarily clear-sky conditions, it is not known if the extinction coefficients will change significantly under overcast conditions. This is an area for further study.

FIGURE 19. PREDICTION OF HOURLY NET RADIATION IN CORN USING THE MODIFIED EXPONENTIAL MODEL

$$Rn_z = Rn_h \exp\left[-k\ Fc\,(\sec z)^{\frac{h-z}{h}} \cos.\left(\phi - \frac{\pi}{2}\right)\right]$$

$k = 0.436$

August 14

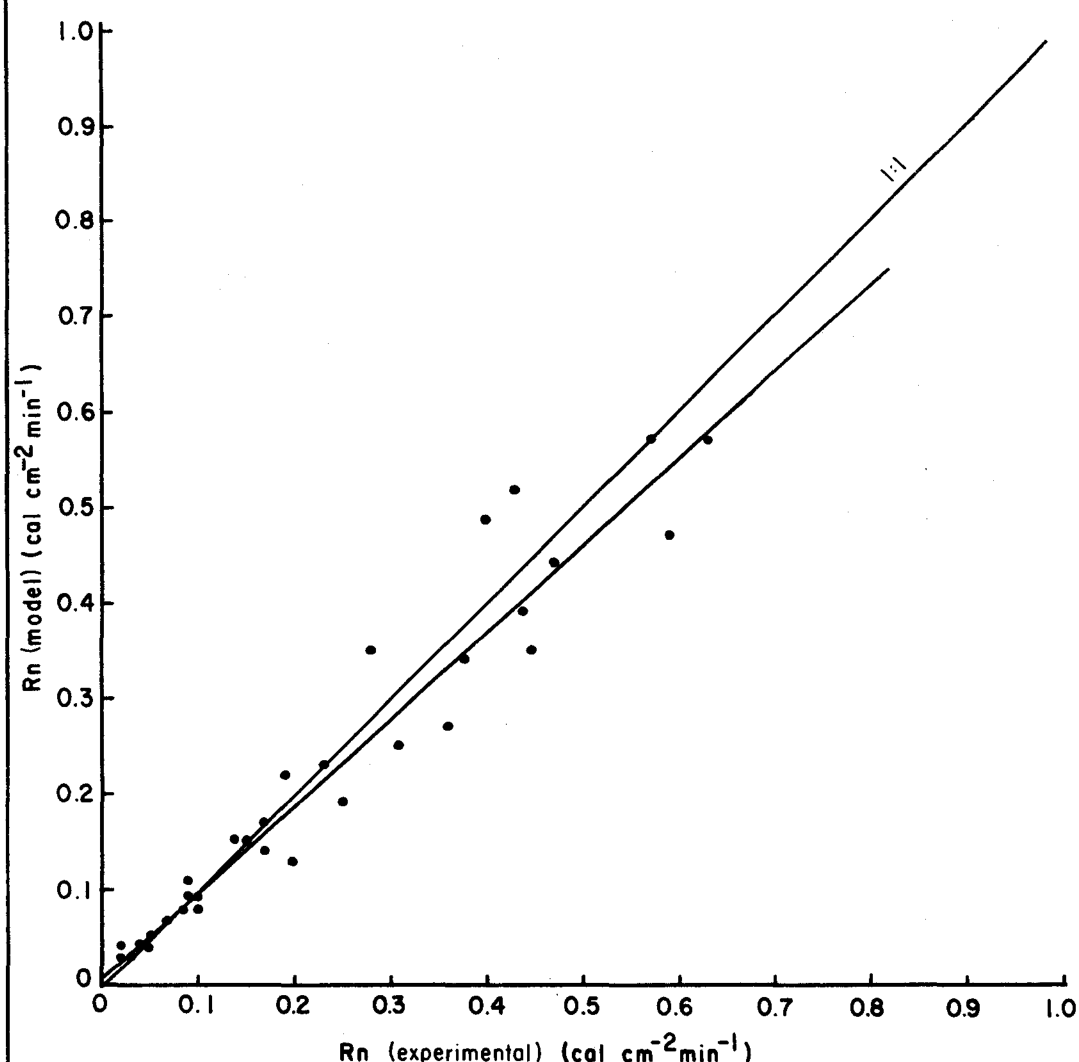

CHAPTER 5

ENERGY BALANCE RESULTS AND DISCUSSION

A ENERGY RELATIONS

Hourly average values of the components of the energy balance were evaluated for various strata, from the base of the canopy to the atmosphere for all sample days from August 1 to 13 (see Table 1). The net radiation within the canopy was calculated from equation 44.

1. Characteristics of Temperature and Humidity Profiles

The data from two contrasting days, August 10 and August 8, are discussed to illustrate the diurnal variation of temperature and vapour pressure profiles within the canopy atmosphere. These profiles are shown in Figures 20 and 21.

(a) August 10. The temperature profile for 0830 was characterized by isothermal conditions at the base of the canopy and lapse conditions at all other levels. From 0900 to 1500, lapse conditions prevailed at all levels, and there was little variation in the magnitude of the temperature gradients for any level. During the late afternoon, the temperature profiles were characterized by the development of a relative minimum in the canopy which changed in position from

FIGURE 20. TEMPERATURE AND VAPOUR PRESSURE PROFILES IN CORN, AUGUST 10, 1969

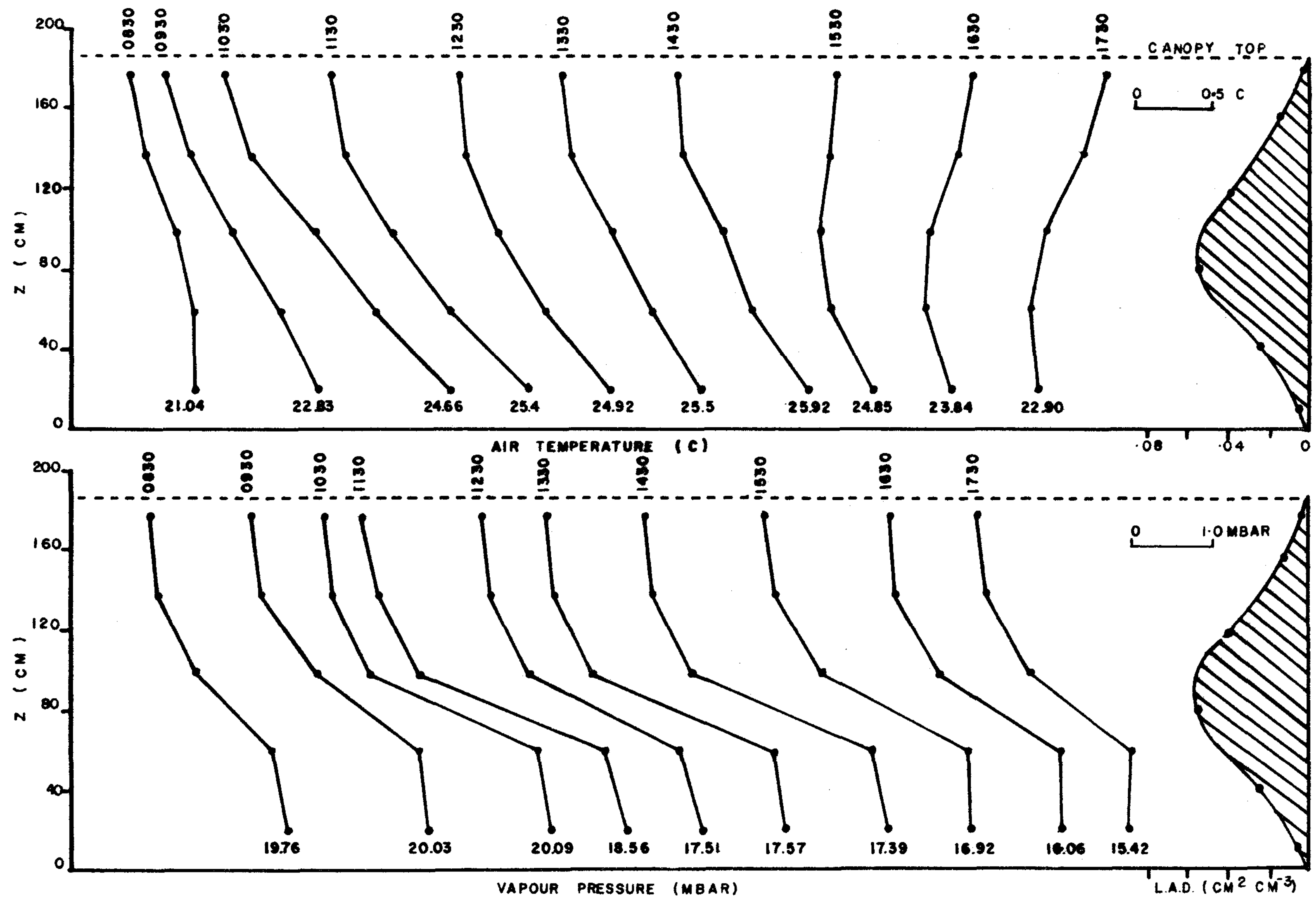

FIGURE 21. TEMPERATURE AND VAPOUR PRESSURE PROFILES IN CORN, AUGUST 8, 1969

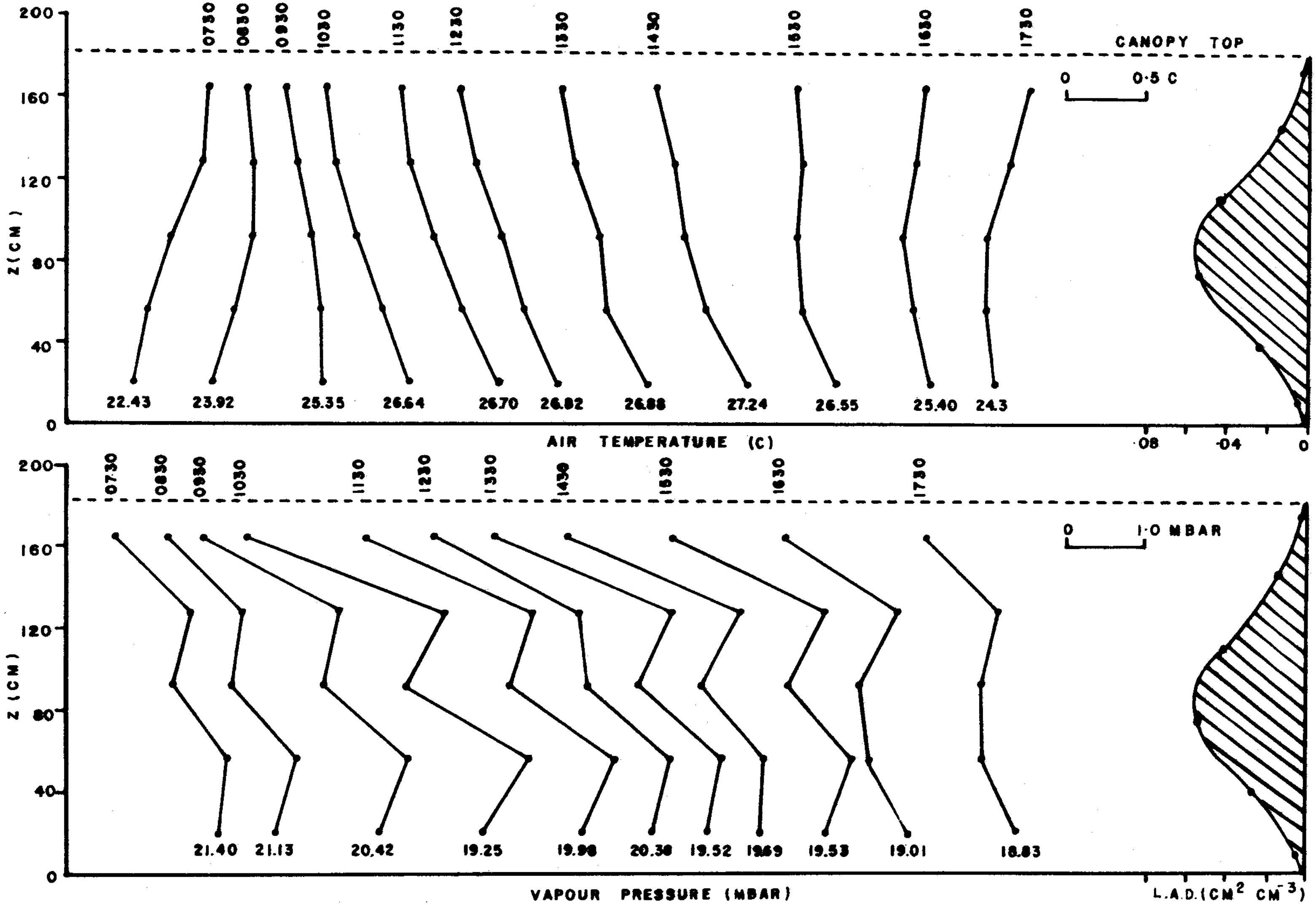

100 cm at 1500 to 60 cm at 1800.

The shapes of the vapour pressure profiles show little change throughout the day. The lowest layers of the canopy, between 20 and 60 cm, showed very small vapour pressure gradients. There was a rapid decrease between 60 and 140 cm, and from there to the top of the canopy, the gradient was again small. Throughout the day, lapse conditions existed at all levels, indicating that the canopy was losing latent heat to the atmosphere. The maximum gradient of vapour pressure occurred in the portion of the canopy where the L.A.D. was at a maximum, and the average daily value was 2.5 mbar m^{-1}.

(b) August 8. The temperature profiles do not exhibit a similar variation with height. All of them indicate two hydro-inversions, except at 1230, 1630 and 1730, which have only one. The most intense inversion occurred between 92 and 128 cm and was present in all profiles except 1230 which shows a very weak lapse. The other zone of inversion, between 20 and 56 cm, persisted from 0730 to 1530, after which it changed to lapse.

The occurrence of hydro-inversions within the canopy is puzzling. If it is accepted that the one-dimensional transfer equation for latent heat (equation 4) completely describes the flux within the canopy atmosphere, then there can be no net transfer across the inflection points in the vapour pressure profiles. For example, if the 1030 profile is considered, it shows that latent heat is diffusing both upward and downward from the second measurement level, indicating a zone of divergence at 56 cm. Similarly, the fourth measurement level at 128 cm is a zone of divergence. Therefore, the third level (92 cm) and the base of the canopy (20 cm) are zones of convergence, or sinks for latent heat. Generally, the hydro-inversion between levels 3 and 4 was the most intense. Convergence of latent heat implies condensation or dew deposition. This is an extremely improbable phenomenon under conditions of positive net radiation, and no dew deposition was observed. Therefore, some other explanation for the occurrence of hydro-inversions is required. It is possible that the reason was instrumental. If values of wet-bulb depression at levels one and three were too large due to error, values of vapour pressure would be too small. However, since the water feed and aspiration of all of the humidity sensors were checked several times during each run, this is unlikely. During the inspection, each sensor was exposed to see if the wicking was damp. When all sensors had been returned to their housings, the aspiration system was examined for leaks. After the inspection, two minutes were allowed for the sensors to reach equilibrium. The data collected during the period were not used in the analysis. Also, the marked contrast between the vapour pressure profiles on the two days suggests that the reason may not have been instrumental.

The occurrence of these inversions within the canopy was not confined to August 8. Out of a total of 106 profiles, 38 showed inversions at one or two levels (Appendix IV). In all cases, these occurred between levels 1 and 2 and between levels 3 and 4. Examination of all profiles showed that the occurrence of hydro-inversions was related to both wind speed and direction. These data are summarized in Figure 22. Wind speed was determined at a height of 1 m above the canopy. All profiles showing hydro-inversions occurred when the wind direction was between south and west-south-west, with 68% occurring with a south wind. Also, 92% occurred when the wind speed was greater than 200 cm sec^{-1}. When the wind speed exceeded 300 cm sec^{-1}, only 2 out of 26 profiles did not show hydro-inversions. Although this evidence suggests that the vertical distribution of latent heat diffusion was strongly influenced by wind speed and direction, the reason for this is not clear. In order to explain the occurrence of these inversions, without condensation, there must have been divergence of latent heat, caused by horizontal wind speed gradients and/or horizontal humidity gradients. If this was the case, then it is reasonable to expect it to have occurred most frequently when the wind was blowing along the rows from the S.E. quadrant, the direction of minimum fetch. This did not happen in this experiment, and the maximum frequency of occurrence of hydro-inversions coincided with a south wind which was at 45° to the rows. The fetch was 108 m. However, there may have been a local heterogeneity in canopy structure in the vicinity of

FIGURE 22. CLASSIFICATION OF HUMIDITY PROFILES IN CORN WITH RESPECT TO WIND SPEED AND WIND DIRECTION

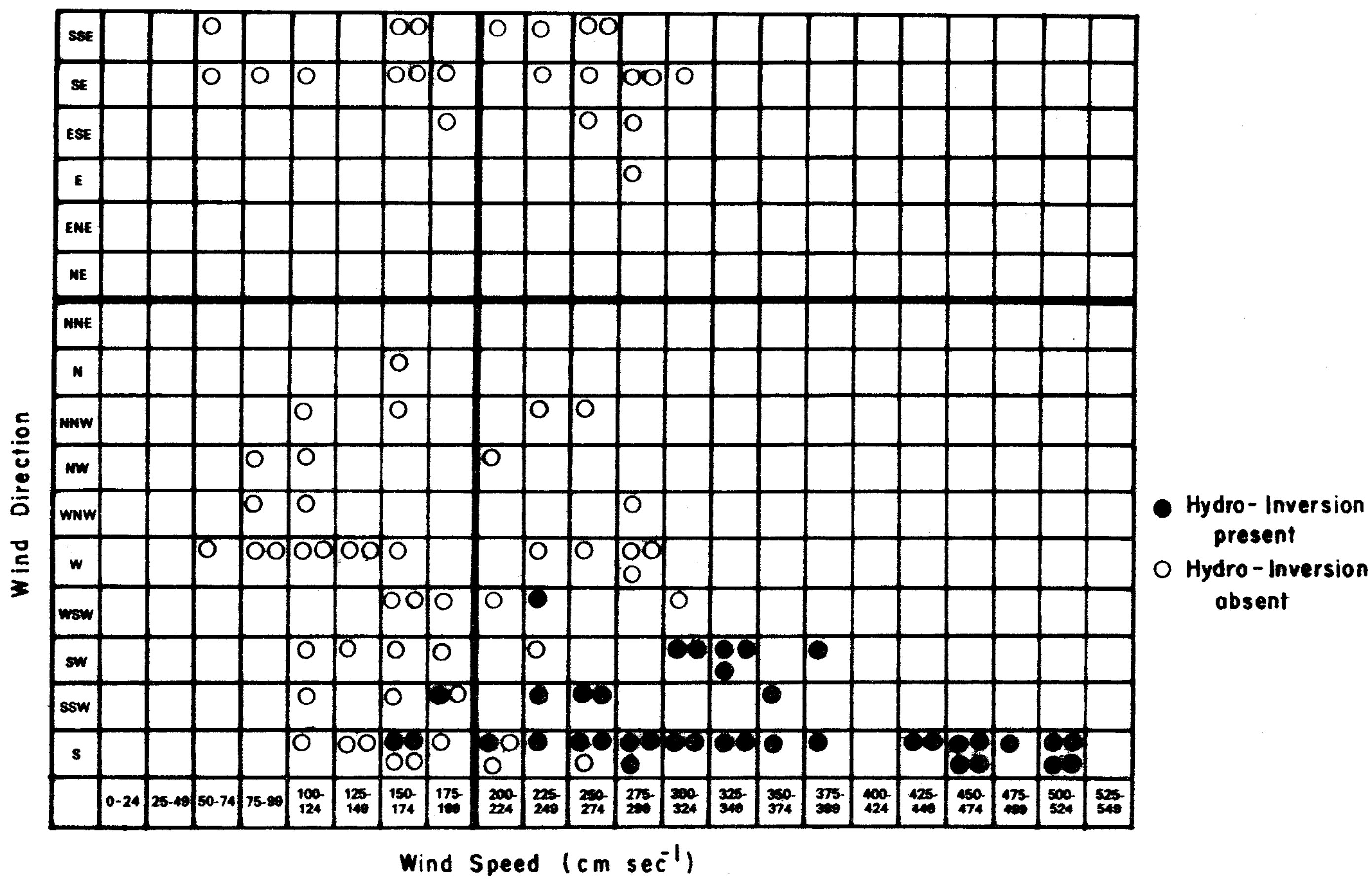

the sampling point. If there were gaps in the canopy towards the south, relatively dry air could have been advected into the canopy from above the crop, causing relative minima in the vapour pressure profiles. If this occurred, the advection of dry air from above the canopy was aided by high wind speeds.

It is interesting to note that hydro-inversions between 0930 and 1530 on August 8 did not coincide with temperature inversions, and this feature was repeated on the other sample days. Rather, the temperature profiles showed weak lapse or isothermal conditions at the levels of hydro-inversions.

2. Classification of Data

When a positive value of available energy (Rn-G) occurs in conjunction with a hydro-inversion and temperature lapse, equation 9 gives negative values of K. Also, the sign of the latent and sensible heat fluxes do not agree with the sign of the gradients of vapour pressure and temperature (equations 6 and 7). This is theoretically impossible. If horizontal divergences of either latent or sensible heat are occurring, the one-dimensional solution to the energy balance of the canopy is insufficient, and it breaks down as an acceptable framework for describing the energy exchange processes.

It was therefore necessary to ignore all levels where negative values of K occurred. Further, if there were a negative value of K at the third stratum, the establishment of any links between the atmosphere and the base of the canopy, in terms of energy transfer or turbulent exchange mechanism, was impossible, and the profile was ommitted from the analysis.

The data most affected by anomalous negative values of K at centre-canopy were concentrated during the first half of the sampling period. In particular, the data for August 1 and August 8 were characterized by negative K values between levels 3 and 4. Only the data for August 3, 5 and 6 exhibited consistent positive values for most of the canopy atmosphere. Similarly, the data for the four days, August 10 to August 13, were characterized by the absence of negative exchange coefficients at the centre of the canopy. It was assumed that these two data sets represented periods when the theoretical framework best described the energy exchange within the canopy. Therefore, the data from these days were chosen as the basis of further analysis. However, negative K values did occur intermittently at the base of the canopy on all of these seven days.

3. Flux Profiles and Sources and Sinks

Smoothed vertical profiles of latent and sensible heat flux were drawn from computed hourly average values of LE and H for each day. In drawing smoothed profiles of latent heat flux, it was assumed that condensation was not occurring at any point in the canopy when there was a positive value of net radiation (Begg et al. 1964).

The shapes of the profiles show good internal consistency for August 3,5 and 6, and for August 10, 11, 12 and 13. Therefore, mean data from these two periods were used in an attempt to generalize the height dependence of the energy exchange within the canopy. The use of mean data is also likely to give a more realistic view of energy use by the crop since more than one sample was employed. The consistency of profile shape within the two sampling periods is apparent from a comparison of the data for 1230 and 1330 on two days within each period (Figures 23 and 24). The error limits are shown for LE and H only when the absolute error >0.01 cal $cm^{-2}min^{-1}$. The errors in Rn, assumed to be ±10% at all levels, are not shown in order to ensure visual clarity. Similarly, the errors in LE and H at the top of the canopy, computed using absolute measurements of temperature and humidity, are not shown on the profiles but are listed in Table 5. It is apparent that the use of the absolute data greatly increases the errors in the fluxes.

(a) Sample period 1. The three-day mean flux profiles for this period are shown in Figure 25. At 0830, the fluxes of latent and sensible heat at the lowest measurement level did not agree with the sign of the gradients of temperature and humidity, and they were omitted. For the whole period, the latent heat flux was the principal energy user at all levels in the canopy. From 0830 until 1030, transpiration in

Figure 23. Rn, LE and H Profiles, August 3 and 5

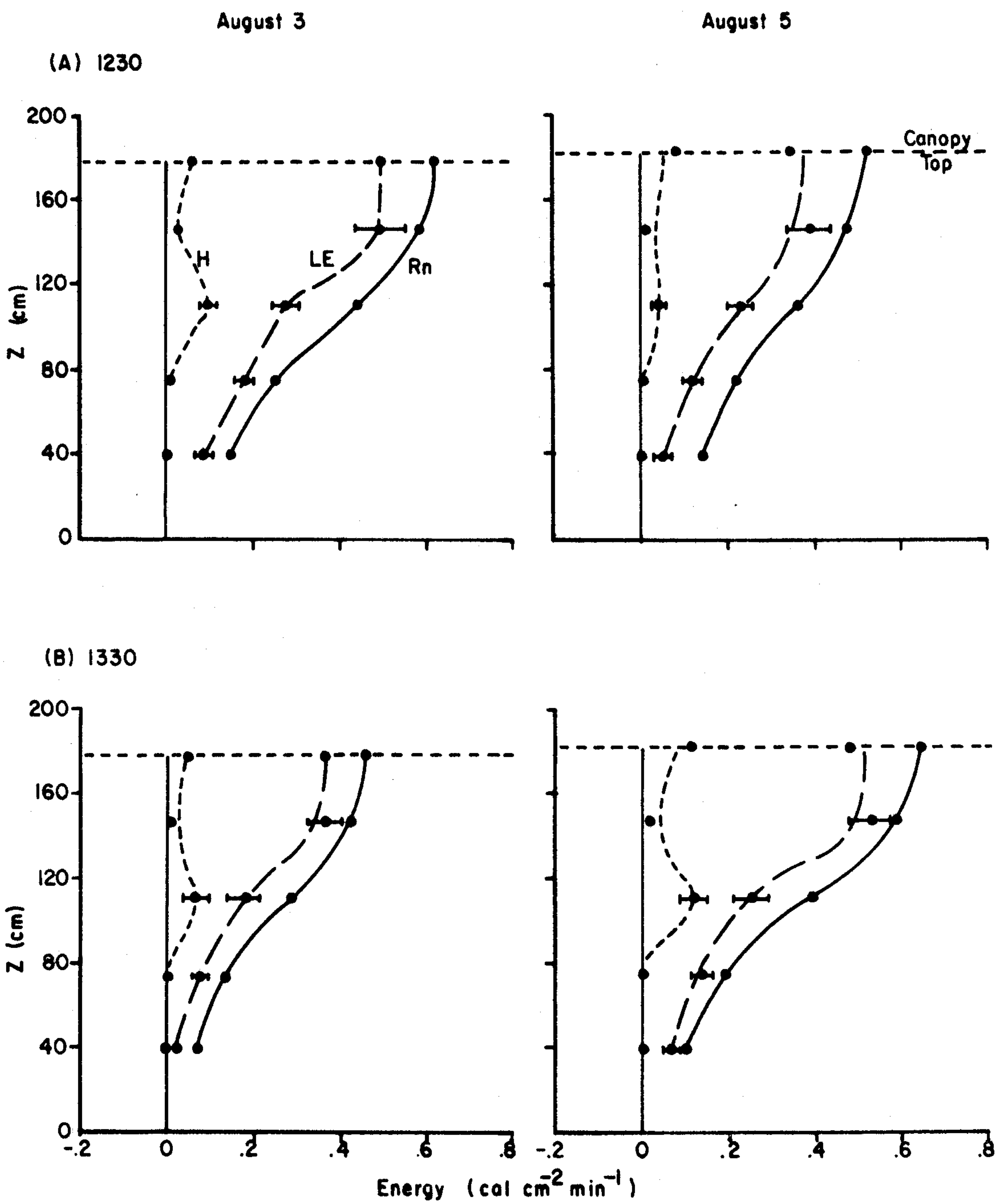

Figure 24. Rn, LE and H Profiles, August 10 and 13

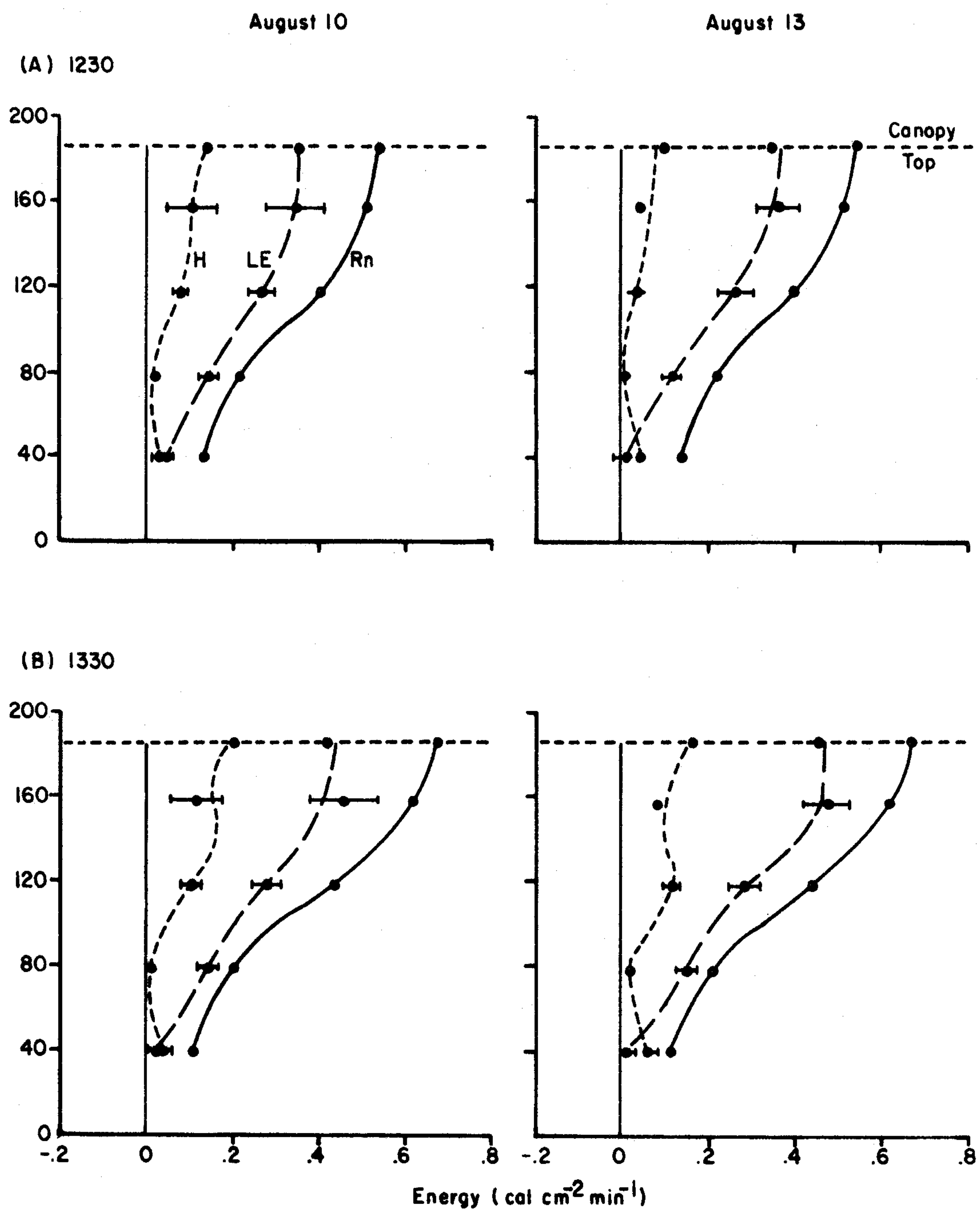

TABLE 5

ERRORS IN LE AND H FOR THE ATMOSPHERE

Date	LE (cal $cm^{-2}min^{-1}$)		H (cal $cm^{-2}min^{-1}$)	
Aug.	1230	1330	1230	1330
3	0.51(±0.17)	0.36(±0.20)	0.05(±0.16)	0.05(±0.19)
5	0.35(±0.18)	0.49(±0.16)	0.08(±0.17)	0.12(±0.15)
10	0.35(±0.12)	0.42(±0.15)	0.14(±0.12)	0.21(±0.14)
13	0.35(±0.10)	0.46(±0.11)	0.10(±0.09)	0.17(±0.10)

FIGURE 25. Rn, LE AND H PROFILES IN CORN, AUGUST 3, 5, 6 (mean data)

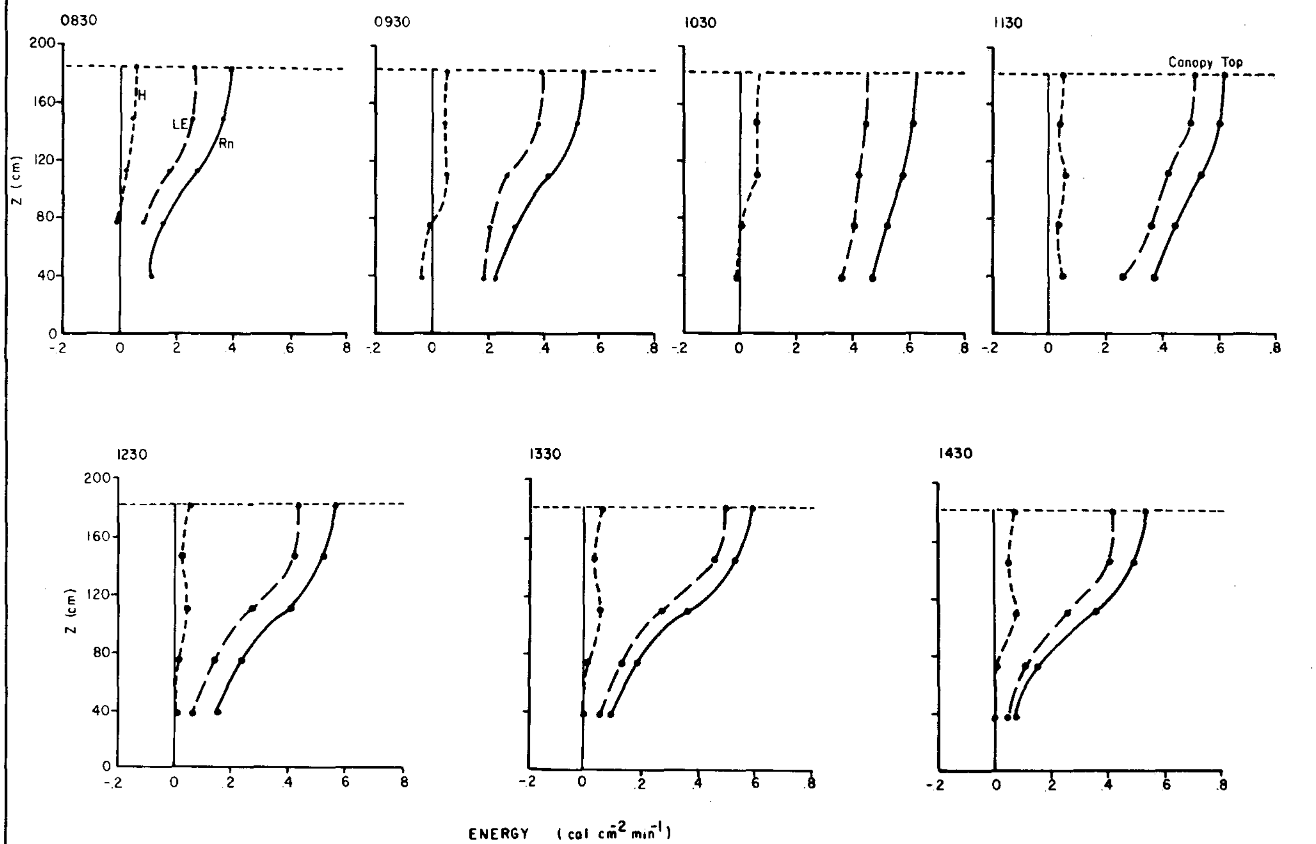

the lowest layer (40 - 80 cm) was supplemented by sensible heat transfer from above. By mid-day (1130), all the fluxes were positive, but the sensible heat term remained very small, and, from 1230 until 1430, H_{40} was zero. The predominance of LE as an energy user is shown by the variation of the ratio LE/Rn within the canopy (Table 6). A diurnal trend is apparent at all levels. For the entire crop, the value of LE/Rn increased from 0.66 in the morning to a maximum of about 0.80 by mid-day. This value was maintained until mid-afternoon. A similar variation is apparent for the upper layer of the canopy, illustrating the close coupling between these zones. However, for the remainder of the canopy, the diurnal pattern is different. The ratios increased from a minimum at 0830 to a maximum around mid-day and then decreased to about the early morning level. This is illustrated in the variation at the 110 cm level. The values of the ratio varied with height, and, for all hours, they tended to decrease with depth. However, the decrease was slight, and the largest variation occurred at 1230 when LE/Rn changed from 0.81 at 146 cm to 0.43 at 38 cm. The reason for this decrease was probably physiological since, towards the base of the canopy, the leaves were older and would be less active in transpiration (Begg et al. 1964).

The source and sink distributions for energy within the canopy were obtained by approximate differentiation of the vertical flux profiles with respect to height. In this

TABLE 6

PERCENT OF NET RADIATION USED IN TRANSPIRATION WITHIN CORN, $LE/Rn \cdot 10^2$. SAMPLE PERIOD 1

Time	Height (cm)				
	38	74	110	146	Entire crop
0830	--	53	65	69	66
0930	83	70	64	73	72
1030	73	76	70	71	70
1130	70	82	78	83	84
1230	43	59	69	81	77
1330	56	71	75	87	83
1430	63	73	68	84	80

context, approximate differentiation means that the finite difference ratios were accepted as a close approximation to the derivative. These data are shown in Figure 26. The shape of the sink distribution for net radiation was approximately Gaussian throughout the day, but the maximum changed in position and in intensity in response to the diurnal variation of the penetration of net radiation. At 0830 and 0930, the maximum absorption of net radiation occurred at 100 cm, which corresponded to the maximum leaf area density. At all levels, the sink strengths were similar. By 1030, when the sun was shining parallel to the rows, the intensity of absorption decreased at all levels, and the level of maximum absorption penetrated to 80 cm. From 1130 until 1430, the sequence of variation of the sink distribution of net radiation represented a return to the early morning pattern, with the maximum absorption again centred at 100 cm. Also, the intensity of the maximum sink strength progressively increased to a maximum value of 6.4×10^{-3} cal $cm^{-3}min^{-1}$ at 1430.

In contrast, the source distributions for latent and sensible heat were not always Gaussian. Also, the maximum source intensities were not at the same level. At 0930, the maximum source strength for latent heat occurred at 120 cm, and it was larger than that for net radiation. The extra energy was drawn from the air, meaning that the plants at this level were cooler than the surrounding air. For all levels above and below, the intensity of the source strengths for

FIGURE 26. SOURCES AND SINKS OF Rn, LE AND H IN CORN, AUGUST 3,5,6 (mean data)

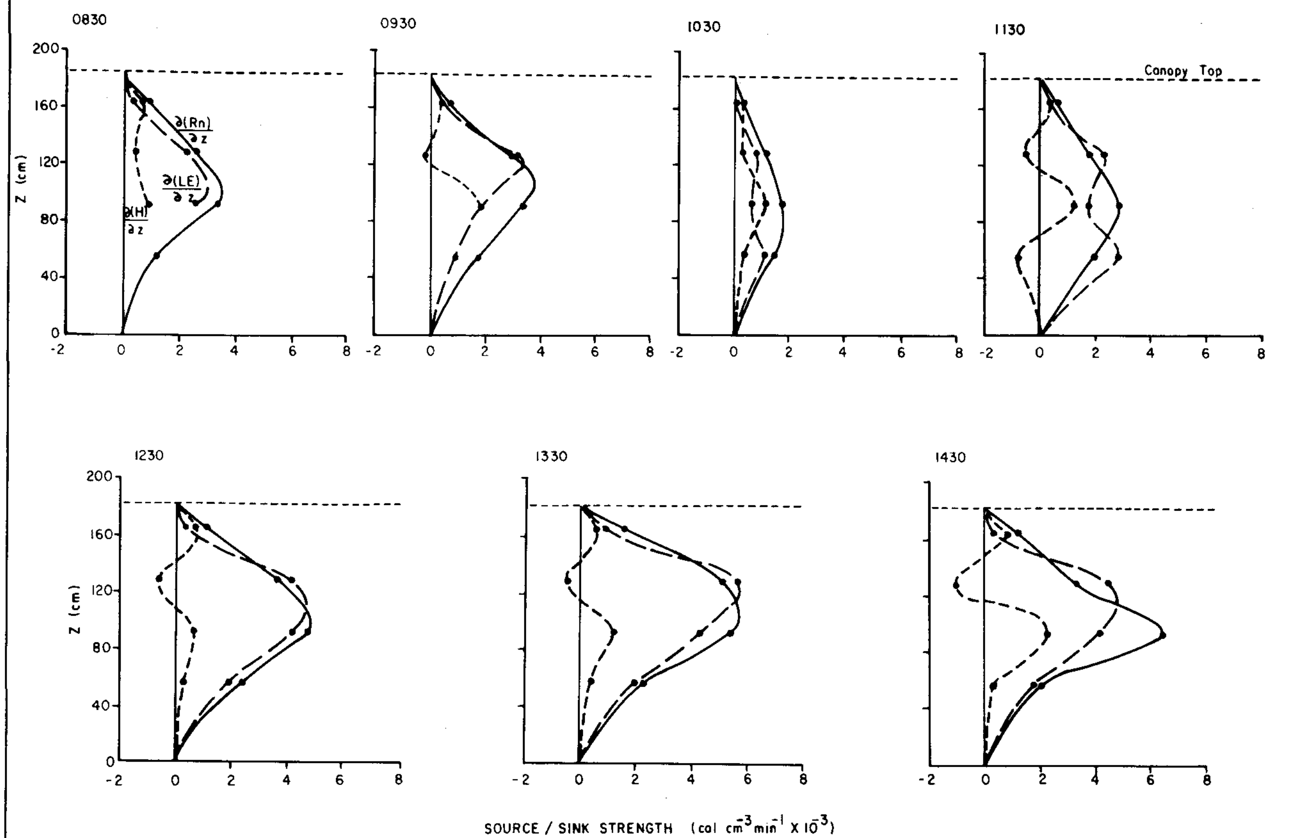

latent and sensible heat were equal. When the penetration of net radiation was at a maximum for all levels at 1030, the source distribution for latent heat exhibited two maxima, one at 60cm and the other at 120 cm, with a relative minima at 100 cm, the point of maximum absorption of net radiation. Other workers have found that the distribution of latent heat sources contained only one maximum for corn in the zone of maximum leaf density (Lemon 1968, Uchijima 1966) and similarly for pine forest (Denmead 1964) and bullrush millet (Begg et al. 1964). The double maxima in the source distribution for latent heat persisted and became more pronounced at 1130, when the intensity of the sources for latent heat exceeded the sink strengths for net radiation, and, therefore, resulted in sinks for sensible heat at the two levels.

Further investigation of the double maxima in the profiles of latent heat source strength is required. The intensity of the latent heat flux depends directly upon biological regulation (stomatal regulation) (Djavanchir 1970, Druilhet et al. 1971). Therefore, it is possible that the relative minimum in the source strength for latent heat at 90 cm was the result of stomatal control. However, since no data on stomatal activity were collected, this remains a point of conjecture.

From 1230 to 1430, the source distribution for latent heat returned to the early morning pattern, with a single maximum centred at 120 cm. The absolute value at this level always exceeded the sink strength for net radiation, and reached a maximum value of 5.6×10^{-3} cal $cm^{-3} min^{-1}$ at 1330. Below the 120 cm level, the source strength for latent heat diminished, and the canopy energy exchange was characterized by an increasing contribution from sensible heat transfer.

(b) Sample period 2. The four-day mean flux profiles for this period appear in Figure 27. The data records for this period were more complete and covered a complete daylight cycle of canopy energy exchange. During this period, sensible heat flux was a more important energy user than in the earlier sampling period which reflects the decrease in the physiological function of transpiration as the canopy approached senescence (Leopold 1961). This is shown in the generally lower values of the ratio LE/Rn (Table 7). The values at the base of the canopy are significantly lower than those for the rest of the canopy, particularly during the mid-day period when the data are most representative. The leaf density had decreased and the older leaves towards the base of the crop were less active in transpiration. In general, the sensible heat flux at the lowest layer was greater than the latent heat flux. This is particularly striking at 1030.

At 0830, the transpiration at the base of the canopy was augmented by negative sensible heat fluxes below 100 cm. Similarly, at 1730, the transpiration was maintained at a rate in excess of the available energy from net radiation for the whole canopy depth below 160 cm.

FIGURE 27. Rn, LE AND H PROFILES IN CORN, AUGUST 10,11,12,13 (mean data)

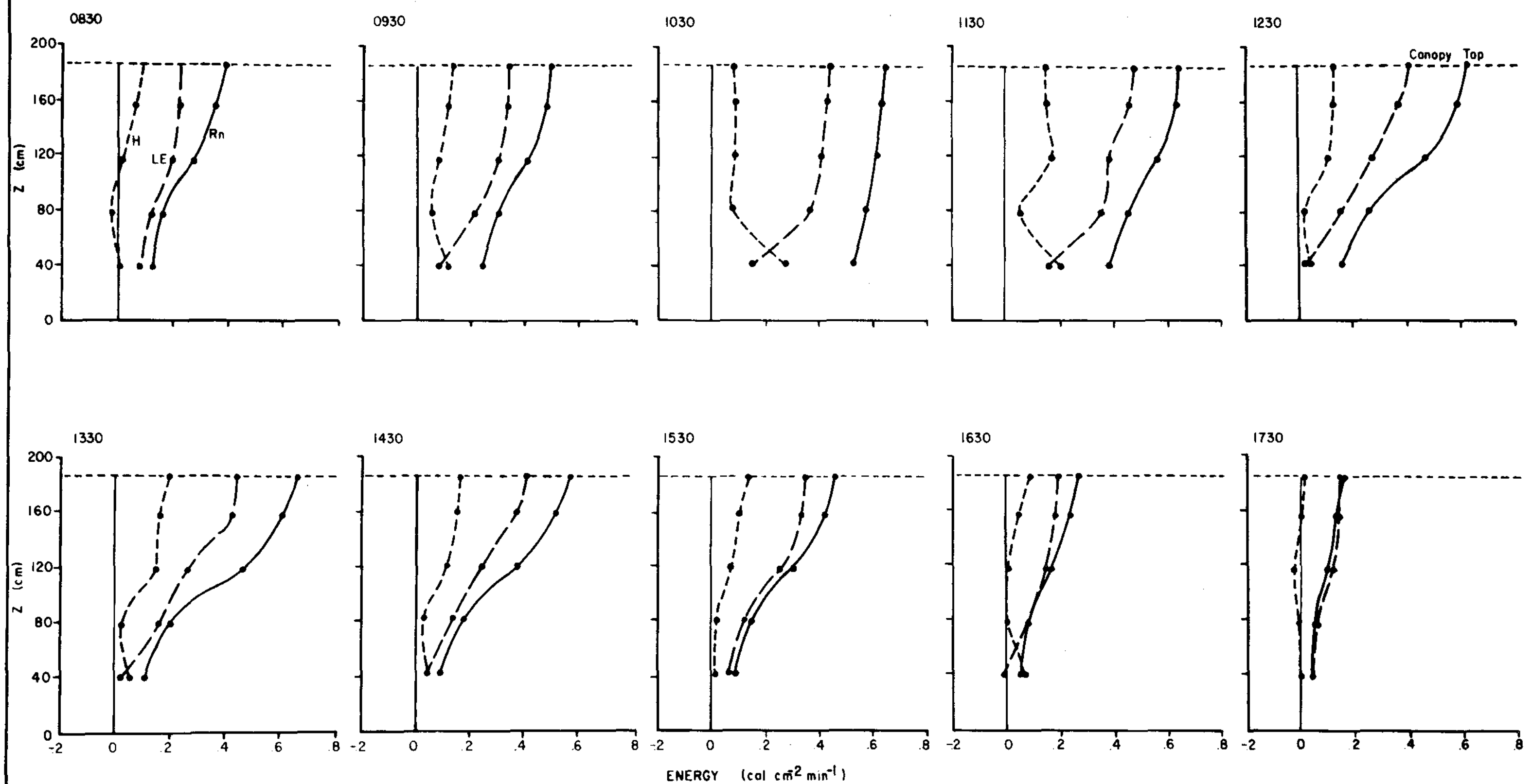

TABLE 7

PERCENT OF NET RADIATION USED IN TRANSPIRATION WITHIN CORN, $LE/Rn \cdot 10^2$. SAMPLE PERIOD 2

Time	Height (cm)				
	40	79	118	157	Entire Crop
0830	67	75	71	61	59
0930	33	77	74	71	68
1030	28	65	67	67	68
1130	42	80	68	73	75
1230	19	58	57	64	65
1330	18	80	59	70	67
1430	44	76	65	71	70
1530	75	85	86	76	73
1630	-20	100	94	78	73
1730	100	120	133	108	87

The relative contribution of different layers of the canopy to the energy exchange is shown in the source strength distributions in Figure 28. At 0830, the maximum source strength for latent heat, at 100 cm, corresponded with the maximum sink strength for net radiation. Above this point, sensible heat was the principal contributor to energy exchange with a source strength of 1.5×10^{-3} cal $cm^{-3}min^{-1}$ compared to 0.3×10^{-3} cal $cm^{-3}min^{-1}$ for latent heat. By 0930, the maximum source strength for latent heat had penetrated to 60 cm, where it was more than double the sink strength for net radiation (3.6×10^{-3} compared to 1.6×10^{-3} cal $cm^{-3}min^{-1}$). By 1130, the source distribution for latent heat was characterized by two maxima: at 140 cm and 60 cm. This is the same pattern as observed during the earlier sampling period, but now the strength of the sources is larger. In contrast to the earlier period, the double maxima in the source distribution for latent heat was maintained until mid-afternoon. By 1530, the pattern of sources for latent heat and sensible heat returned to the early morning configuration with the maximum source strength for latent heat at 100 cm.

The most striking feature of the source distribution for latent heat is the magnitude of the source at the base of the canopy. It was always equal to or greater than the sink strength for net radiation. Also, for all profiles except those at 1330 and 1430, the region of the canopy below 100 cm was the most important source area for water vapour.

FIGURE 28. SOURCES AND SINKS OF Rn, LE AND H IN CORN, AUGUST 10, 11, 12, 13 (mean data)

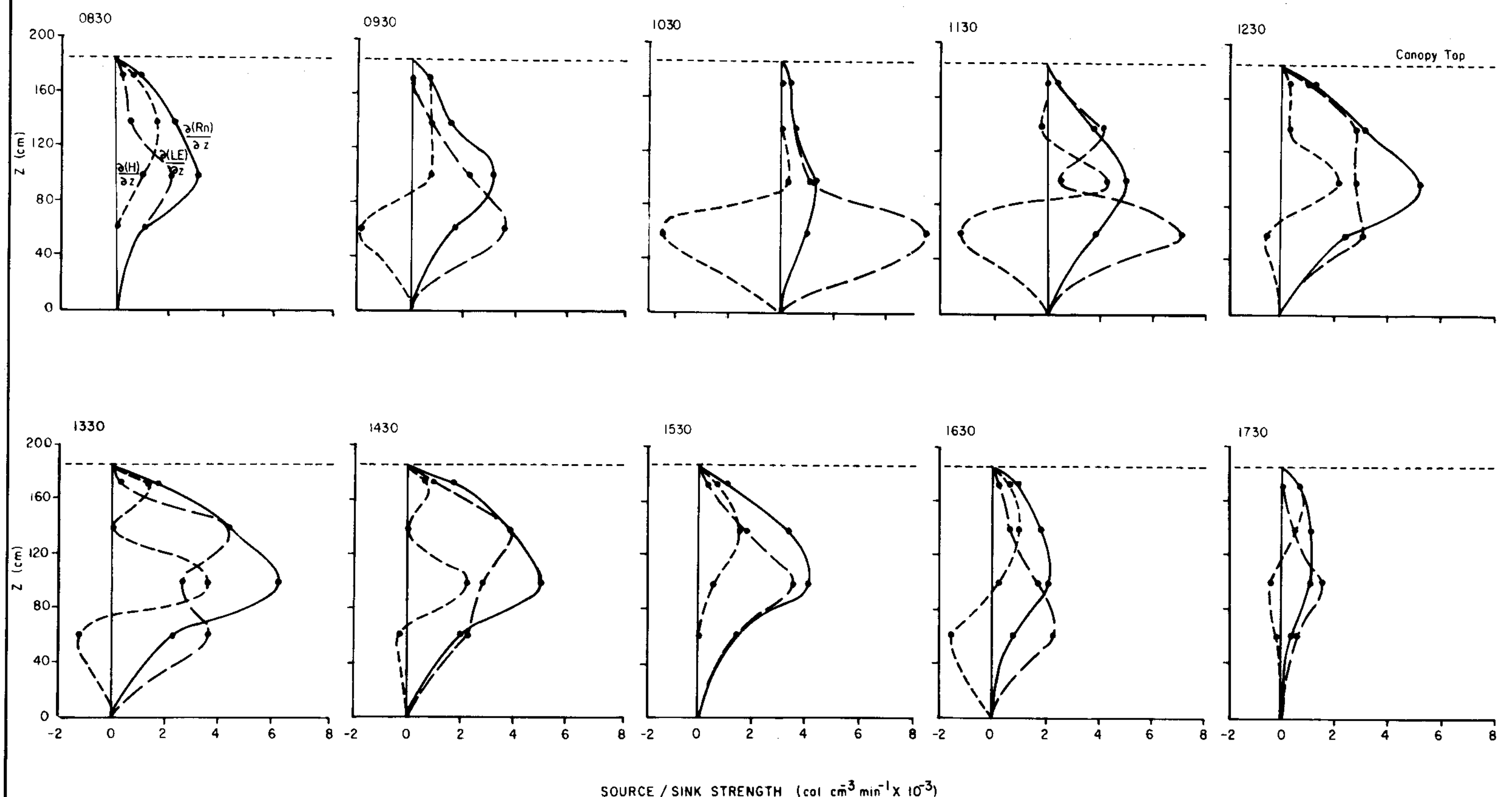

4. Apparent Transfer Coefficients

Previous studies have shown that K decays approximately exponentially with depth in mature crop canopies during daylight periods. These include studies for rice (Uchijima 1962), for a pine forest (Denmead 1964), for bullrush millet (Begg et al. 1964), for corn (Brown and Covey 1966, Wright and Brown 1967) and for sunflowers (Impens 1970). The intensity of the exchange process was visualized as decreasing with depth because of the increased interference of the vegetation. Uchijima (1962) expressed the decay as a function of height as

$$K_z = K_h \exp\{-a(1-z/h)\} \quad , \tag{47}$$

where

K_z = exchange coefficient at height z,

K_h = exchange coefficient at canopy top,

h = canopy height,

a = extinction coefficient.

This model has been evaluated by several workers, and some computed values of the extinction coefficient are presented in Table 8.

However, there is evidence that the decay of turbulence within vegetation is not always exponential. Gillespie and King (1971) found that the transfer coefficient for latent heat did not decrease exponentially in a corn canopy at night.

TABLE 8

EXTINCTION COEFFICIENTS OF THE TRANSFER COEFFICIENT IN SEVERAL CROPS

Crop	a	Source
Corn	2.6	Brown and Covey (1966)
Corn	2.8	Wright and Brown (1967)
Rice	3.1	Uchijima (1962)
Pine	4.25	Denmead (1964)

The minimum occurred at the centre of the canopy, and the value at the base was double that at the top. Allen (1969) presented similar results for corn at mid-day. His explanation for a mid-canopy minimum was that at this point the leaf area density was very large and mixing of air from above was suppressed. This conclusion was based on the fact that simultaneous determination of the profile of K in a thinned corn canopy did not exhibit any minimum at mid-canopy. Druilhet et al. (1971) argued that local large thermal gradients between the plant and the air could induce a significant increase in turbulent mixing within the canopy. Therefore, it appears insufficient to interpret the pattern of turbulence in vegetation on purely mechanical arguments. In corn, they found a marked non-monotonic decrease in K throughout the day. There was a marked local increase in K in the middle zone of the canopy associated with the maximum source strength of sensible heat.

Values of K for the two sample periods in this experiment are shown in Figures 29 and 30. For both periods, the decay of K is not exponential. This is illustrated in Figure 31, which shows the performance of Uchijima's model using a mean value of 2.7 for the extinction coefficient for corn (Table 8). Each point represents a three-day mean value for the first sample period, and a four-day mean for the second. The agreement between actual and predicted decay is poor. In particular, significant departures occur at the middle and

FIGURE 29. TRANSFER COEFFICIENT AS A FUNCTION OF HEIGHT, AUGUST 3,5,6 (mean data)

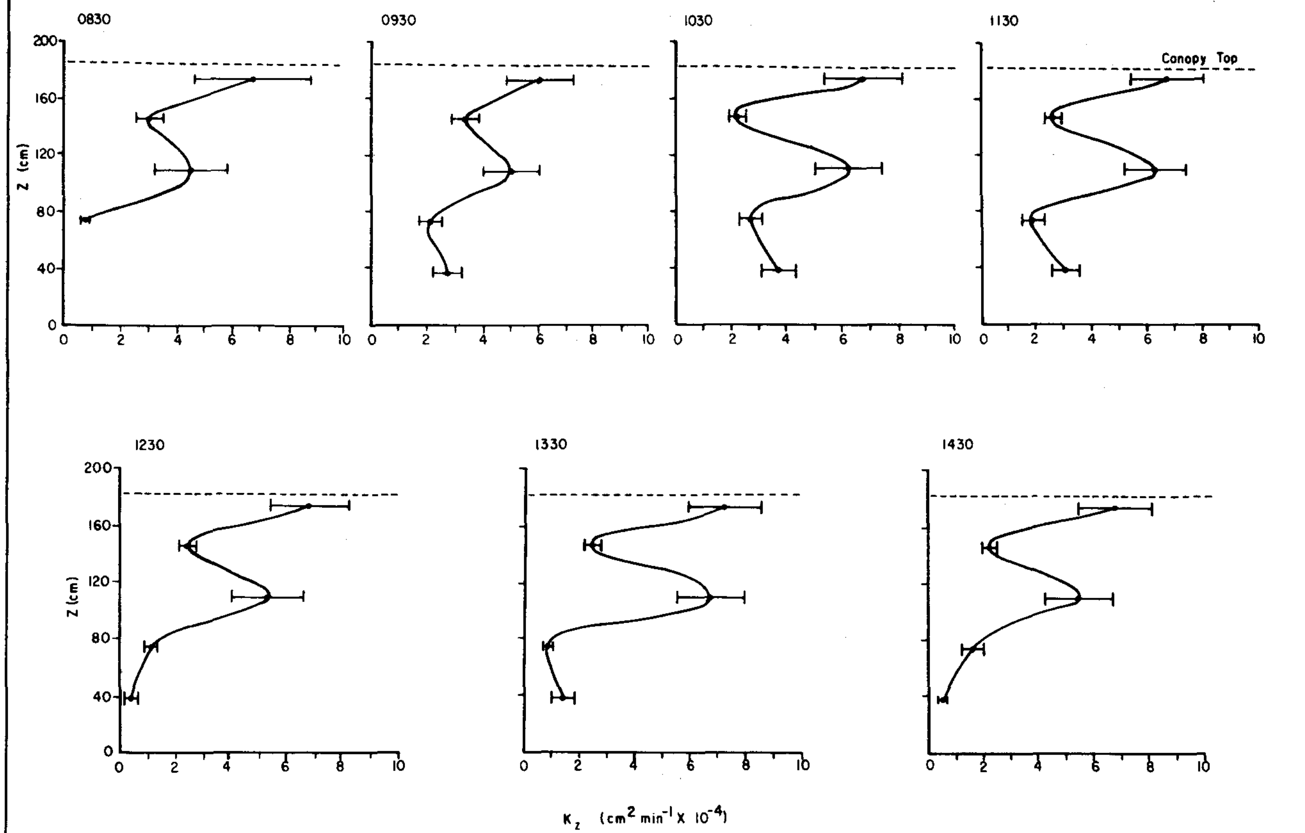

FIGURE 30. TRANSFER COEFFICIENT AS A FUNCTION OF HEIGHT, AUGUST 10, 11, 12, 13 (mean data)

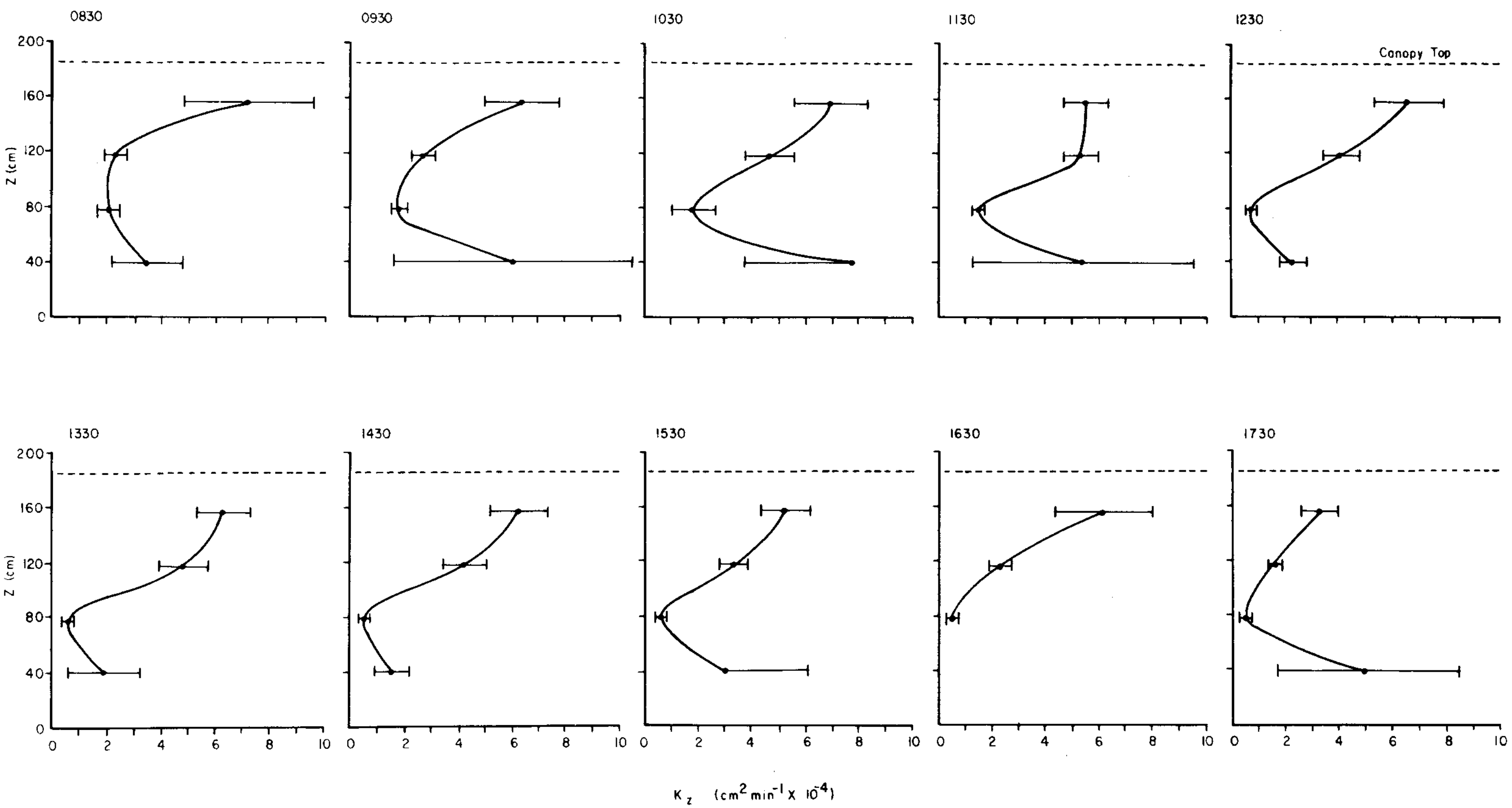

Figure 31. Variation of Dimenionless Transfer Coefficient as a Function of (1-z/h)

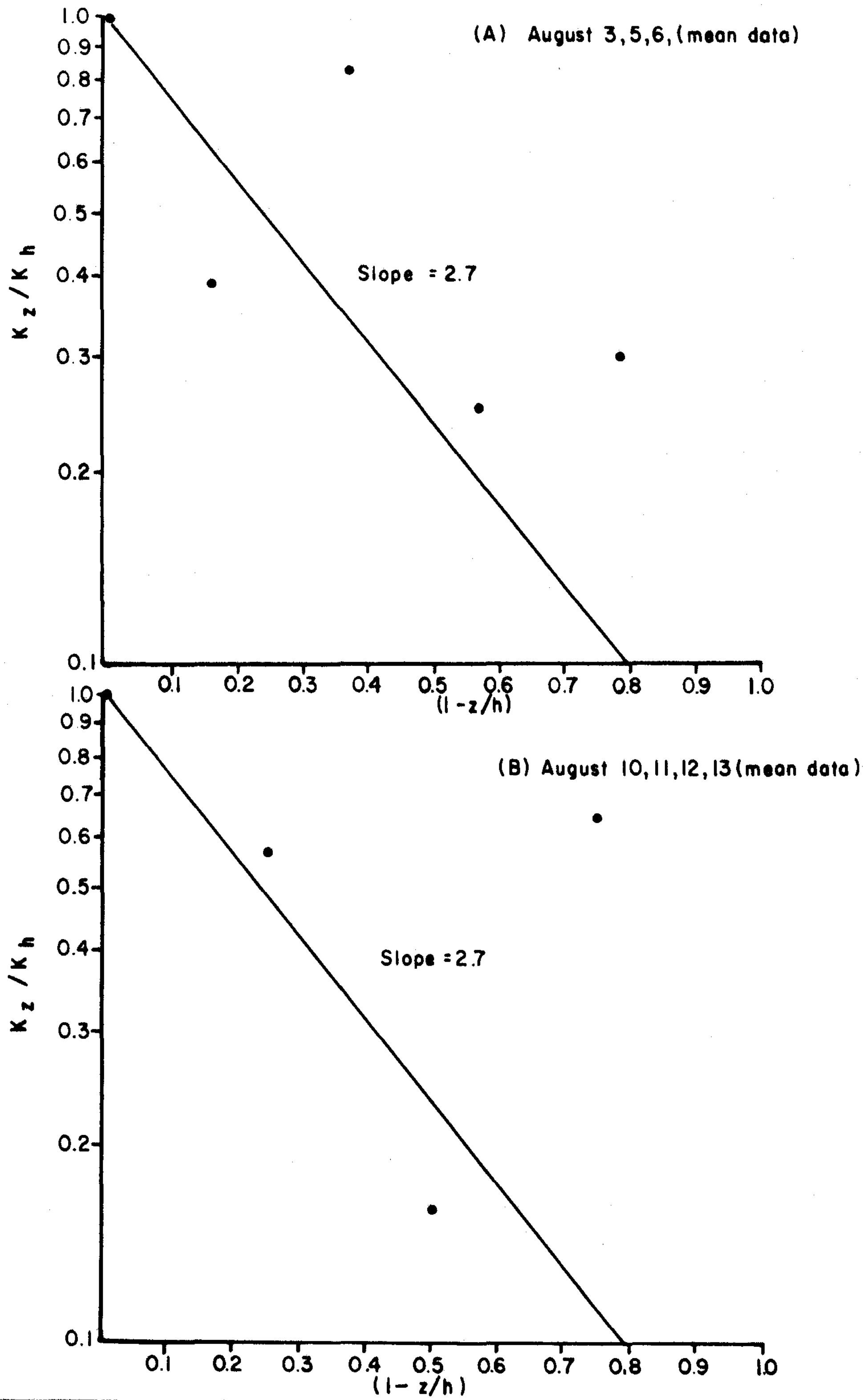

base of the canopy during the first sample period, and at the base of the canopy for the second sample period.

During the first period, the shape of the profiles of K between 80 cm and the top of the canopy is similar. For all hours, K declined rapidly from the top of the crop to a relative minimum at 140 cm. It then increased to a mid-canopy maximum which coincided with the area of maximum leaf area density. For all hours, the magnitude of K_{110} was not significantly different from the value at the top of the crop. The value then declined to another relative minimum at 80 cm. For all hours, except 1230 and 1430, the value at 40 cm was larger than the value at 80 cm. This general tendency for an increase towards the base of the crop was probably a result of the rapid decrease of leaf area density at this level, leading to greater turbulent mixing. The presence of a mid-canopy maximum cannot be explained using the simple argument that the intensity of turbulent mixing is inversely related to leaf area density (Allen 1969). However, the mid-canopy increase in K coincided with the occurrence of the maximum source strength for sensible heat (Figure 26). Therefore, the largest thermal gradients between the plant surfaces and the air occurred at this level, and the intensity of turbulent mixing was augmented by the increased thermal convection (Druilhet et al. 1971).

In contrast, during the second sample period, there was no evidence of a mid-canopy maximum in the profiles of K.

This is attributed to the occurrence of the maximum thermal convection towards the base of the canopy (Figure 28). The values of K declined to a minimum at 80 cm for all profiles, and, as in the first period, the value at the base of the canopy (40 cm), exceeded the value at 80 cm. Also, the values of K at the base of the canopy for the second period were greater than those for the first, for all comparable hours (Table 9). This was probably due to decreased leaf area density at this level, and the larger temperature gradients characteristic of the second period in response to the decreased transpiration. The increase in the magnitude of the temperature gradients would have enhanced convective mixing, and, therefore, caused an increase in K. Also, during the period of maximum penetration of net radiation, the value of K at the lowest level increased sharply. This is shown in the 0930, 1030 and 1130 profiles (Figure 30) where $K_{40} > K_{156}$.

In conclusion, the diffusion for all levels in this canopy was turbulent since K greatly exceeded the molecular diffusivities of sensible heat and water vapour in air. For both sample periods, the pattern of turbulence did not show an exponential decrease with depth. There were significant increases in K, probably due to thermal convection. The level of maximum thermal convection changed from the middle to the base of the canopy from the first to the second sample periods.

TABLE 9

TRANSFER COEFFICIENTS ($cm^2 min^{-1} \times 10^{-4}$),

AT THE BASE OF THE CANOPY

Time	Sample period 1	Sample period 2
	K_{38}	K_{40}
0930	2.7	6.1
1030	3.7	7.8
1130	3.1	5.4
1230	0.45	2.3
1330	1.4	1.9
1430	0.5	1.6

CHAPTER 6

CONCLUSIONS

The principal finding of this study is that the attenuation of net radiation within the canopy shows a significant diurnal variation. Even though the crop was very dense (max. L.A.I. = 5.6), the effect of row orientation was pronounced. When the sun was shining parallel to the row, irrespective of the zenith angle, the attenuation of net radiation was at a minimum. Hourly values of canopy net radiation could not be satisfactorily estimated under these conditions by a simple form of the exponential model which uses the cumulative L.A.I. and a constant extinction coefficient (k). The Impens and Lemeur (1969) modification to the exponential model did not improve the estimate. It is shown that a satisfactory estimate (±10%) is possible with a modified exponential model which incorporates both a zenith and azimuth angle dependence of k. In this model, k showed no significant variation for the essentially clear sky conditions encountered. Further studies are required to determine whether or not it will vary for different sky conditions. Also, since satisfactory estimates of canopy net radiation for corn have been found using the simple exponential model (Allen et al. 1962, Brown and Covey 1966), it is apparent that all corn canopies do not possess similar radiation climates. Future studies could determine the variation in net radiation attenuation for different varieties of the same crop.

Special efforts are necessary to ensure that representative spatial samples of canopy net radiation are obtained. The data collected with the manual probe show that there were large horizontal variations in the flux, particularly in the zone of maximum leaf density. Routine measurements were impossible with a single standard radiometer. The measurement problem and errors were minimized by the use of linear sensors.

Similarly, temperature and humidity measurements are difficult in canopies. The attempt at solving this problem by the use of long, perforated, plastic sampling tubes fixed at each level failed. Large systematic errors (1.5C) resulted from radiative heating. Also, the temperature and humidity differences should be of high accuracy (±0.01C and ±0.05mbar, respectively) to preserve an accuracy of ±10% to ±20% in the computed fluxes of latent and sensible heat, and an accuracy of ±25% in the turbulent transfer coefficient. It is shown that this accuracy is possible using a combination of thermopiles and thermocouples but is impossible using single thermocouples.

The one-dimensional flux equations for latent and sensible heat transfer did not always provide a satisfactory framework for the study of diffusion within the canopy. It is inferred that significant horizontal divergence occurred under certain conditions of wind speed and wind direction. Since horizontal gradients of temperature and humidity were not measured, a complete analysis of the problem was impossible.

Evaporation was the principal energy user in the canopy for both sample periods. During the second period, the sensible heat flux increased in importance because the canopy was older and less active in transpiration. The most interesting feature of the source/sink distributions was the double maxima in the source strength for LE. This feature appeared during both periods and was most pronounced around solar noon. It is hypothesized that the relative minimum at the centre of the canopy could have been caused by stomatal control on the intensity of the latent heat flux. However, since no data on stomatal activity were available, this remains a point of conjecture. As the attenuation of net radiation increased after solar noon, the profiles of the source strength for LE returned to a single maximum which was located in the zone of maximum leaf area density (two-thirds canopy height). In contrast, during the second period, the most important source region for LE moved to a lower level which coincided with the centre of the tiller layer (one-third canopy height).

The diffusion for all levels in the canopy was turbulent. The turbulence did not decay exponentially as has been indicated by some previous studies in corn during daylight periods (Brown and Covey 1966, Wright and Brown 1967). There were zones which experienced marked increases in turbulence probably as a result of increased thermal convection (Druilhet et al. 1971). During the first sample period, well-developed relative maxima in the profiles of K occurred at the centre and base of the canopy. The former was probably caused by increased thermal convection and the latter by decreased leaf density. During the second sample period, the base of the canopy exhibited a significant increase in turbulent exchange. Also, for the whole canopy, the K values were higher during the second period.

Further studies are necessary to provide more information on the characteristics of the exchange process and energy partitioning within canopies, since they are basic inputs into existing simulation models of canopy microclimate (Waggoner and Reifsnyder 1968).

APPENDIX I

LIST OF SYMBOLS

Roman Capital Letters

A Leaf area (cm^2)

C Calibration constant ($C\mu v^{-1}$)

Ca Heat capacity of air (cal $cm^{-3}C^{-1}$)

Cc Specific heat of plant material (cal $g^{-1}C^{-1}$)

Cm Heat capacity of mineral matter in soil (cal $cm^{-3}C^{-1}$)

Co Heat capacity of organic matter in soil (cal $cm^{-3}C^{-1}$)

Cp Specific heat of moist air at constant pressure (0.2396 cal $g^{-1}C^{-1}$)

Cs Heat capacity of soil (cal $cm^{-3}C^{-1}$)

Cw Heat capacity of water (cal $cm^{-3}C^{-1}$)

D Wet-bulb depression (C)

DA Disc area (cm^2)

DW Disc weight (g)

Fc Downward cumulative leaf area index (dimensionless)

Fc' Effective downward cumulative leaf area index (dimensionless)

G Soil heat flux (cal $cm^{-2}min^{-1}$)

H Sensible heat flux between surface and air (cal $cm^{-2}min^{-1}$)

I&Io Final and initial monochromatic radiant fluxes in Beer's Law (cal $cm^{-2}min^{-1}micron^{-1}$)

K Apparent transfer coefficient ($cm^2 min^{-1}$)

K_H Transfer coefficient for sensible heat ($cm^2 min^{-1}$)

K_W Transfer coefficient for water vapour ($cm^2 min^{-1}$)

L Latent heat of vapourization for water (594.9 - 0.51T cal g^{-1})

LE Latent heat flux between surface and air (cal $cm^{-2} min^{-1}$)

P Rate of energy consumption by photosynthesis (cal $cm^{-2} min^{-1}$)

R Recorder output (μV)

R' Specific gas constant (mbar $cm^3 g^{-1} C^{-1}$)

Rn Net radiation flux (cal $cm^{-2} min^{-1}$)

Sy Standard error of estimate (various units)

T Dry-bulb temperature (C)

Ts Soil temperature (C)

Tw Wet-bulb temperature (C)

W Leaf weight (g)

Xa Volume fraction of air in soil (dimensionless)

Xm Volume fraction of mineral matter in soil (dimensionless)

Xo Volume fraction of organic matter in soil (dimensionless)

Xw Volume fraction of water in soil (dimensionless)

Roman Lower Case Letters

a Extinction coefficient for turbulent transfer coefficient (dimensionless)

e Vapour pressure (mbar)

e_s Saturation vapour pressure (mbar)

h Canopy height (cm)

k	Extinction coefficient for net radiation (dimensionless)
k_*	Extinction coefficient in Beer's Law (dimensionless)
m	Optical air mass (dimensionless)
p	Atmosphereic pressure (mbar)
r	Correlation coefficient (dimensionless)
t	Time (min)
u	Horizontal wind speed (cm $time^{-1}$)
z	Height (cm)

Greek Letters

$\alpha,\beta'\gamma'$	Constants in saturation vapour pressure equation of Murray
β	Bowen ratio (dimensionless)
γ	Psychrometric constant (mbar C^{-1})
ε	Ratio of mole weight of water to air (dimensionless)
ζ	Zenith angle (^{o})
θ	Potential temperature (C)
λ	Thermal conductivity of soil (cal $C^{-1}cm^{-1}min^{-1}$)
ρ	Density of air (g cm^{-3})
ρ_c	Density of plant material (g cm^{-3})
ϕ	Relative solar azimuth (^{o})

Suffixes and Mathematical Operators

(B is sample parameter)

$\overline{B}$	Time-average
B_z	Value at reference level z

B_0	Value at ground surface
∇_H	$\partial/\partial x + \partial/\partial y$
Δ	Finite increment

APPENDIX II

SOLUTIONS FOR EQUATIONS 32 AND 34

Equation 32 written for LE and H becomes

$$\delta LE = \frac{\partial LE}{\partial Rn}\,\delta Rn + \frac{\partial LE}{\partial G}\delta G + \frac{\partial LE}{\partial \overline{\Delta\theta}}\,\delta\overline{\Delta\theta} + \frac{\partial LE}{\partial \overline{\Delta e}}\,\delta\overline{\Delta e} \quad ,$$

and

$$\delta H = \frac{\partial H}{\partial Rn}\,\delta Rn + \frac{\partial H}{\partial G}\,\delta G + \frac{\partial H}{\partial \overline{\Delta\theta}}\,\delta\overline{\Delta\theta} + \frac{\partial LE}{\partial \overline{\Delta e}}\,\delta\overline{\Delta e} \quad ,$$

in which

$$\frac{\partial LE}{\partial Rn} = \left(1 + \gamma\,\frac{\overline{\Delta\theta}}{\overline{\Delta e}}\right)^{-1} \quad ,$$

$$\frac{\partial LE}{\partial G} = -\left(1 + \gamma\,\frac{\overline{\Delta\theta}}{\overline{\Delta e}}\right)^{-1} \quad ,$$

$$\frac{\partial LE}{\partial \overline{\Delta\theta}} = -\frac{Rn - G}{\left(1 + \gamma\,\frac{\overline{\Delta\theta}}{\overline{\Delta e}}\right)^2} \cdot \frac{\gamma}{\overline{\Delta e}} \quad ,$$

$$\frac{\partial LE}{\partial \overline{\Delta e}} = \frac{Rn - G}{\left(1 + \gamma\,\frac{\overline{\Delta\theta}}{\overline{\Delta e}}\right)^2} \cdot \gamma\,\frac{\overline{\Delta\theta}}{\overline{\Delta e}^2} \quad ,$$

and

$$\frac{\partial H}{\partial Rn} = \frac{\gamma\overline{\Delta\theta}}{\overline{\Delta e} + \gamma\,\overline{\Delta\theta}} \quad ,$$

$$\frac{\partial H}{\partial G} = -\frac{\gamma\overline{\Delta\theta}}{\overline{\Delta e} + \gamma\ \overline{\Delta\theta}} \quad ,$$

$$\frac{\partial H}{\partial\overline{\Delta\theta}} = -\frac{(Rn-G)\ \gamma^2\ \overline{\Delta\theta}}{(\overline{\Delta e} + \gamma\ \overline{\Delta\theta})^2} + \frac{(Rn-G)\ \gamma}{\overline{\Delta e} + \gamma\ \overline{\Delta\theta}} \quad ,$$

and

$$\frac{\partial H}{\partial\overline{\Delta e}} = -\frac{(Rn-G)\ \gamma\ \overline{\Delta\theta}}{(\overline{\Delta e} + \gamma\overline{\Delta\theta}\ )^2} \quad .$$

The solution to the partial derivatives in equation 34 are

$$\frac{\partial K}{\partial LE} = \frac{\Delta z}{\rho\ L\ \frac{\varepsilon}{p}\ \overline{\Delta e}} \quad ,$$

and

$$\frac{\partial K}{\partial\overline{\Delta e}} = \frac{\Delta z\cdot LE}{\rho\ L\ \frac{\varepsilon}{p}\ \overline{\Delta e}^2} \quad .$$

APPENDIX III

DIURNAL VARIATION IN RELATIVE INTENSITY OF CANOPY NET RADIATION (LINEAR SENSORS)

DATE	TIME	Rn_h (cal $cm^{-2}min^{-1}$)	$\frac{Rn_{z_3}}{Rn_h}$	$\frac{Rn_{z_2}}{Rn_h}$	$\frac{Rn_{z_1}}{Rn_h}$
August	E.S.T.				
14	0730	.18	.50	.28	.17
	0830	.32	.72	.63	.28
	0930	.47	.94	.77	.40
	1030	.59	.97	.73	.68
	1130	.65	.97	.72	.43
	1230	.64	.92	.48	.23
	1330	.52	.73	.28	.17
	1430	.55	.82	.31	.13
	1530	.30	.83	.33	.17
	1630	.27	.63	.26	.15
	1730	.15	.67	.13	.13
20	0830	.38	-	.58	.24
	0930	.56	.93	.68	.36
	1030	.70	1.10	-	-
	1130	.78	1.14	.85	.46
	1230	.80	1.05	.53	.24

DATE	TIME	Rn_h (cal $cm^{-2}min^{-1}$)	$\frac{Rn_{z_3}}{Rn_h}$	$\frac{Rn_{z_2}}{Rn_h}$	$\frac{Rn_{z_1}}{Rn_h}$
<u>August</u>	<u>E.S.T.</u>				
20	1330	.76	.84	.12	.09
	1430	.67	.58	.07	.06
	1530	.52	.73	.12	.12
	1630	.36	.31	-	-
	1730	.16	.56	-	-
21	0730	.19	.32	.21	.11
	0830	.38	.58	.47	.29
	0930	.55	1.02	.73	.71
	1030	.69	1.07	1.13	.91
	1130	.76	1.09	.89	.39
	1230	.78	.96	.54	.22
	1330	.75	.99	.09	.11
	1430	.66	.61	.12	.06
	1530	.53	.72	.13	.11
	1630	.37	.32	-	.08
	1730	.16	.56	-	-
22	0730	.20	.30	.25	.15
	0830	.38	.61	.50	.24
	0930	.55	1.00	.76	.69
	1030	.68	1.06	1.16	.90
	1130	.76	1.07	.79	.37
	1230	.78	.97	.55	.28

DATE	TIME	Rn_h (cal $cm^{-2}min^{-1}$)	$\frac{Rn_{z_3}}{Rn_h}$	$\frac{Rn_{z_2}}{Rn_h}$	$\frac{Rn_{z_1}}{Rn_h}$
August	E.S.T.				
22	1330	.75	.69	.12	.08
	1430	.65	.49	.08	.05
	1530	.52	.81	.08	.17
	1630	.35	.34	.03	.09
	1730	.16	.44	-	-
23	0730	.22	.41	.32	.23
	0830	.37	.57	.49	.24
	0930	.54	.85	.72	.67
	1030	.67	.99	.99	.88
	1130	.60	-	.66	.33
	1230	.73	-	.48	.26
	1330	.75	.71	.19	.11
	1430	.64	.50	.13	.06
	1530	.51	.80	.14	.24
	1630	.34	.35	.15	.09
	1730	.16	.56	-	-
24	0730	.19	.26	.26	.16
	0830	.38	.53	.53	.26
	0930	.54	.91	.76	.67
	1030	.66	.98	1.05	.89
	1130	.74	.97	.77	.34
	1230	.75	.92	.51	.32

DATE	TIME	Rn_h (cal $cm^{-2}min^{-1}$)	$\frac{Rn_{z_3}}{Rn_h}$	$\frac{Rn_{z_2}}{Rn_h}$	$\frac{Rn_{z_1}}{Rn_h}$
August	E.S.T.				
24	1330	.73	.66	.19	.15
	1430	.61	.49	.13	.07
	1530	.50	.68	.14	.22
	1630	.33	.27	.09	.12
	1730	.14	.50	-	.07
25	0830	.36	.58	.56	.22
	0930	.52	.94	.85	.63
	1030	.65	1.00	1.08	.86
	1130	.73	.97	.71	.30
	1230	.75	.84	.45	.32
	1330	.61	.67	.26	.13
	1430	.61	.52	.20	.05
	1530	.48	.48	.25	.10
	1630	.28	.39	.14	.45

APPENDIX IV

TEMPERATURE AND VAPOUR PRESSURE PROFILES IN CORN

TEMPERATURE AND VAPOUR PRESSURE PROFILES IN CORN, AUGUST 1, 1969

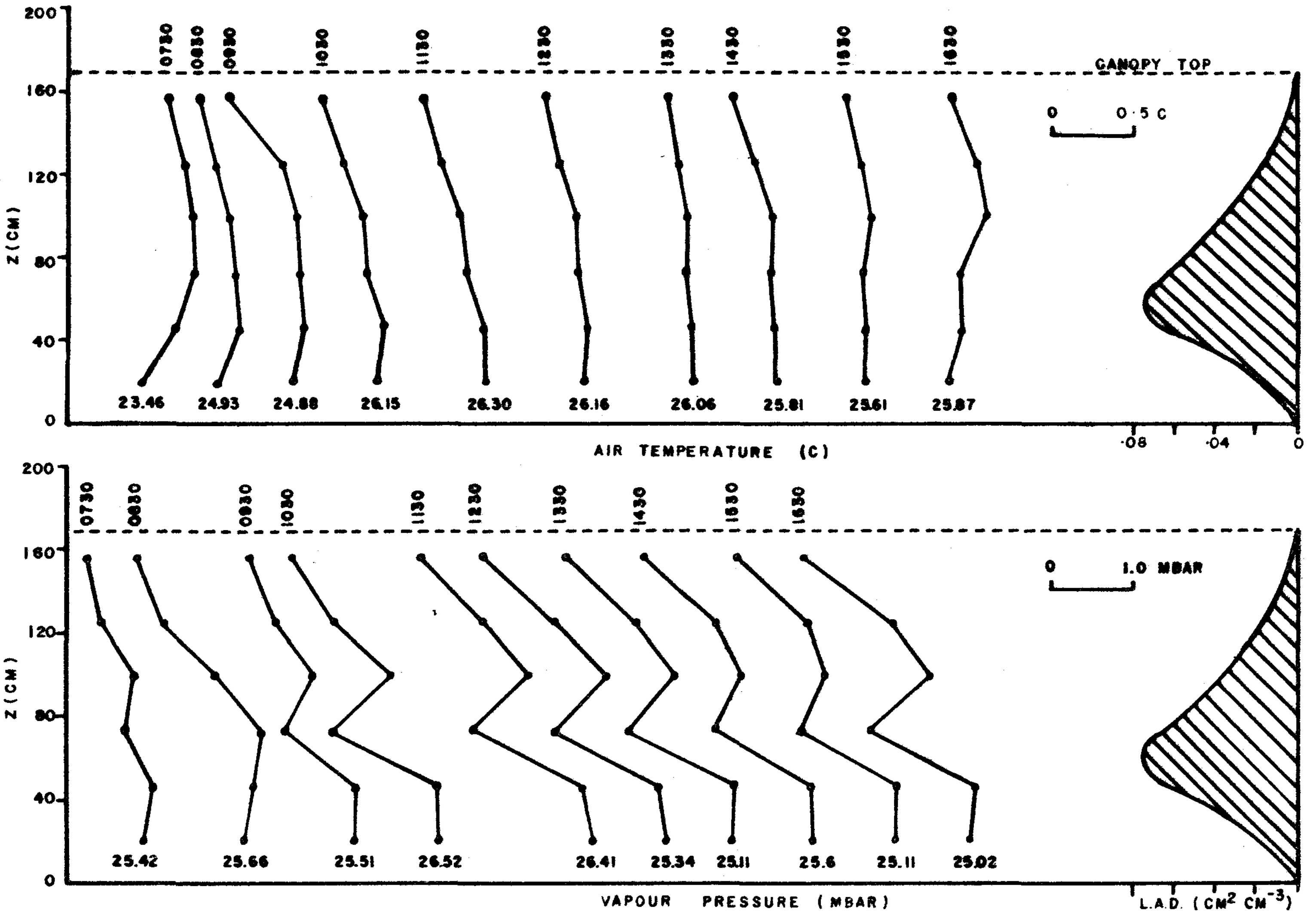

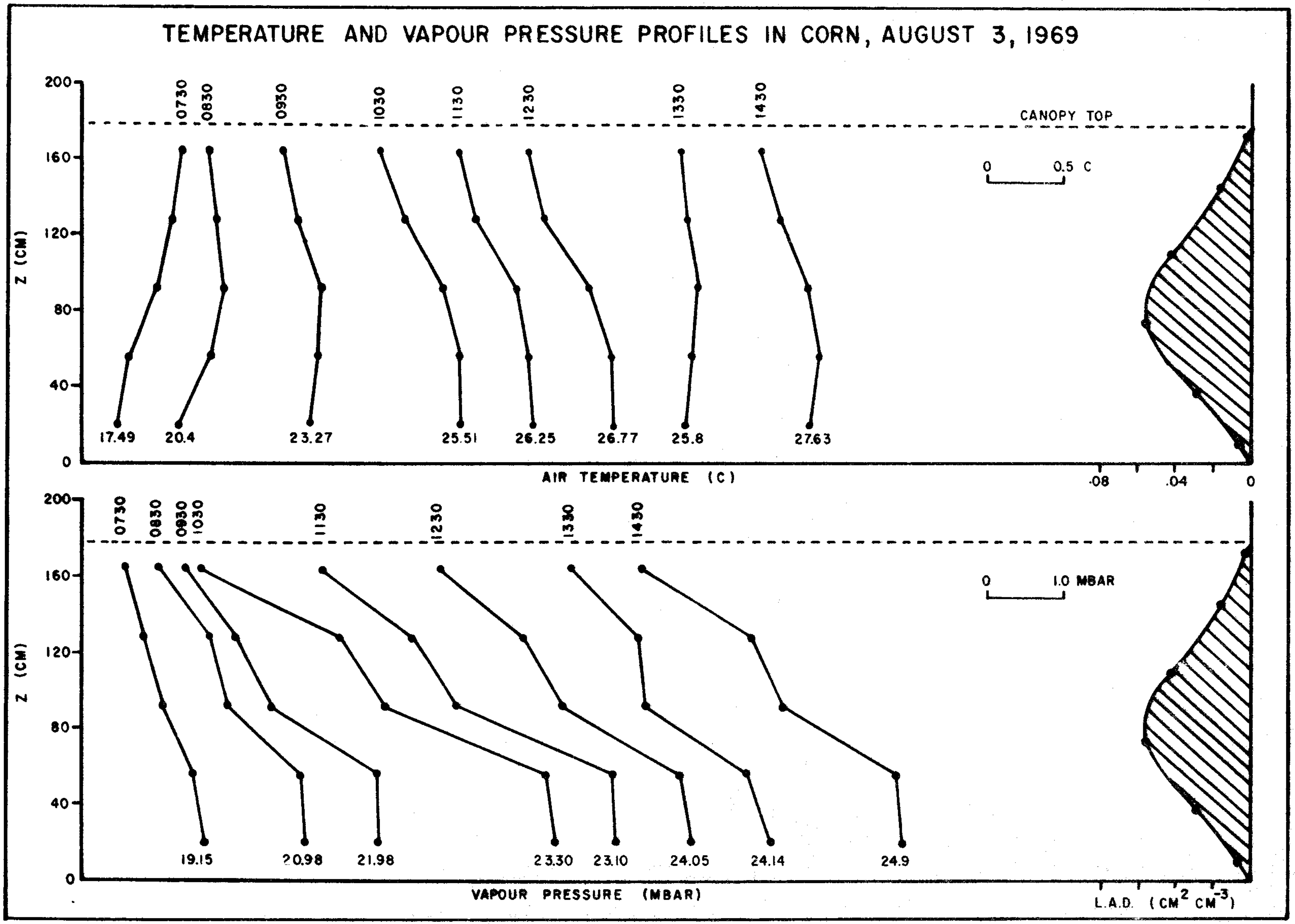
TEMPERATURE AND VAPOUR PRESSURE PROFILES IN CORN, AUGUST 3, 1969
Z (CM)
0730
0830
0930
1030
1130
1230
1330
1430
CANOPY TOP
0 0.5 C
17.49
20.4
23.27
25.51
26.25
26.77
25.8
27.63
AIR TEMPERATURE (C)
.08
.04
0
0 1.0 MBAR
19.15
20.98
21.98
23.30
23.10
24.05
24.14
24.9
VAPOUR PRESSURE (MBAR)
L.A.D. (CM² CM⁻³)

TEMPERATURE AND VAPOUR PRESSURE PROFILES IN CORN, AUGUST 5, 1969

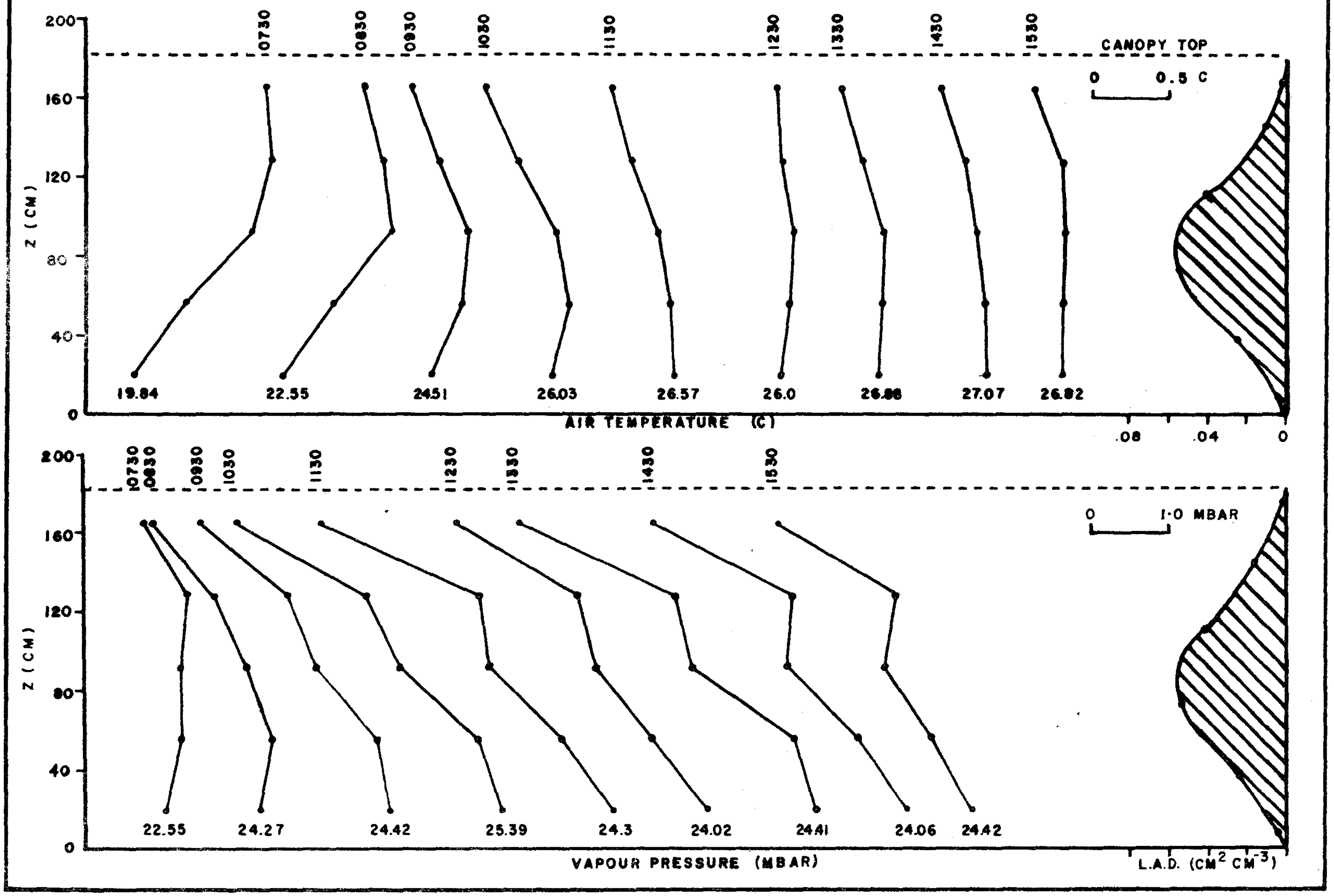

TEMPERATURE AND VAPOUR PRESSURE PROFILES IN CORN, AUGUST 6, 1969

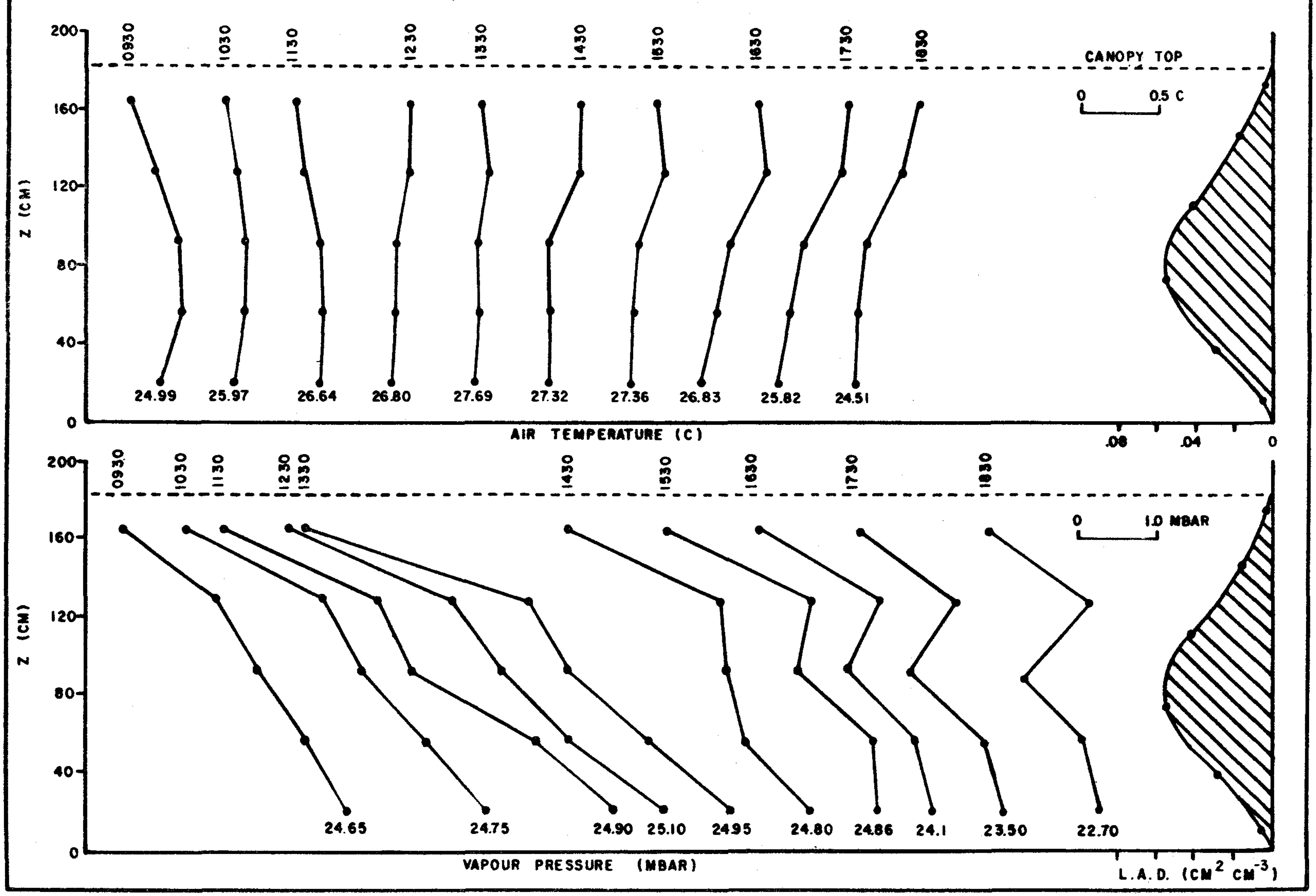

TEMPERATURE AND VAPOUR PRESSURE PROFILES IN CORN, AUGUST 7, 1969

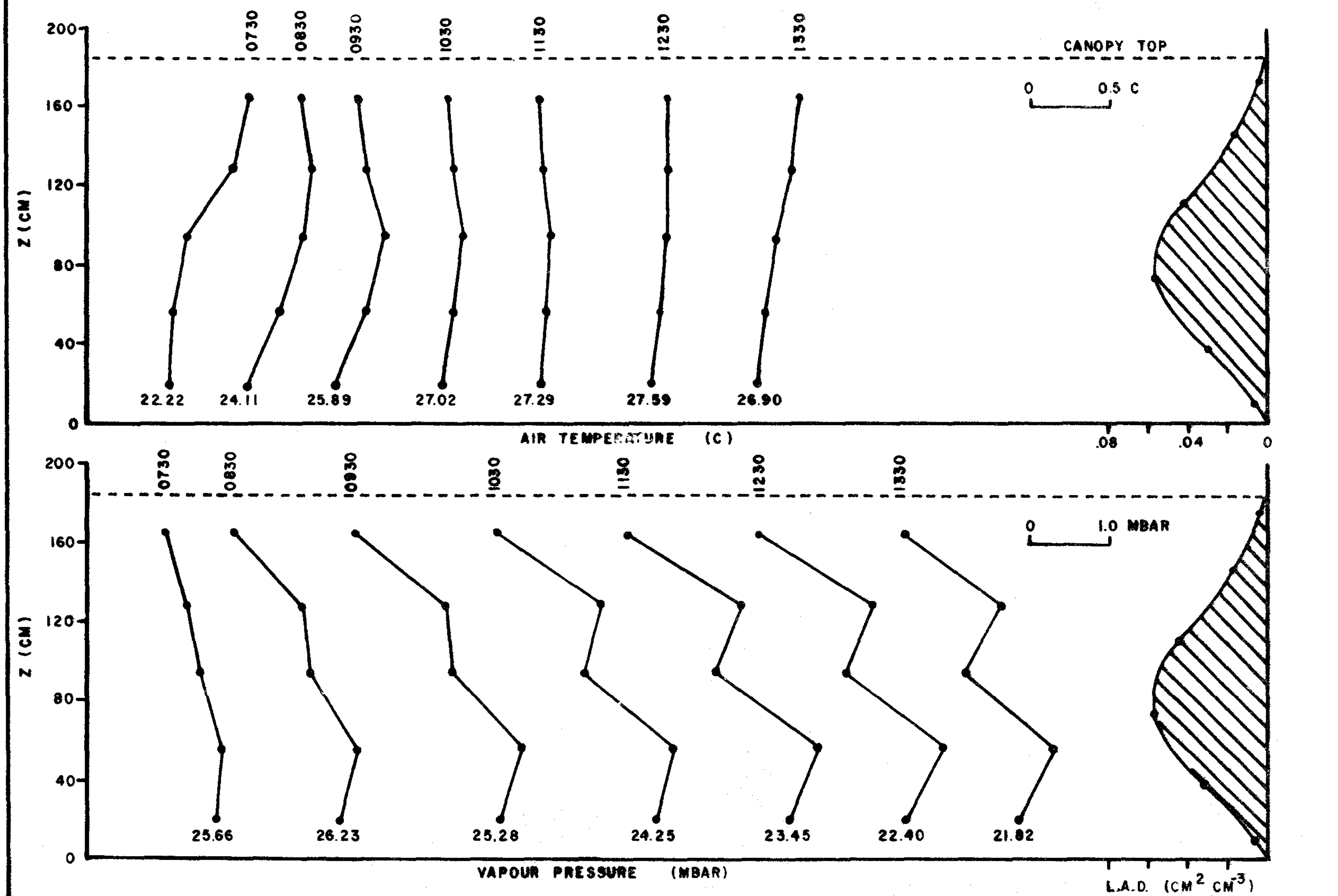

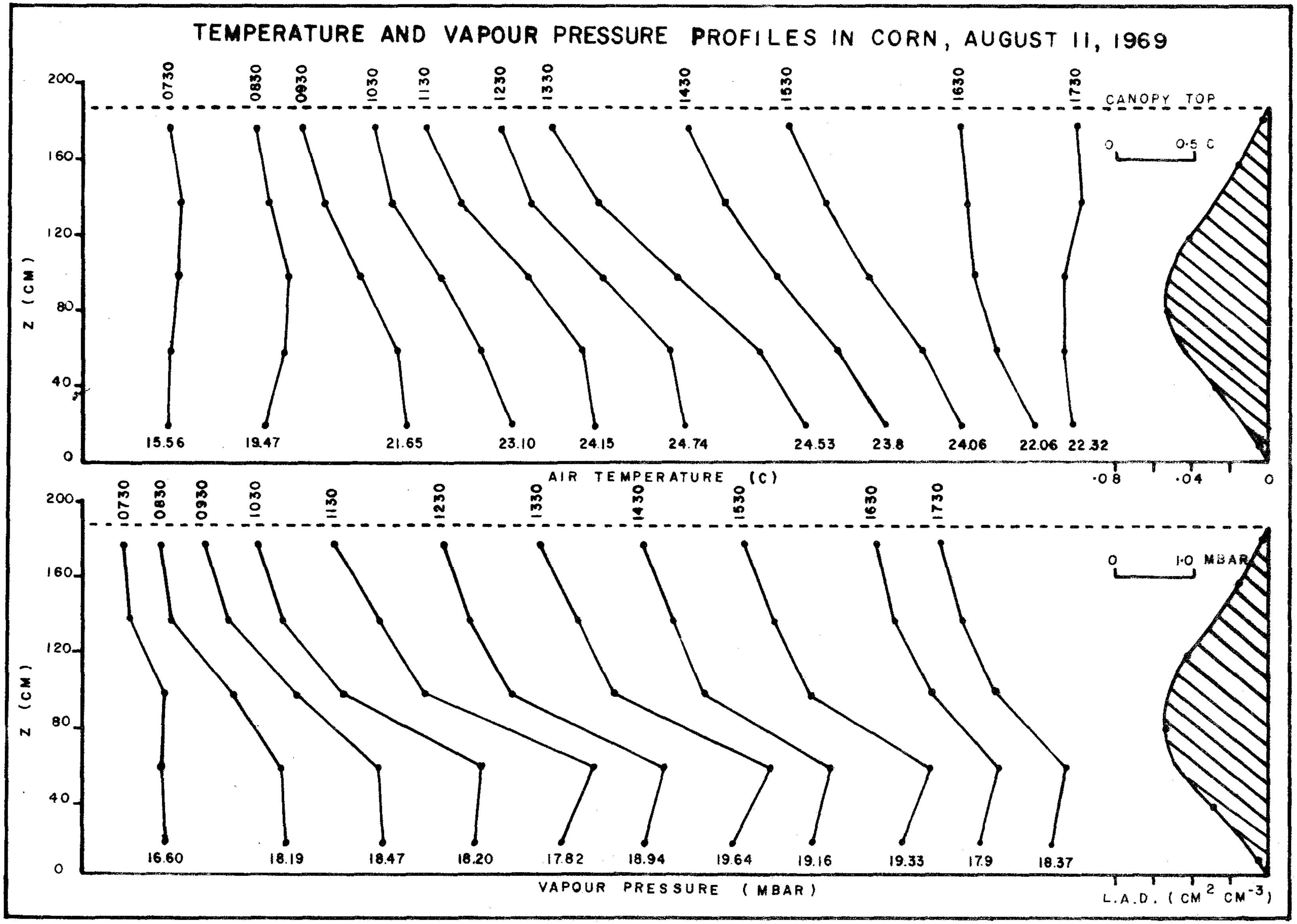
TEMPERATURE AND VAPOUR PRESSURE PROFILES IN CORN, AUGUST 11, 1969
CANOPY TOP
0 0.5 C
0730 0830 0930 1030 1130 1230 1330 1430 1530 1630 1730
15.56 19.47 21.65 23.10 24.15 24.74 24.53 23.8 24.06 22.06 22.32
AIR TEMPERATURE (C)
Z (CM)
0 1.0 MBAR
16.60 18.19 18.47 18.20 17.82 18.94 19.64 19.16 19.33 17.9 18.37
VAPOUR PRESSURE (MBAR)
·08 ·04 0
L.A.D. (CM² CM⁻³)

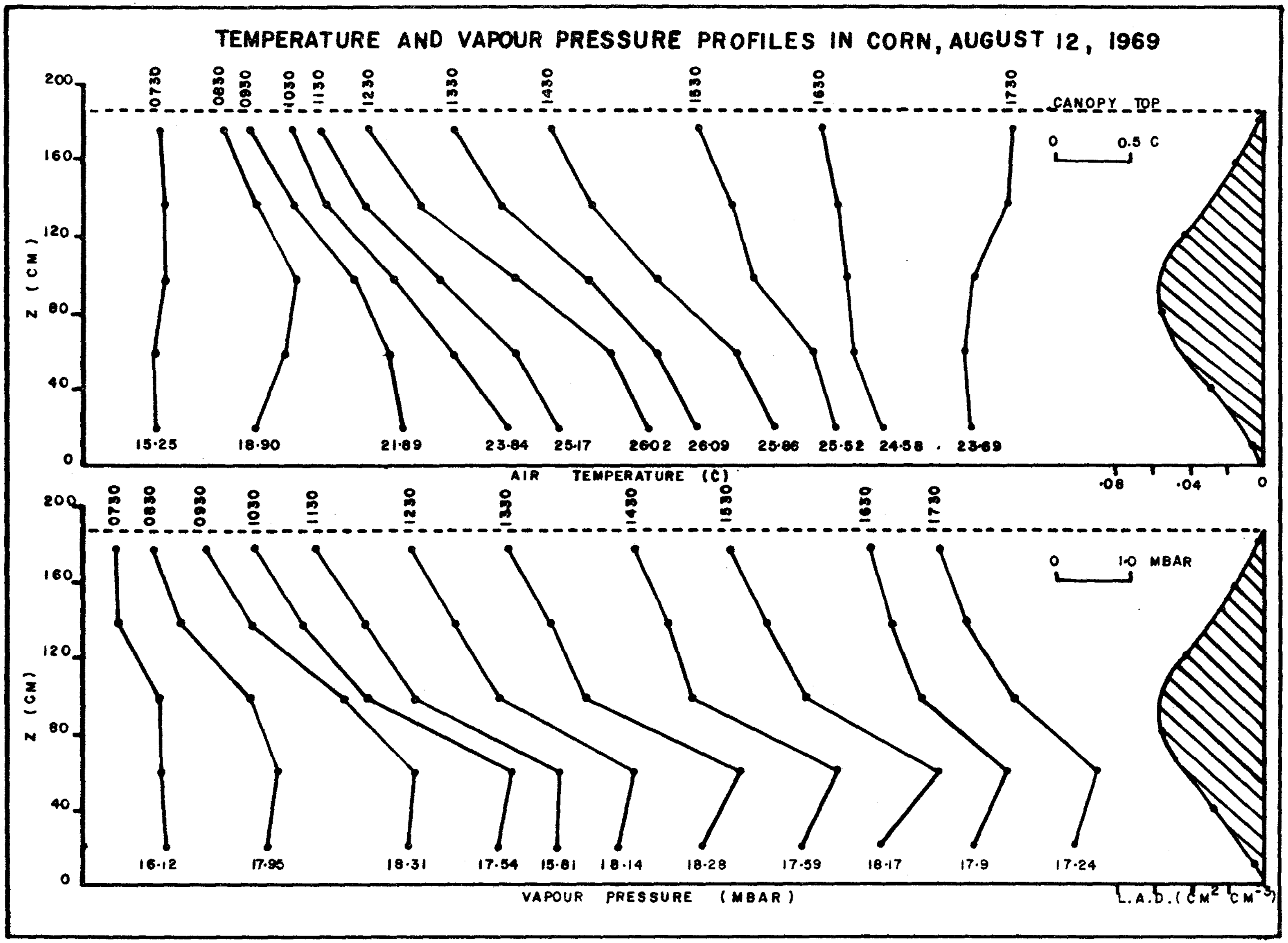
TEMPERATURE AND VAPOUR PRESSURE PROFILES IN CORN, AUGUST 12, 1969
0730
0830
0930
1030
1130
1230
1330
1430
1530
1630
1730
CANOPY TOP
0 0.5 C
Z (CM)
15·25
18·90
21·89
23·84
25·17
26·02
26·09
25·86
25·52
24·58
23·69
AIR TEMPERATURE (C)
·08
·04
0
0 1·0 MBAR
16·12
17·95
18·31
17·54
15·81
18·14
18·28
17·59
18·17
17·9
17·24
VAPOUR PRESSURE (MBAR)
L.A.D.(CM² CM⁻³)

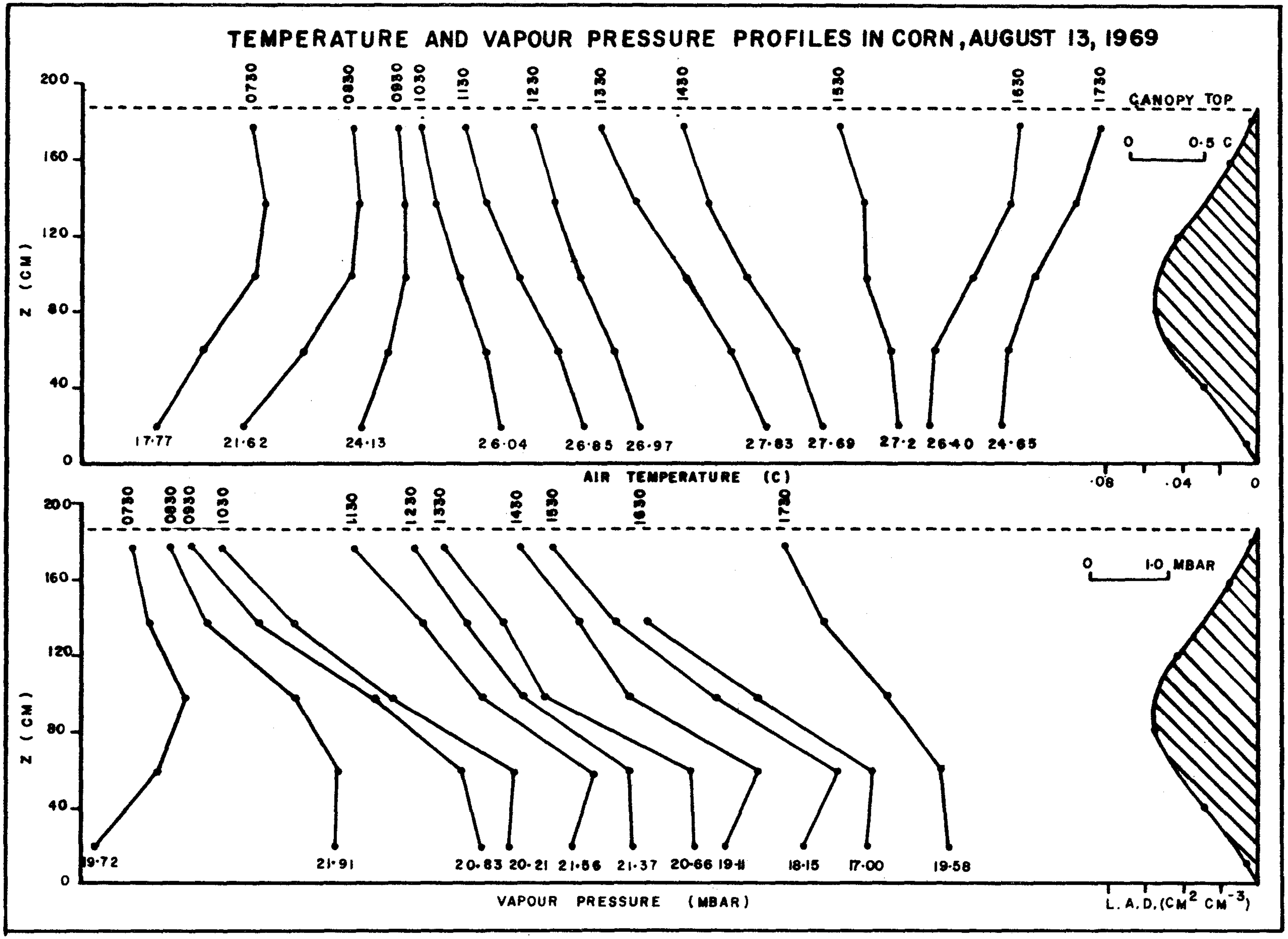
TEMPERATURE AND VAPOUR PRESSURE PROFILES IN CORN, AUGUST 13, 1969
0730
0830
0930
1030
1130
1230
1330
1430
1530
1630
1730
CANOPY TOP
0 0.5 C
Z (CM)
17·77
21·62
24·13
26·04
26·85
26·97
27·83
27·69
27·2
26·40
24·65
AIR TEMPERATURE (C)
·08
·04
0
0 1·0 MBAR
19·72
21·91
20·83
20·21
21·56
21·37
20·66
19·11
18·15
17·00
19·58
VAPOUR PRESSURE (MBAR)
L. A. D. (CM² CM⁻³)

REFERENCES

Allen Jr., L.H., 1969: An operational system for: (1) sampling and sensing micrometeorological elements: and (2) logging and processing micrometeorological data. Proceedings of the Third Microclimate Symposium, Kananaskis; Alberta, 1969, Calgary, Canadian Forestry Service, pp. 91-116.

Allen Jr., L.H., C.S. Yocum, and E.R. Lemon, 1962: The energy budget at the earth's surface. Interim Rep. No. 62-64, 3A99-27-055-08, N.Y. State Coll. Agr., Cornell Univ., Ithaca, New York. 23 pp.

Allen Jr., L.H., C.S. Yocum, and E.R. Lemon, 1964: Photosynthesis under field conditions VII. Radiant energy exchanges within a corn crop canopy and implications in water use efficiency. Agron. J., 56, 253-259.

Anderson, M.C., 1966: Stand structure and light penetration. II. A theoretical analysis. J. Appl. Ecol., 3, 41-54.

Anderson, M.C., 1966: Radiation and crop structure. IBP/PP Handbook, Canberra, C.S.I.R.O., 86 pp.

Angus, D.E., 1963: The influence of meteorological and soil factors on the rate of evapotranspiration of a crop. Ph.D. Thesis, University of California, Davis, California.

Begg, J.E., J.F. Bierhuizen, E.R. Lemon, D.K. Misra, R.O. Slatyer, and W.R. Stern, 1964: Diurnal energy and water exchanges in bullrush millet in an area of high solar radiation. Agr. Meteorol., 1, 294-312.

Bowen, I.S., 1926: The ratio of heat-losses by conduction and by evaporation from any water surface. Phys. Rev., 27, 779-787.

Brown, K.W., and W. Covey, 1966: The energy budget evaluation of the micrometeorological transfer processes within a cornfield. Agr. Meteorol., 3, 73-96.

Collins, B.G., 1963: An integrating temperature and humidity gradient recorder. In: A. Wexler (ed), Humidity and Moisture, Vol. 1, Principles and Methods of Measuring Humidity in Gases. New York, Reinhold Publ. Corp., pp. 83-94.

Cook, N.H., and E. Rabinowicz, 1963: Physical Measurement and Analysis. Reading, Mass., Addison-Wesley Pub. Co., 312 pp.

Daynard, T.B., 1971: Characterization of corn canopies from measurements of individual plants. Agron. J., 63, 133-135.

Denmead, O.T., 1964: Evaporation sources and apparent diffusivities in a forest canopy. J. Appl. Meteorol., 3, 383-389.

Denmead, O.T., 1967: A strip net radiometer. Aust. J. Instr. Control, 61.

Denmead, O.T., L.J. Fritschen, and R.H. Shaw, 1962: Spatial distribution of net radiation in a cornfield. Agron. J., 54, 505-510.

Denmead, O.T., and I.C. McIlroy, 1970: Measurements of non-potential evaporation from wheat. Agr. Meteorol., 7, 285-302.

De Vries, D.A., 1963: Thermal properties of soil. In: W.R. Van Wijk (ed), Physics of Plant Environment. New York, John Wiley and Sons, pp. 210-235.

Djavanchir, A., 1970: Mise au point d'une chambre de transpiration pour mesurer la résistance stomatique. Oecol. Plant., 5, 301.

Druilhet, A., A. Perrier, J. Fontan and J.L. Laurent, 1971: Analysis of turbulent transfers in vegetation: Use of thoron for measuring the diffusivity profiles. Boundary-Layer Meteorology, 2, 173-187.

Dyer, A.J., 1963: The adjustment of profiles and eddy fluxes. Quart. J. Roy. Meteorol. Soc., 89, 276-280.

Dyer, A.J., 1967: The turbulent transport of heat and water vapour in an unstable atmosphere. Quart. J. Roy. Meteorol. Soc., 93, 501-508.

Dyer, A.J., 1968: The role of fetch in plant studies. Proceedings of the Copenhagen Symposium, Natural Resources Research V, Functioning of Terrestrial Ecosystems at the Primary Production Level, UNESCO, pp. 493-498.

Dyer, A.J., B.B. Hicks, and K.M. King, 1967: The Fluxatron - a revised approach to the measurement of eddy fluxes in the lower atmosphere. J. Appl. Meteorol., 6, 408-413.

Dyer, A.J., and F.J. Maher, 1965: Automatic eddy-flux measurement with the Evapotron. J. Appl. Meteorol., 4, 622-625.

Elliott, W.P., 1964: The height variation of vertical heat flux near the ground. Quart. J. Roy. Meteorol. Soc., 90, 260-265.

Fuchs, M., and C.B. Tanner, 1965: Radiation shields for air temperature thermometers. J. Appl. Meteorol., 4, 544-547.

Fuchs, M., and C.B. Tanner, 1968: Calibration and field test of soil heat flux plates. Soil Sci. Soc. Amer. Proc., 32, 326-328.

Fuchs, M., and C.B. Tanner, 1970: Error analysis of Bowen ratios measured by differential psychrometry. Agr. Meteorol., 7, 329-334.

Funk, J.P., 1959: An improved polythene-shielded net radiometer. J. Sci. Instr., 36, 267-270.

Gillespie, T.J., 1971: Carbon dioxide profiles and apparent diffusivities in corn fields at night. Agr. Meteorol., 8, 51-57.

Gillespie, T.J., and K.M. King, 1971: Night-time sink strengths and apparent diffusivities within a corn canopy. Agr. Meteorol., 8, 59-67.

Goff, S.A., and S. Gratch, 1946: Low-pressure properties of water from -160 to 212°F. Trans. Amer. Soc. Heat. Vent. Eng., 52, 95-121.

Groom, M., 1968: The heat budget model for calculating the gaseous exchange in crop canopies and estimates of errors. Annual Progress Report of Microclimate Investigations, Cornell Univ., Ithaca, New York, 74-83.

Impens, I.I., 1970: Daytime distribution of energy sinks and sources and transfer processes within a sunflower canopy. Preprints of Papers, Symposium on Plant Response to Climatic Factors, Uppsala, Sweden, pp. 1-19.

Impens, I.I., and R. Lemeur, 1969: Extinction of net radiation in different crop canopies. Arch. Met. Geoph. Bioph., Ser. B, 17, 403-412.

Impens, I.I., R. Lemeur, and R. Moermans, 1970: Spatial and temporal variation of net radiation in crop canopies. Agr. Meteorol., 7, 335-337.

Kalma, J.D., and G. Stanhill, 1969: The radiation climate of an irrigated orange plantation. Solar Energy, 12, 491-508.

Kiesselbach, T.A., 1950: Progressive development and seasonal variations of the corn crop. Nebraska Agr. Exp. Sta. Res. Bull., 166.

King, K.M., 1961: Evaporation from land surfaces. Proceedings of Hydrology Symposium No. 2, Evaporation, Toronto, National Research Council of Canada, Associate Committee on Geodesy and Geophysics, Subcommittee on Hydrology, pp. 55-82.

Lemon, E.R., 1960: Photosynthesis under field conditions II: An aerodynamic method for determining the turbulent CO_2 exchange between the atmosphere and a corn field. Agron. J., 52, 697-703.

Lemon, E.R., 1965: Micrometeorology and the physiology of plants in their natural environment. In: F.C. Steward (ed), Plant Physiology, Vol. IVA. New York, Academic Press, pp. 203-227.

Lemon, E.R., 1968: The measurement of height distribution of plant community activity using the energy and momentum balance approaches. Proceedings of the Copenhagen Symposium, Natural Resources Research V, Functioning of Terrestrial Ecosystems at the Primary Production Level, UNESCO, pp. 381-389.

Leopold, A.C., 1961: Senescence in plant development. Science, 134, 1727-1732.

Lourence, F.J., 1967: Instrumentation development and calibration. Final Rept., U.S.A.E.C. Contract No. DA-02-086-AMC-0447(E), University of California, Davis, 29-36.

Middleton, W.E.K., and A.F. Spilhaus, 1953: Meteorological Instruments. Toronto, University of Toronto Press, 286 pp.

Monsi, M., and K. Saeki, 1953: Über den Lichtfaktor in den Pflanzengesellschaften und seine Bedeutung für die Staffproduktion. Japan. J. Botany, 14, 22-52.

Monteith, J.L., 1968: Analysis of the photosynthesis and respiration of field crops from vertical fluxes of carbon dioxide. Proceedings of the Copenhagen Symposium, Natural Resources Research V, Functioning of Terrestrial Ecosystems at the Primary Production Level, UNESCO, pp. 349-358

Montgomery, E.G., 1911: Correlation studies in corn. Nebraska Agr. Exp. Sta. Res. Bull., 166

Munn, R.E., 1966: Descriptive Micrometeorology. New York, Academic Press, 245 pp.

Murray, F.W., 1967: On the computation of saturation vapour pressure. J. Appl. Meteorol., 6, 203-204.

Panofsky, H.A., and A.A. Townsend, 1965: Change of terrain roughness and the wind profile. Quart. J. Roy. Meteorol. Soc., 91, 240-242.

Penman, H.L., and I.F. Long, 1960: Weather in wheat. An essay in micrometeorology. Quart. J. Roy. Meteorol. Soc.,86, 16-50.

Philip, J.R., 1964: Sources and transfer processes in the air layers occupied by vegetation. J. Appl. Meteorol., 3, 390-395.

Rider, N.E., and G.D. Robinson, 1951: A study of the transfer of heat and water vapour above a surface of short grass. Quart. J. Roy. Meteorol. Soc., 77, 375-401.

Suomi, V.E., and C.B. Tanner, 1958: Evapotranspiration estimates from heat-budget measurements over a field crop. Trans. Amer. Geophys. Union, 39, 2, 298-304.

Swinbank, W.C., and A.J. Dyer, 1967: An experimental study in micrometeorology. Quart. J. Roy. Meteorol. Soc., 93, 494-500.

Szeicz, G., J.L. Monteith, and J.M. Dos Santos, 1964: Tube solarimeter to measure radiation among plants. J. Appl. Ecol., 1, 169-174.

Tanner, C.B., 1957: Factors affecting evaporation from plants and soils. J. Soil Water Conserv., 12, 221-227.

Tanner, C.B., 1960: Energy balance approach to evapotranspiration from crops. Soil Sci. Soc. Amer. Proc., 24, 1-9.

Tanner, C.B., 1963: Basic instrumentation and measurement for plant environment and micrometeorology. Univ. Wisc., Dept. Soil Sci., Soils Bull., 6.

Tanner, C.B., A.E. Peterson, and J.R. Love, 1960: Radiant energy exchange in a cornfield. Agron. J., 52, 373-379.

Taylor, R.J., 1962: Small-scale advection and the neutral wind profile. J. Fluid Mech., 13, 529-539.

Tetens, O., 1930: Über einige meteorologische Begriffe. Z. Geophys., 6, 297-309.

Uchijima, Z., 1962: Studies on the microclimate within the plant communities. 1. On the turbulent transfer coefficient within the plant layer. J. Agr. Meteorol. (Tokyo), 18, 1-9.

Uchijima, Z., 1966: Micrometeorological evaluation of integral exchange coefficient at foliage surfaces and source strengths within a corn canopy. Bull. Natl. Inst. Agr. Sci. (Japan), Ser. A, 13, 81-92.

Van Wijk, W.R., 1965: Soil microclimate, its creation, observation and modification. Agr. Meteorol., Meteorol. Mono., 6, 59-73.

Waggoner, P.E., and W.E. Reifsnyder, 1968: Simulation of the temperature, humidity and evaporation profiles in a leaf canopy. J. Appl. Meteorol., 7, 400-409.

Webb, E.K., 1970: Profile relationships: the log-linear range, and extension to strong stability. Quart. J. Roy. Meteorol. Soc., 96, 69-90.

Wesely, M.L., G.W. Thurtell, and C.B. Tanner, 1970: Eddy correlation measurements of sensible heat flux near the earth's surface. J. Appl. Meteorol., 9, 45-50.

Wilson, R.G., 1971: Evapotranspiration estimates from the water balance and equilibrium models. Ph. D. Thesis, McMaster University, Hamilton, Ontario.

Wright, J.L., and K.W. Brown, 1967: Comparison of momentum and energy balance methods of computing vertical transfer within a crop. Agron. J., 59, 427-432.

Wylie, R.G., 1962: Psychrometry. In: J. Thewlis (ed), Encyclopaedic Dictionary of Physics, Vol. 5. New York, Macmillan, pp. 692-693.

Yocum, C.S., L.H. Allen Jr., and E.R. Lemon, 1964: Photosynthesis under field conditions. VI. Solar radiation balance and photosynthetic efficiency. Agron. J., 56, 249-253.